BLAST FURNACE MODELLING AND CONTROL

~~OF A BLAST FURNACE~~

BARRY IVOR WOOD

A thesis submitted for the Degree of Doctor of Philosophy

Date Submitted May, 1972

Department of Computing & Control,

Imperial College of Science & Technology,

University of London

ABSTRACT

Following a systematic classification of relevant literature a numerical simulation of the blast furnace process is developed on sound mathematical principles. Both steady and transient operation can be simulated directly. The thesis is concerned with a model for the purposes of computer control and, therefore, particular emphasis is placed on a simplified, but realistic, analysis of the process.

The validity of the simulation is considered in three areas, steady operation, response to step input signals and response to the changes experienced under normal operation. Off-line simulation exercises are discussed in relation to manual parameter tuning and provide further insight into furnace dynamics.

Finally, the role of the simulation in both silicon control and plant set up is discussed. Various dynamic control techniques and parameter adaption strategies are developed.

ACKNOWLEDGMENTS

I would like to thank Mr. G. F. Bryant, of the Department of Computing and Control and Project Director of the Industrial Control Group at Imperial College, Mr. D. H. A. Harvey of British Steel Corporation, Strip Mills Division and Mr. M. G. Shortland ex of British Steel Corporation, Corporate Laboratories, for their guidance, encouragement and continued backing. Mr. Bryant is particularly thanked for reading the proofs of the thesis and making several valuable suggestions.

I would also thank the Directors of the British Steel Corporation, Strip Mills Division for permission to submit this thesis.

My research started at the Corporate Laboratories at Battersea and has been continued at Port Talbot. Many thanks are, therefore, due to a number of people associated with the computer control project at Port Talbot for their assistance and for the many fruitful discussions.

Finally, I would like to thank my wife, Denise, for typing the script of this thesis and for her patience and understanding over the past years.

CONTENTS

		Page
Title Page		1
Abstract		2
Acknowledgments		3
Contents		4
Introduction		7
Contributions of this thesis		9
Chapter 1	Description of the plant, process and its control problems.	11
	1.1 The plant and process	11
	1.2 Manual operation	14
	1.3 Aspects of computer control	17
Chapter 2	Discussion of the developments to date.	19
	2.1 Various computer control techniques	19
	2.1.1 Simple heuristic methods	19
	2.1.2 Linear regression methods	20
	2.1.3 Non-linear regression methods	22
	2.1.4 Difference equation methods	23
	2.1.5 Classical material balance methods	23
	2.2 Off-line process simulation	30
Chapter 3	The development of a dynamic model.	40
	3.1 The form of the equations	41
	3.2 The chemical and thermodynamic forcing functions	43

		Page
	3.2.1 Reduction of iron oxides	45
	3.2.2 Reduction of metalloids	51
	3.2.3 Heat transfer	56
	3.2.4 Reactions in the Tuyere Region	56
	3.2.5 Heat and material balances	57
	3.3 A numerical solution	59
Chapter 4	Some simulation and trial results.	69
	4.1 The problem of initial parameter estimates	69
	4.2 An assessment of certain dynamic responses	78
	4.2.1 Steam injection	81
	4.2.2 Blast temperature	84
	4.2.3 Coke rate	84
	4.2.4 Oil injection	84
	4.2.5 Oxygen enrichment	84
	4.3 A simulation of normal furnace working	85
Chapter 5	Methods of control using the simulation.	89
	5.1 Control of silicon using a single variable	91
	5.1.1 Manual control	92
	5.1.2 Systems using the model as an 'observer'	95
	5.1.3 Feedforward prediotive control	101
	5.1.4 Comments on the above systems	106

		Page
	5.2 Control of silicon using a blast variable and the coke rate	107
	5.3 Attainment of efficient operation	110
	5.4 Concluding remarks	114
Chapter 6	Methods for improving simulation accuracy in an on-line environment.	115
	6.1 Estimating the silicon bias	115
	6.2 Correction of material flow	116
	6.3 Measurements from the top gas	120
Conclusions and Future Research		124
References		127
Appendix 1	The fundamental differential equations.	129
Appendix 2	Error calculations.	132

INTRODUCTION

The blast furnace performs the first stage in the transformation of natural iron bearing ores into steel. In recent years the introduction of fast and sophisticated basic oxygen steelmaking has been accompanied by quite large increases in blast furnace production rates and larger furnaces are now producing more than 7000 tons of hot metal per day.

The process itself has a long history and notable among its characteristics are the acceptance of materials with widely varying properties and the extremely slow dynamic behaviour of the process. Furnace control is further complicated by the large number of interactive inputs and difficulties of measurement.

Research into furnace control has to a large extent been stimulated by the potential rewards from even a moderately successful system and to date quite a number of on-line process control computer systems have been installed, with varying results. The majority of these applications have been based on a steady state analysis of the process.

The aim of research described in this thesis is the development of dynamic control techniques and in order to make progress a process model is proposed and developed.

The presentation of work is divided into chapters as follows:-

Chapter 1 A brief description is given of the plant and process followed by a discussion of the control problems.

Chapter 2 Here computer control techniques already in use and several of the more abstract mathematical models which, due to recent advances in process control computers, may be of use in the control field, are discussed in some detail.

Chapter 3 A dynamic simulation of the process is developed from first principles. Particular attention is paid to a realistic and sufficiently simplified analysis of the process chemistry, and the numerical method of solution.

Chapter 4 Parameter tuning is discussed and results from both off-line and on-line simulation exercises presented.

Chapter 5 This chapter deals with methods of control based on the simulation, and discusses use of the blast variables, the coke rate, and plant set up.

Chapter 6 Here certain techniques aimed at improving the accuracy of the simulation in its on-line environment, and in particular use of the top gas analysis and temperature, are discussed.

CONTRIBUTIONS OF THIS THESIS

The introduction has indicated the scope of this thesis. These studies appear to the author to advance knowledge of blast furnace control systems in the following ways:-

1. A systematic classification of the large number of published papers on blast furnace modelling and control is presented.

2. A numerical method for simulating the process in both steady and transient operation is developed on sound mathematical principles. To the best of the author's knowledge the method of characteristics has not been applied and developed in connection with this problem. This in contrast to other approaches yields both an accurate and numerically viable solution.

3. A simplified, but realistic, analysis of the process is developed specifically for the control application. This reduces the manual tuning of parameters to manageable proportions and ensures a practical application.

4. Simulation studies are presented which increase ones understanding of the process and its dynamics.

5. The role of the simulation in respect to on-line control is developed in depth. Application of the observer principle and predictive control to the blast furnace process is to the author's knowledge novel.

6. The problem of establishing optimal steady working conditions quickly is non-trivial. For instance, the calculation of changes to the coke rate and their timing is time consuming and demands considerable operator skill and insight. Guide lines are given for the use of the simulation in this area and as an operator guide.

CHAPTER 1

Description of the plant, process and its control problems.

1.1 The plant and process

Iron is first produced from its oxide ore in the blast furnace and then further processed in the steelmaking plant to remove much of the carbon. The blast furnace is basically a vertical shaft furnace which is charged periodically at the top with various iron ores, coke, flux and possibly scrap material, while a blast of hot enriched air is injected through a number of water-cooled nozzles, called tuyeres, near the base. Iron and slag are removed independently through tap holes at intervals of about 3-4 hours. Iron production can range from typically 1000 tons/day from smaller units to perhaps 7000 tons/day from the larger furnaces. The gaseous products leave through off-take mains at the top of the furnace. A typical blast furnace is shown in Fig. 1.1.

The mechanism is most easily explained in three parts. Firstly, while the iron ores are being preheated in the furnace Stack, they react with both carbon monoxide and hydrogen and are thus progressively reduced to a viscous primary slag. Typical reactions, termed as Indirect Reduction, are

$$Fe_xO_y + CO \rightleftharpoons Fe_xO_{y-1} + CO_2$$

$$Fe_xO_y + H_2 \rightleftharpoons Fe_xO_{y-1} + H_2O$$

Some of the resulting carbon dioxide reacts further with carbon from the preheated coke, thus regenerating reducing gas for use higher in the Stack. This reaction, known as Carbon Solution Loss, is

$$C + CO_2 \rightleftharpoons 2CO$$

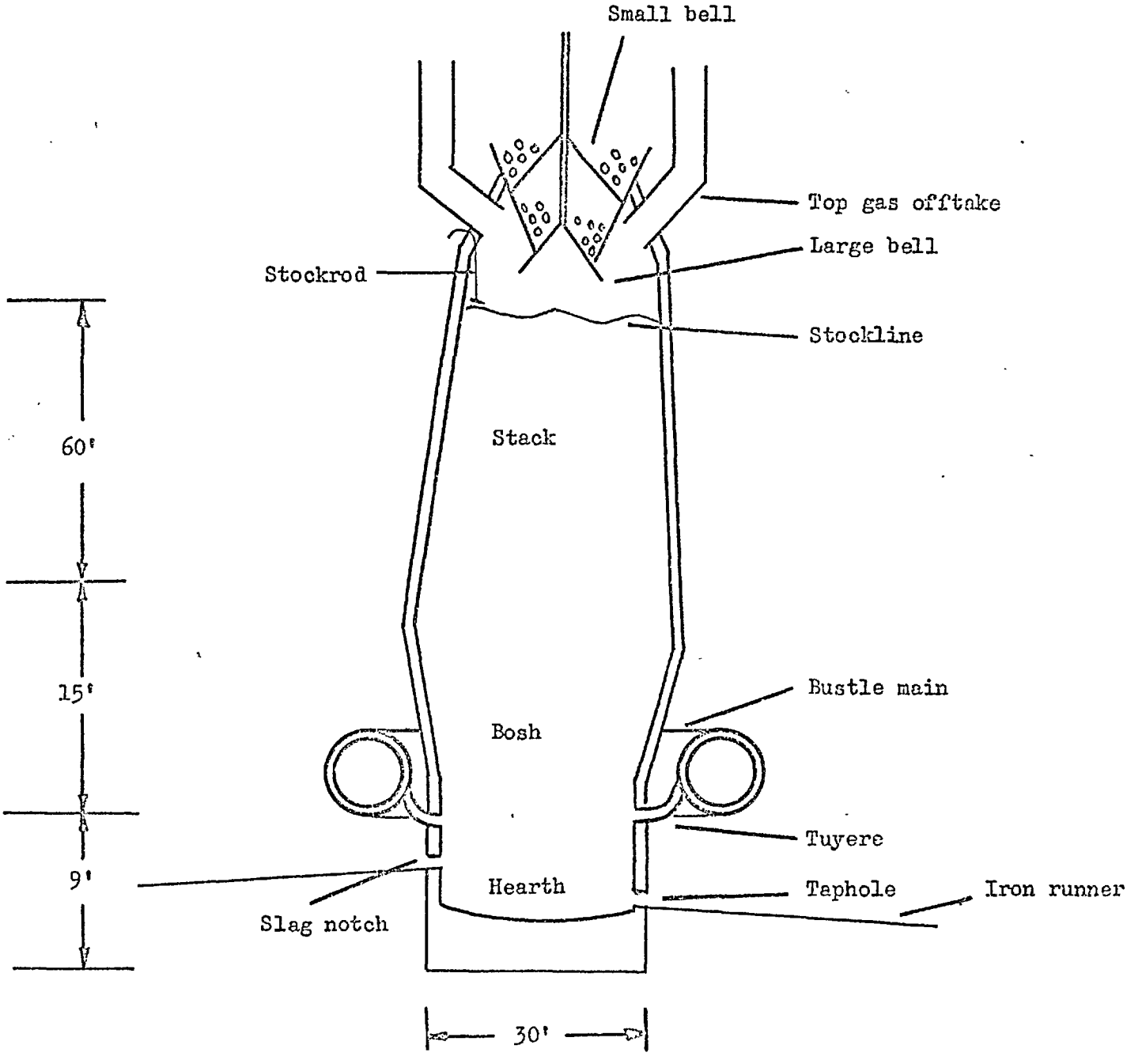


Fig. 1.1 A Typical Blast Furnace

and is highly endothermic. Secondly, as the primary slag passes slowly through a bed of hot coke, sited in the lower Bosh area, the reduction to metallic iron is completed by Direct Reduction, i.e.

$$FeO_{slag} + C_{coke} \rightleftharpoons Fe_{metal} + CO$$

Various metalloids are also reduced at this stage. For example

$$SiO_{2\,slag} + 2C \rightleftharpoons Si_{metal} + 2CO$$

These metalloids have a particularly important bearing on the thermal condition of the furnace in view of the large amounts of heat consumed in their reduction. Lastly, the metallic iron is separated from the gange and from ash left by coke burning at the tuyeres; differences in density cause the formation of a layer of slag which floats on top of the pool of liquid iron in the furnace hearth.

The usual criteria for quantifying furnace performance and in particular the degree of control obtained are:-

(i) hot metal production rate

(ii) furnace fuel rate

(iii) iron quality, whereby this one usually considers the mean level and variation in the percentages of silicon and sulphur in the hot metal.

Thus, the percentage of silicon in the hot metal is particularly important for two reasons:-

(i) it is closely related to the thermal state of the furnace and has a considerable bearing on the efficiency (in terms of fuel rate). Extreme thermal conditions can introduce adverse physical conditions in the hearth, and drastically affect overall performance,

(ii) it considerably affects the heat balance for the steelmaking process. Variations are, therefore, disturbances to routine operation at the steelplant and result in a drop in the production rate of steel.

1.2 Manual Operation

The generally accepted method for setting up and controlling a furnace is firstly to fix the blend of ores and sinters to be used, a slag analysis and weight per ton of iron and the initial coke rate, by theoretical and emperical calculations; here the ironmaker relies heavily on his operating experience and on his knowledge of the individual characteristics of his particular plant. Materials balance calculations are then performed to determine the amounts of flux and additives to be added to the basic burden.

The various measurements allowing the operator to monitor the plant are shown in Table 1 and are generally restricted to measurements of plant input and output variables. Certain internal measurements have been made using probes to sample gas and solids from within the furnace. However, such methods are still considered as research tools rather than routine aids to production and are rarely used in plant control.

Control takes the form of successive adjustments to the blast variables or to the ore/coke ratio and continues until satisfactory working conditions are reached. These adjustments to the furnace inputs are based mainly on the following:-

(i) the iron and slag appearance and analysis at recent casts

TABLE 1 Measurements from a Furnace

CHARGE		
*Charging rates of:-	Sinter	t/hr
	Rubble Ores	t/hr
	Carbonates	t/hr
	Additives	t/hr
	Scrap	t/hr
	Coke	t/hr
Charging rate		charges/hr
BLAST		
Volume		m^3/hr
Temperature		^oC
Moisture		Grains/m^3
Oil Injection Rate		gals/hr
Oxygen Content		% of dry volume
Pressure		psi
TOP GAS		
Temperature		^oC
Pressure		psi
%CO		
$\%CO_2$		
$\%H_2$		
Stockline ht		m
Stockline descent rate		m/hr
HOT METAL		
Iron temperature		^oC
Tonnage		t
%Si		
%S		
%Mn		
%P		
%C		
ROUGHING & FLUSHING SLAG		
Slag weight		t/t iron
%FeO		
$\%SiO_2$		
$\%Al_2O_3$		
%CaO		
%MnO		
%MgO		
%S		

* the analyses of individual constituents are available from time to time.

(ii) the state of the furnace hearth as viewed through the tuyere peepholes

(iii) the blast volume relative to blast pressure

(iv) the rate and regularity of burden descent.

The blast furnace process when under control is, therefore, in a delicately balanced condition. Both feedback and feedforward control techniques are used by the operator, against a background of disturbances in both the blast and the charge inputs, in order to minimise any deviation from balanced conditions.

One factor limiting the performance of this manual process control system is the frequency at which control actions are made by the operator. Two reasons for this very slow frequency are suggested:-

(i) Low information sampling rate and high signal to noise ratio.

This relates to the amount of information available and to the confidence the operator has in this. As an example, consider cast analyses, an important set of variables used in the control of iron quality. Several samples are taken and analysed at each cast (every 3 hours) and an average given to the operator. However, knowing that there are sometimes large variations in analysis during a cast, that samples can be contaminated and allowing for errors at the laboratory, the operator would wait for at least another cast before finally identifying a trend in the heat level of the furnace hearth or a variation in slag chemistry and subsequently making a control action.

(ii) The interaction problem.

Time constants - ranging from 2 to 12 hours - and long transport delays give rise to many complex interactions after control actions involving several inputs; these are difficult for the operator to follow and encourage him to wait and measure the full effect of his

actions before making other adjustments. As furnace production rates rise and fuel rates fall control of hot metal quality will become both more difficult and more critical.

While discussing the performance of manual control, it must be noted that large improvements both in furnace production and control have been made using improved burdening and charging practice. In this way many of the previously unknown disturbances in the burden i.e. in sizing and analysis, are greatly reduced; the major disturbances to the system then take the form of manual changes to the blast variables, and can more easily be compensated for. Improvements in these areas are generally considered a necessary prerequisite to computer control.

1.3 Aspects of computer control

Computers have, or are being linked to the plant to perform various functions. For example:-

(i) Sequence control of the material charging system.

(ii) D.D.C. of the air flow, temperature and additive injection rates.

(iii) Calculation of limestone and magstone additions for the burden.

(iv) Supervision of material weighing systems and compensation for variations in the analysis of materials charged.

(v) Variation of the blast inputs and the coke rate in order to stabilise hot metal quality - in particular the % Silicon and % Sulphur in the hot metal.

(vi) Selection of input operating levels which reduce the process costs.

This thesis is concerned in particular with items (v) and (vi) above.

CHAPTER 2

Discussion of the developments to date.

During the last decade many researchers have studied the blast furnace process from standpoints covering process technology, furnace design, furnace performance and control, and in many cases some form of mathematical model has evolved. In discussing the developments relevant to furnace control it is beneficial to consider the subject in two areas, one dealing with computer control systems that are in use and the models associated with them, the other covering the more abstract mathematical models that have for example been used to improve process technology and which may now, due to recent advances in process control computers, have considerable potential in the control field.

2.1 Various computer control techniques

The first papers on this subject appeared in the early sixties and dealt with systems designed to rationalise manual control into a sequence of logical and consistent actions.

2.1.1 Simple heuristic methods

K. H. Gee (Ref. 1) argued that control of temperature within the furnace was the key to good operation. Operators traditionally take the silicon analysis of the hot metal as an indication of this. Gee, however, notes that the dependence of silicon content on temperature is affected by changes in slag analysis and the slag weight per ton of hot metal, and also that there are often delays in the confirmation of cast analyses by the laboratory. He, therefore, takes hot metal temperature, measured continuously by an immersion thermocouple in

the iron runner, as his basis. A comparison is made between the curve of iron temperature at the current cast, that of the previous cast and a standard curve, to determine whether the furnace is heating or cooling and thus the required change in blast temperature.

Shellenberger and Powell (Ref. 2) develop a similar method based on the maximum temperature during the cast. The difference between this and an aim temperature, and the change in temperature since the previous cast, are used to calculate the necessary change in the blast moisture. This calculation includes some consideration of transient behaviour. Changes in blast moisture are made at each cast and variation of the coke rate is used to centralise the moisture in its operating range. Plant trials lasting two months using this method in conjunction with control of slag basicity - based on the amount of limestone charged - show that the standard deviation of silicon content taken from cast to cast drops from 0.23 to 0.15.

2.1.2 Linear regression methods

An approach taken by some researchers involves a multiple regression analysis of furnace operating data and has the advantage that control is based on continuously measured variables rather than those available only while casting. G. H. McCleskey (Ref. 3) suggests a fairly simple controller to regulate production rate:-

$$PR = 1.019 + 0.082\,W - 0.0226M - 0.476P - 0.0014T$$

where PR = iron production rate

W = blast volume

M = blast moisture

P = blast pressure (plant output)

T = top gas temperature (plant output)

Blast pressure is included as a measure of the resistance of the burden to the blast and top gas temperature indicates the extent to which the burden and blast are combining. Control actions are made every 15 minutes to the blast volume and moisture to compensate for variations in top gas temperature and blast pressure.

Robins (Ref. 4) suggests regulating the silicon content by controlling the heat input to the furnace, and achieves this using a mixture of feedforward and feedback control. The regression equations used are suggested by a theoretical examination of the process - a heat effect for each of the measured variables is calculated and compared with that for blast temperature,

i.e. $\Delta B_m = k_1 \Delta B_t$ $\quad\quad$ $\Delta L = k_4 \Delta B_t$

$\Delta B_v = k_2 \Delta B_t$ $\quad\quad$ $\Delta G_t = k_5 \Delta B_t$

$\Delta C = k_3 \Delta B_t$ $\quad\quad$ $\Delta CO = k_6 \Delta B_t$

$$\Delta h = k_7 \Delta B_t$$

where B_t = blast temperature

B_m = blast moisture

B_v = blast volume

C = coke/ore ratio (5 hour moving average)

L = limestone/ore ratio (5 hour moving average)

G_t = top gas temperature (dependent variable)

CO = top gas CO analysis (dependent variable)

h = heat loss to cooling water (dependent variable)

Using blast temperature to compensate for changes in the other variables the standard deviation of silicon content is decreased from 0.22 to 0.14, although no consideration is given to changes in

production rate or to transient effects, and no use is made of the current silicon level.

2.1.3 Non-linear regression methods

So far in the discussion the regression equations have been linear in terms of input/output variables. One consequence of including accurate and contiruous top gas analysis - the instrumentation first became available in 1965 - is that some of the fundamental reactions and heat transfers associated with the process can be evaluated and this leads to non-linear equations in terms of the input/output variables. The advantages of this can be seen by considering a change in the CO content of the top gas. This can be produced by variations in the reactions in either the Stack or Bosh areas and can, therefore, cause different thermal effects.

Katsura and Yamamoto (Ref. 5) set out to control the heat level in the hearth and use % Silicon to indicate this. Their regression equation is based on the assumption that change in silicon is proportional to the heat stored between casts. A heat balance over the furnace as a whole suggests that

$$\Delta Si_n = C_o + C_1\, Si_{n-1} + C_2 \alpha_n + C_3\, (\alpha_n + \beta_{n-1} + \gamma_{n-1}) + C_4\, M_n + C_5\, P_n$$

where α = amount of direct reduction

β = amount of indirect reduction

γ = amount of hydrogenous reduction

M = blast humidity

P = permeability (blast volume/pressure drop in furnace)

n = sample instant

Using this difference equation to estimate % Silicon, the correlation between plant and model is 0.65.

Control using blast moisture was based on feedback of the estimated value of the current % Silicon in the hot metal.

2.1.4 Difference equation methods

A similar approach is suggested by Spallanzani (Ref. 6). The important difference is that the blast volume and temperature terms are also delayed. So, although only one term is included, the equation gives some consideration to the transient relationships between the blast variables and Silicon. 95% confidence limits for estimates of Silicon concentration are $\pm$ 0.2%.

Rebeko et al (Ref. 7) take this approach one step further using the modern methods of statistical dynamics to develop an equation for predicting % Silicon from normal operating records. Both auto and cross correlation functions are used to investigate the time relationships between Silicon content and ore/coke ratio, blast temperature and composition, amounts of indirect and direct reduction, and hydrogen utilisation.* They conclude that these transients can be approximated by first order systems plus a pure lag. Estimates of % Silicon given by a linear equation involving the above variables displaced in time and their preceding values, when compared with plant silicon values, show a correlation coefficient of 0.82 to 0.86.

2.1.5 Classical material balance methods

In the preceding systems a theoretical analysis of the process has been used to give qualitative information which has then been refined by statistical techniques. Several organisations (Refs. 8, 9, 10, 11, 12 and 13) have reported controllers which are based totally on theoretical analyses and which have usually resulted in improved operation at quite a number of European Works. The common

*This is a measure of the indirect reduction associated with hydrogen.

approach is to use heat and materials balance equations to continually calculate the thermal state of the furnace hearth, from data regarding the top gas, blast and charge. A feedback controller uses one of the blast parameters - humidity, temperature or oil injection rate - to regulate the heat level of the hearth to some reference level, and thus indirectly stabilises the hot metal analysis.

It is beneficial at this stage to develop this technique further in order to gain some insight into the process and in particular into factors affecting the top gas analysis and the coke rate. For simplicity a base practice using 100% fluxed sinter and no blast enrichment will be examined using the graphical technique of Rist (Ref. 14).

Consider Fig. 2.1. The oxygen in the top gas initiates from three sources:-

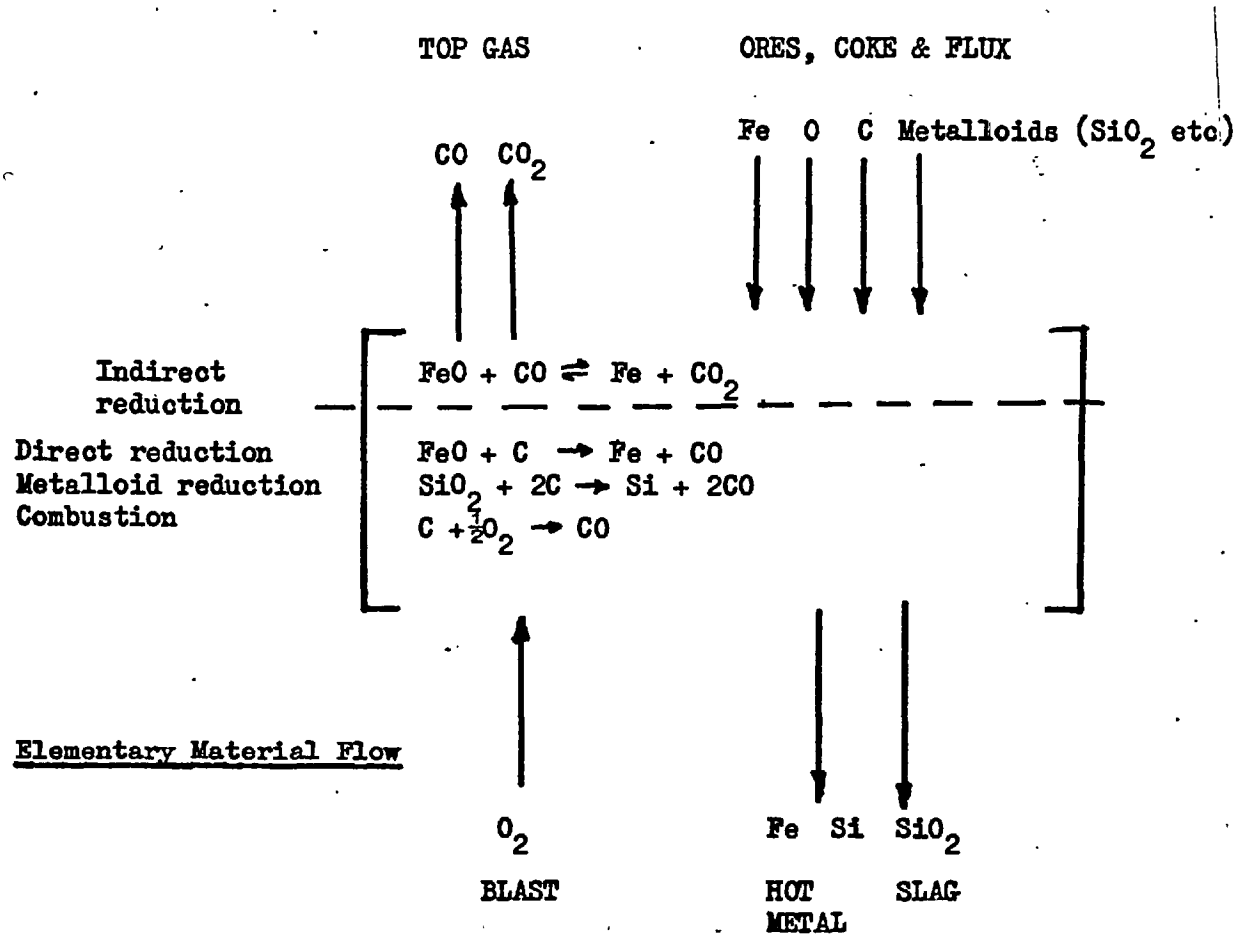
(i) oxygen in blast

(ii) oxygen initially bound to iron

(iii) oxygen released by the reduction of metalloids.

These quantities of oxygen per unit iron produced can be established given the hot metal analysis, the oxygen/iron ratio of the burden and the amount of iron produced by one unit of blast.

With the furnace in a steady state there are fixed ratios relating the amount of iron charged to the amount of carbon charged and to the amount of carbon in the top gas - hence the linear relationship shown in Fig. 2.1, known as the Operating Line. Once direct reduction ceases, the carbon content of the gas as it ascends the Stack is fixed and so the section of the oxygen/carbon axis between 1 and 2 represents the O/C ratio of the gas as it ascends the furnace stack. The area to the left of the ordinate O/C = 1 refers to the generation of reducing gas, that to the right to its utilisation in the Bosh and Stack.



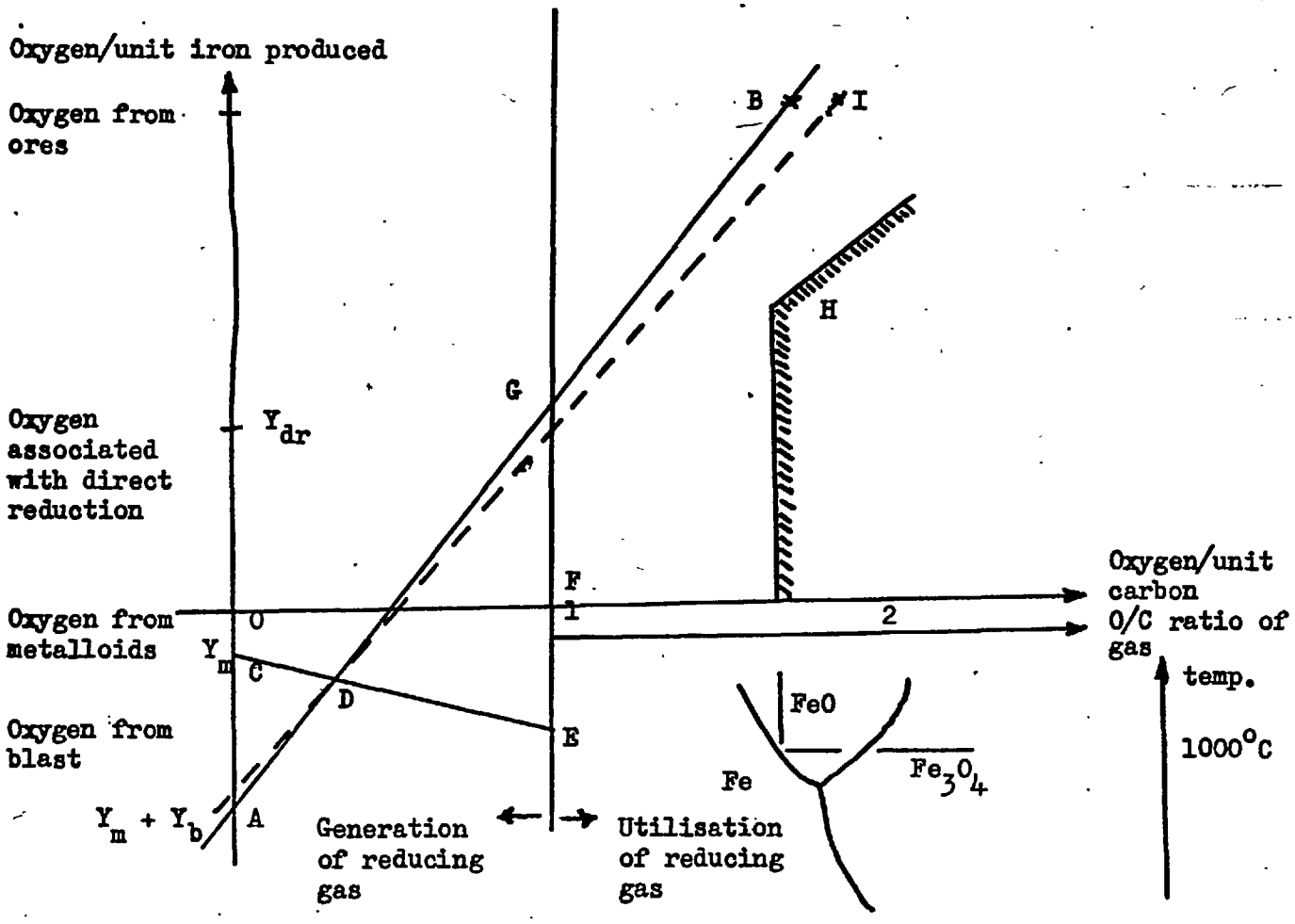


Fig. 2.1 The Rist Operating Diagram

The point H (Fig. 2.1) represents the chemical equilibrium for the system - the process is at its most efficient when the operating line passes through this point.

To fix the operating line for a given operating condition the amount of iron produced per unit of blast, Pi, is first calculated using an oxygen balance, with base the unit of blast. That is

$$Pi = \frac{\text{Oxygen in top gas - Oxygen in blast}}{\text{Oxygen from iron ores and metalloids per ton of iron}}$$

Using this the amount of oxygen from the blast (Y_b) and the amount associated with metalloid reduction (Y_m) are calculated, which fixes point A on the operating line. A second point (B) is found from the O/C ratio of the top gas and the O/Fe ratio of the burden when charged.

A thermal reserve is now assumed, at a temperature of 1000°C, in which the gas/solid temperature difference approaches zero. This allows a heat balance over the lower (or production) zone to be performed (Table 2).

Inputs	Outputs
Blast enthalpy	Direct reduction
Combustion	Reduction of SiO_2, MnO & P_2O_5
Burden at 1000°C	Heating and melting of metal and slag
Coke at 1000°C	Gas at 1000°C
Heat from Indirect reduction	Losses

Table 2. Terms in the heat balance for the 'production' zone.

So $Wu = h_b y_b - h_{dr} Y_{dr} + \text{const.}$

where Y_b = amount of oxygen from blast

Y_{dr} = amount of oxygen associated with carbon solution loss

Wu = heat for raising the temperature of iron and slag above 1000°C, heat losses, and the reduction of metalloids

h_{dr} = reaction heat for direct reduction

h_b = heat from blast (enthalpy and combustion)

and this equation fixes Wu, the heat level of the hearth.

In order to examine changes in the steady state this equation is rewritten as

$$\frac{Y_b}{Y_{dr}+\frac{1}{h_{dr}}\,Wu} = \frac{h_{dr}}{h_b}$$

Now h_{dr}/h_b is a known constant for any particular set of blast conditions. If EF on Fig. 2.1 is made equal to $\frac{1}{h_{dr}}$ Wu then, because of the similarity of triangles ADC and DEG, the line CE defines a fixed point D through which the operating line passes. For example, if the blast volume drops without changing the production rate or the cast analysis, then the operating line pivots about the point D, the amount of direct reduction drops and the point I indicates the new top gas analysis. On the other hand, a change in blast temperature will vary h_b, which in turn means a repositioning of point D and a change in Wu.

In viewing these changes in the process variables it must be remembered that in theory the information applies only to the initial and final steady states and yields no details regarding the transient period. In practice, however, Staib et al. (Ref. 15) note that in many cases a good degree of correlation exists between % Silicon and Wu during transient conditions. They go on to identify 1st order

dynamic relationships between Wu and the blast variables and use these to tune their controller.

Several authors (Ref. 16, 17 and 13) extend the method by examining the relationship between the thermal index (Wu, Ec, K_w, M depending on origin) and % Silicon during normal operation. Vidal notes that the best filter is

$$G_{\Delta\%Si,\ \Delta Ec} = \frac{K}{(1 + sT_1)(1 + sT_2)}$$

and goes on to show that estimates of % Silicon (Fig. 2.2) explain 50% of the natural variation in the plant values. A point to note here is that the relationship between Ec and % Silicon depends on the origin of the disturbance in Ec; if a change occurs to the reactions in the Stack its effect on Silicon will appear much later than that from a change at the Bosh or Hearth levels.

A promising extension to the balance technique has been proposed by T. Barbieri et al. (Ref. 18) and is designed to overcome some of the deficiencies of the Wu technique. For example, accumulations of heat and carbon in the solids are allowed for in the material balances, variations in slag weight and analysis are taken into account and the calculation of production index using an oxygen balance - this is sensitive to errors in the measurement of blast volume and O/Fe ratio of the burden - is replaced by an iron balance in which stock line velocity is used to predict furnace driving rate. After a considerable amount of linearisation about the working point the following remarkably simple equation evolves:-

$$\alpha \frac{dSi(t)}{dt} + \beta Si(t) = Q(t)$$

and $Q(t)$, the heat input to the production zone, is given by

$$Q(t) = A(t) + a_1C + a_2S_v + a_3b + a_4 Mn + a_5P + a_6S + a_7$$

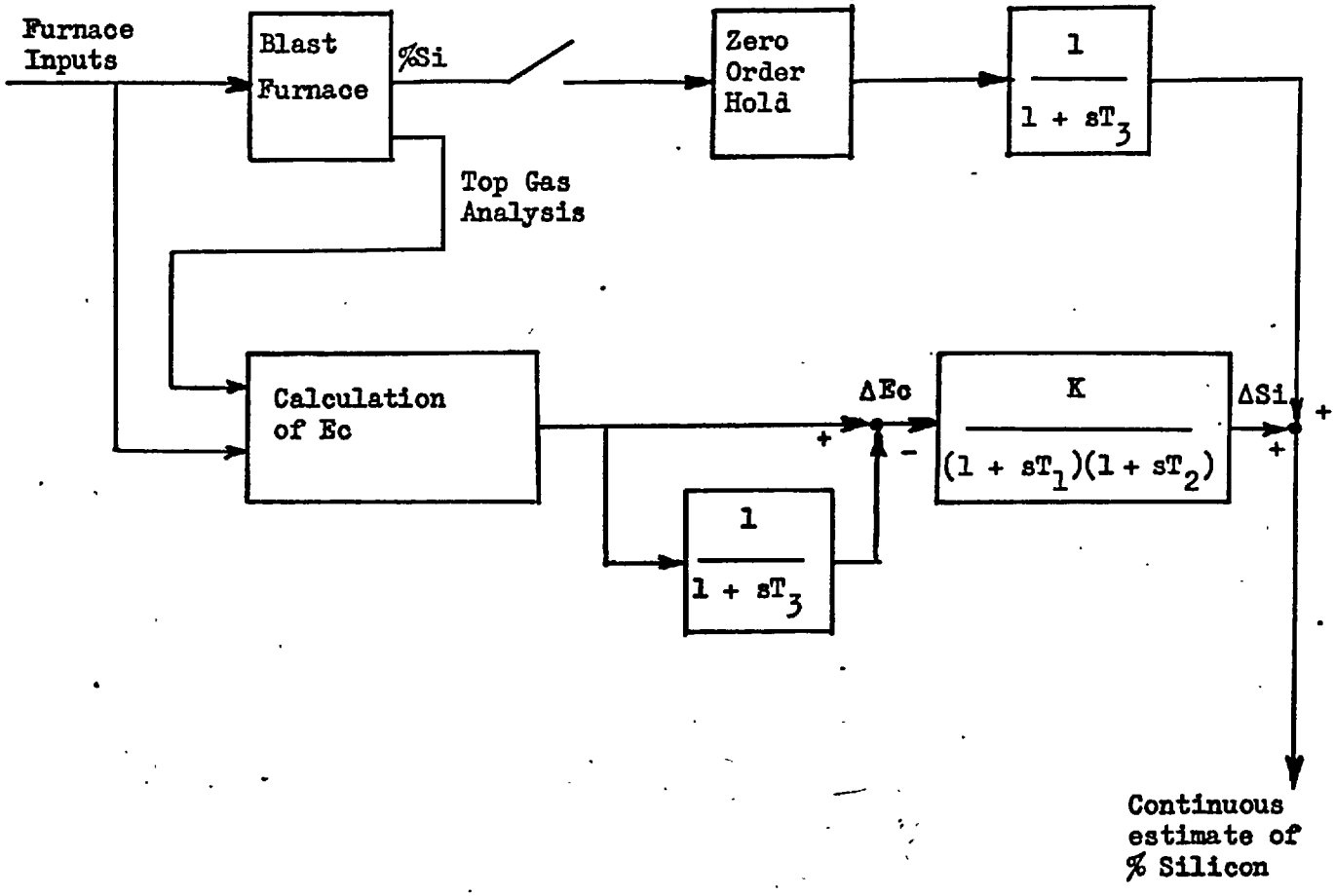


Fig. 2.2 Vidal's System for Estimating % Silicon

where α, β , $a_1 - a_7$ are constants, A(t) is a term resembling Wu and including production rate, S_v, b, C, Mn, S, P are the calculated slag weight, basicity, C/Fe ratio, Mn/Fe ratio, S/Fe ratio and P/Fe ratio, respectively, all delayed by 6.8 hours.

The Silicon prediction equation, therefore, takes the form

$$Si(t) = \frac{\alpha}{\alpha + \beta\Delta t} Si(t-\Delta t) + \frac{\Delta t}{\alpha + \beta\Delta t} Q(t)$$

and explains 60% of the natural variation in % Silicon.

In concluding this section it must be noted that it is difficult to measure and compare the improvements in control claimed at different iron works because of variations in operating practice, in the type of inputs available and in the disturbance levels. The amount of variation that can be explained in the silicon content is more meaningful and gives some indication of the relative merits of the various systems.

2.2 Off-line process simulation

The models so far discussed deal almost entirely with input/output relationships and offer little information about the process itself. To gain such information it is necessary to write and solve the differential equations applying to an incremental volume in the furnace. This approach, however, produces many difficulties. For example, partial differential equations must be solved during transient operation, boundary conditions are given at both the top and bottom of the furnace, and our knowledge and ability to describe mathematically the kinetic and thermodynamic phenomena involved leave much to be desired.

However, considerable progress has been made on the calculation of longitudinal distributions of process variables (Ref. 19, 20, 21, 22 and 23), particularly for steady state conditions.

These models normally involve many complicated equations and so here the discussion concentrates on the fundamental approach used to derive the differential equations and the method of solution. Koump et al. (Ref. 21) and Muchi (Ref. 19) treat the furnace as a one dimensional counter current reactor with heat and material transfer between the streams. A set of simultaneous ordinary differential equations covering steady state operation are derived from first principles and a numerical solution obtained using the Runge Kutta method as modified by Gill, with boundary conditions specified at the furnace top. Okabe (Ref. 22) uses an analogue computer to find the solution. A typical equation is

$$\frac{dx}{dz} = \frac{22.4\ A\ R}{F}$$

where R = reaction speed of $Fe_2O_3 + 3CO \rightleftharpoons 2Fe + 3CO_2$

x = molar fraction of CO in bulk of gas

F = Vol. rate of flow of gas

A = Area of reactor

z = Longitudinal co-ordinate

The following phenomena are considered by Muchi:-

Indirect reduction by CO: $Fe_2O_3 + 3CO \rightleftharpoons 2Fe + 3CO_2$

Carbon solution loss: $C + CO_2 \rightleftharpoons 2CO$

Direct reduction by solid carbon: $FeO + C \rightarrow Fe + CO$

Decomposition of limestone: $CaCO_3 \rightarrow CaO + CO_2$

Reaction between carbon and steam: $H_2O + C \rightarrow H_2 + CO$

Reduction of silica in slag: $SiO_2 + 2C \rightarrow Si + 2CO$

Water gas shift reaction: $H_2O + C \rightleftharpoons H_2 + CO$

Heat transfer between gas and solids (using the theory of packed beds)

Each reaction is considered in great detail and its speed is calculated after consideration of gas film diffusion, intraparticle diffusion and speed of chemical reaction, and requires a knowledge of gas analysis, pressure and temperature, solid temperature and mean size, and many constants.

The integration procedure requires that boundary conditions are given at one point - two point boundary problems generally call for iteration. Koump avoids this by assuming a knowledge of top gas temperature, analysis and flow. Muchi neatly solves the problem for steady states by using overall heat and mass balances to transform the boundary conditions at tuyere level into ones at the furnace top.

Typical longitudinal distributions are shown in Fig. 2.3.

Lahiri and Seshadri (Ref. 24) take this approach a stage further by defining both radial and axial co-ordinates; the associated partial differential equations are solved using a backward finite difference method from boundary conditions given at the furnace top.

St. Clair (Ref. 25) develops a numerical simulation of a much simplified version of the process (Fig. 2.4). The complete reaction for producing one mole of Fe in the Reducing Zone is

$$gCO + ZC + FeO_{3/2} \rightarrow Fe + (g - 3/2 + 2Z)CO + (3/2 - Z)\ CO_2$$

where g = moles of CO/mole Fe entering Reduction Zone

Z = moles of C reacting with CO_2 per mole Fe

The Reduction Zone is divided into N reactors of varying sizes such that 1/N moles of $FeO_{3/2}$ are reduced in each. Consider reactors 1 through j. The composition of solids entering this region is j/N moles of $FeO_{3/2}$, (1-j/N) moles of Fe and (g + Zj) moles of C, and that of gas leaving the region is ($g - 3j/2N + 2Z_j$) moles of CO, ($3j/2N - Z_j$) moles of CO_2 and 1.88 g moles of N2. Hence, if Z_j

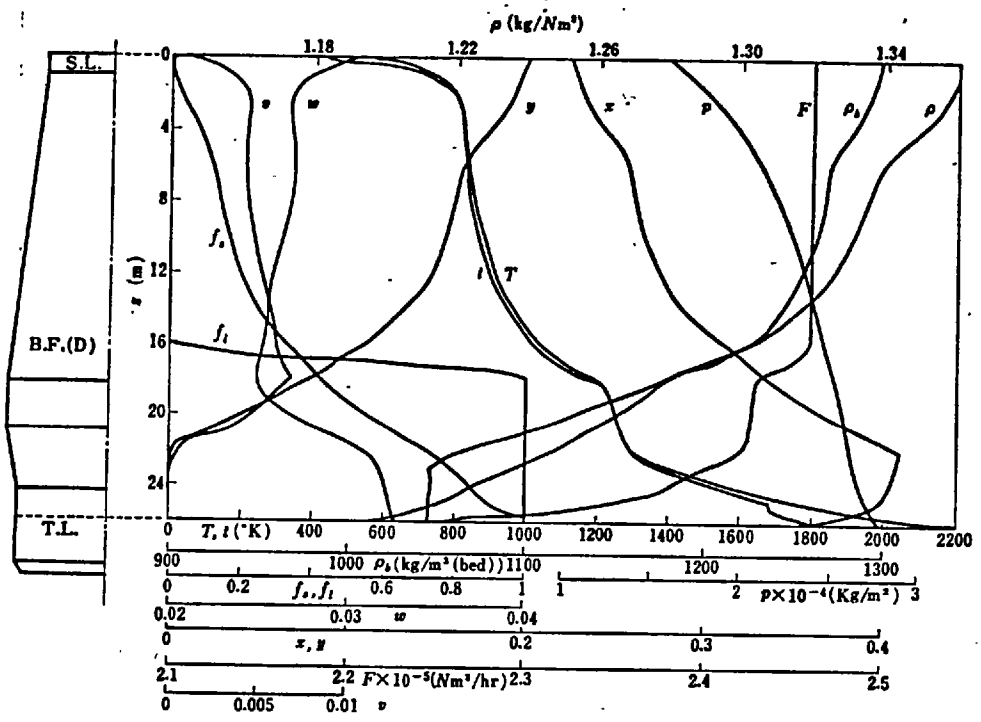


Fig. 2.3 Analytical results obtained by I. Muchi (Ref. 18)

Symbols

f_l	fractional decomposition of limestone	y	molar fraction of CO_2
f_s	fractional decomposition of iron ore	x	molar fraction of CO
v	molar fraction of H_2O	p	gas pressure
w	molar fraction of H_2	ρ_b	bulk density of solids
T	gas temperature	ρ	density of gas
t	solid temperature		

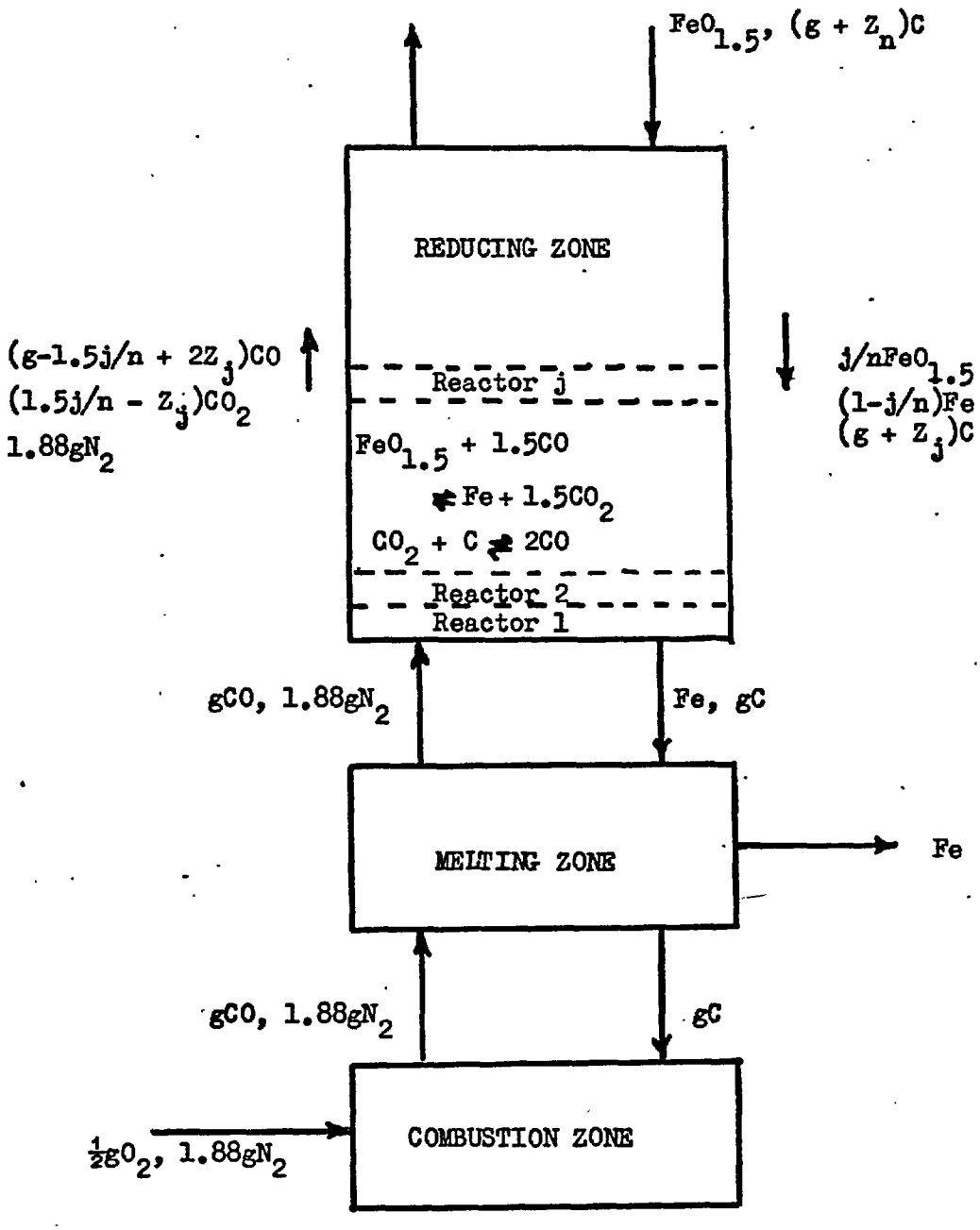


Fig. 2.4 The simplified process studied by St. Clair

Symbols

g	moles of CO entering per mole/Fe
Z_j	moles of carbon reacting with CO_2 per mole of Fe in reactors 1 to j
n	number of reactors

can be calculated for j = 1 - N, then the longitudinal distribution of CO and CO_2 are also known.

The reaction occurring within the region j = 1 - N is

$$gCO + Z_j C + \frac{j}{N} FeO_{3/2} \rightarrow \frac{j}{N} Fe + (2Z_j - \frac{3j}{2N} + g)CO + (\frac{3j}{2N} - Z_j)\ CO_2$$

and the heat of reaction is

$$\Delta H = 41.22\ Z_j + 3.05\ j/N$$

Now if M moles of iron/min are to be produced, then for reactor j the following typical reaction rate equations give

$$\frac{M}{N} = a_1\ Fe_j\ \Phi_1(CO_j,\ CO_{2j})$$

$$(Z_j - Z_{j-1})M = a_2\ Fe_j\ (g + Z_j)\ \Phi_2\ (CO_{2j})$$

where Fe_j = moles of iron in reactor j

a_1 and a_2 = rate and equilibrium coefficients

and Φ_1 & Φ_2 are known functions.

The longitudinal distributions of CO and CO_2 are known in terms of Z_j and so the combination of these two equations eliminates Fe_j and results in a difference equation for Z_j.

To initiate the procedure values must be known for the initial reactor temperatures and the production index i.e. the amount of iron produced by 1 unit of blast for the period to be simulated. The calculation then proceeds from the boundary condition at j = o up through the reducing zone giving Z_j and points on the longitudinal distributions of variables at each stage. Having found the amount of reaction in each of the reactors, heat balances are used to calculate the new gas temperatures and the rate of accumulation of heat in the solids. Finally, the reactor temperatures after Δt mins are calculated, the time increased by Δt and the whole

process repeated to form the simulation. This simulation, unlike other models in this section is valid under certain transient conditions (e.g. changes in blast temperature) but it is not clear whether the technique can be extended to include the highly endothermic and temperature dependent hearth reactions without introducing further iteration.

In the preceding models the treatment of reaction speeds has engulfed much detail. Flierman and Van Langen (Ref. 26) were the first to suggest simplified rate equations, and provided a steady state solution using incremental balances.

Consider the movement of burden from level b to level a (Fig. 2.5). A heat balance gives

$$Wm(t_a - t_b) + VQ\tau = Wg\,(T_a - T_b)$$

$$Wg(T_a - T_b) = \alpha\tau\left(\frac{T_a + T_b}{2} - \frac{t_a + t_b}{2}\right)$$

and a typical materials balance gives

$$Fe_3O_{4a} = Fe_3O_{4b} - V\tau$$

The reaction speed is approximated by $V = a(CO - KCO_2)^{\Phi}(T_a, T_b)$ and a and K are parameters found by laboratory experiments.

The path of a typical burden unit is calculated from tuyere level back up through the furnace. From a knowledge of the blast volume required to reduce each burden unit, boundary conditions at tuyere level are established. Then knowing the materials at level a, t_a and T_a, and fixing t_b, the equations can be solved for τ (the holding time), T_b and the composition of material at level b using an iterative procedure. These values are then used as initial conditions for the next level, the procedure continuing until a solid temperature of 25°C is reached. Various constants are then

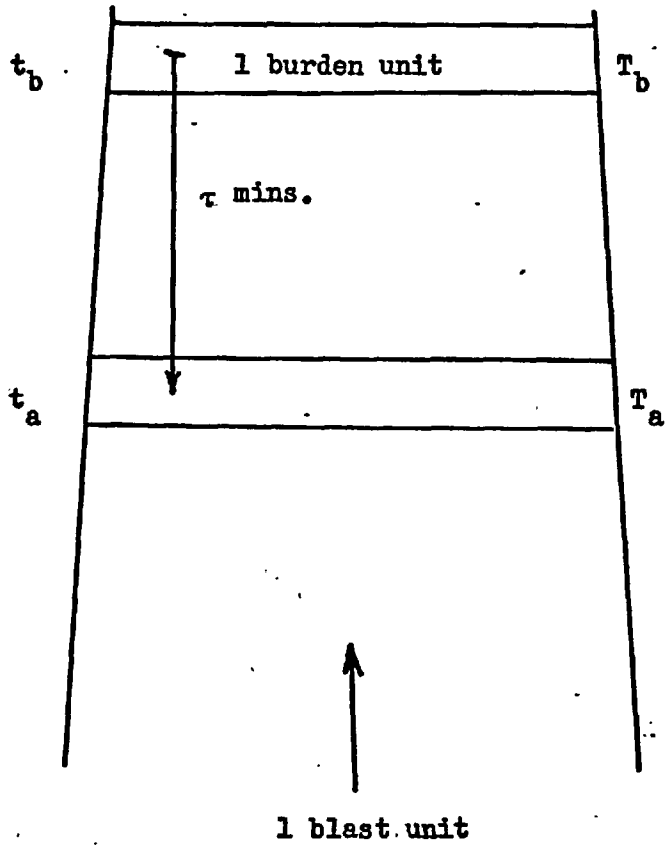


Fig. 2.5 Schematic Representation of Burden Descent

Symbols

t	solid temperature
T	gas temperature
W_m	water equivalent of solids
W_g	water equivalent of gas
α	heat transfer coefficient
τ	transport time
V	reaction speed
Q	heat of reaction

1 burden unit	the amount of ore and coke from which 1 kgm of iron can be produced
1 blast unit	amount of wind required to produce 1 kgm of iron

adjusted and the procedure repeated until the composition of the burden unit agrees with that of the initial charge.

This method has been used successfully to investigate the effects of higher blast temperatures and changes in the type of ores charged on the steady state. If this method is extended so that each burden unit is tracked rather than a typical unit then transient conditions could also be simulated. However, the number of iterations may now be prohibitive.

Tsuchiya and Mori (Ref. 27) have rearranged the classical balance techniques discussed in 2.1.5 to form a simulation which treats transient conditions as a succession of steady states. The important point here is that top gas temperature and analysis are taken as inputs for the simulation.

In order to by-pass the need to consider reaction kinetics, the furnace is divided into five successive stages such that each reaction continues to completion at each stage. For example;

Stage 1 material pre-heat occurs

Stage 2 all Fe_2O_3 reacts to Fe_3O_4

Stage 3 all Fe_3O_4 reacts to FeO

Stage 4 all FeO reacts to Fe, carbon solution loss occurs

Stage 5 complete combustion occurs

Using the top gas analysis, overall balances for CO and CO_2 fix the amount of carbon solution loss, individual materials balances give (for the steady state) the amount of material flowing from stage to stage and an energy balance gives its temperature. Certain additional assumptions have to be introduced to ensure a unique solution.

In testing the simulation with plant data the temperature of material leaving stage 5 has been shown to correlate well with the plant silicon percentage - this reinforces the successful results claimed for the balance methods of 2.1.5.

In concluding this section it can be said that researchers have put a great deal of work into establishing simulations of the process and in particular several configurations have been suggested upon which to quantify the process. Namely: zones of fixed volume, zones in which a given amount of reduction occurs or zones in which the temperature changes by a given amount. However, the iron production per unit of blast or the top gas analysis - unknowns during transient operation following for example a change in the coke rate - are usually assumed to be known. This forms a serious limitation on the use of simulation for an investigation of furnace dynamics and prompts the conclusion that none of the simulation techniques discussed are at present developed sufficiently to simulate transient operation of the complete process, a necessity if process control is to be the objective.

CHAPTER 3

The development of a dynamic model.

In Chapter 2, two distinct types of model evolve, one involving regression formulae relating measured plant variables and possibly their past values to a particular output. The other involving the numerical solution of a set of either ordinary or partial differential equations. From the control point of view the regression approach presents few difficulties as far as the implementation of a feedback controller is concerned. However, the approach almost invariably assumes steady (or near steady) conditions and some degree of over simplification of the dynamics about this state. Thus, particular care must be taken to establish the range of operation over which the model is valid.

The more formal solution of the differential equations offers detailed information about the state of the process itself and will allow operators to follow and predict the evolution of knowndisturbances as they pass through the furnace. This should, of course, promote a greater understanding of the process and thus improve manual control. The extreme and wide ranging conditions under which a large scale metallurgical process such as the blast furnace operates make the precise description of the process needed for this approach difficult to formulate and has in the work described in Chapter 2 lead to complicated equations containing many unknown quantities. In this chapter this problem is re-examined and the equations taylored to suit the control application.

Having developed such a simulation of the process, one is still faced with the problem of designing the associated controller. The

equations become difficult to use directly for controller design but do give considerable insight into control problems. In principle, modern optimal control techniques can be applied, but because partial differential equations are involved their application is by no means straightforward and is likely to lead to considerable numerical difficulty. This problem is examined in detail in Chapter 5.

In many cases the more theoretically detailed the model is, the more rapidly the law of diminishing returns applies, and so a compromise approach seems logical. Here a model is proposed in which the differential equation formulation is retained, and the kinetic and thermodynamic phenomena describing the process (that is the forcing terms) are considerably simplified. One notes that for steady conditions the characteristics of the longitudinal distributions of Figs. 3.2 and 3.3 would be reproduced fairly accurately by considering the furnace in three zones and using first order ordinary differential equations with linear forcing terms - the calculated distributions would then consist of three exponential curves. If a fundamental parameter of the process such as the pressure distribution or the size of materials charged changes then the coefficients in the forcing terms may need modification.

In practice, however, such a drastic linearisation is unnecessary. The fundamentals of Chemical Engineering and researchs into the blast furnace process yield the type of rate equations to be used and suggest where non-linearities such as temperature effects or the effect of basicity should be included.

3.1 The form of the equations

The derivation of the partial differential equations describing a counter-current reactor with heat and mass transfers between the

streams can be found in Chemical Engineering texts. However, in order to establish clearly the underlying assumptions the derivation for a unidimensional system is given in Appendix 1. The system of equations relating the concentration of materials and their temperatures to space and time are:-

$$\frac{\partial c_i}{\partial t} + \frac{\partial}{\partial x}(V_x c_i) = G_i \quad \text{for } i = 1 \ldots m$$

$$W_s \left(\frac{\partial T_s}{\partial t} + V_x \frac{\partial T_s}{\partial x}\right) = G_{H_s}$$

$$W_g \left(\frac{\partial T_g}{\partial t} + V_x \frac{\partial T_g}{\partial x}\right) = G_{H_g}$$

where c_i = the concentration of the i^{th} chemical element, these being for solids

Fe O C H_2O SiO_2 MnO P_2O_5 Si Mn P Al_2O_3 CaO S $CaCO_3$ MgO

and for gases

CO CO_2 N_2 O_2 H_2 H_2O

m = the total number of chemical elements considered

t = time

x = distance from the stockline

G_i = rate of generation of the i^{th} element

V_x = velocity of gas or solids as appropriate

W = water equivalent per unit volume

T = temperature

G_H = rate of generation of heat

The subscripts s and g refer to solids and gas.

Notable omissions from the above system are equations determining the gas and solid velocities from considerations of continuity. These equations are particularly complex and demand an understanding of many factors.

For example, the voidage, the pressure distribution within the gas stream, the changes in volume of burden materials as they are heated and reduced, and the behaviour of liquids in the furnace hearth. It is expedient, therefore, at this stage to assume that these are known functions of x and t. The problem of estimating these velocities in an on-line environment is considered in detail in Chapter 4.

The boundary conditions are as follows:-

(1) $c_i(x,o)$ is given for $o \leq x \leq h$ and $i = 1 \ldots m$

(2) $T_s(x,o)$ and $T_g(x,o)$ are given for $o \leq x \leq h$

(3) $T_s(o,t)$ and $T_g(h,t)$ are given for $t > o$

(4) $c_i(x,t)$ is given for $t > o$ at either $x = o$ or $x = h$ as appropriate and $i = 1 \ldots m$

(1) and (2) refer to the initial furnace state and (3) and (4) refer to the composition of gas and solid at tuyere and stockline levels respectively.

The problem is then to find a solution of this system of equations subject to the mixed boundary conditions.

3.2 The chemical and thermodynamic forcing functions

Before considering possible methods of solution, the process and its equations must be defined more precisely. Throughout the discussion reference is made to five regions (Fig. 3.1).

(1) Stack region.

(2) Upper Bosh region.

(3) Lower Bosh region.

(4) Tuyere region.

(5) Hearth region.

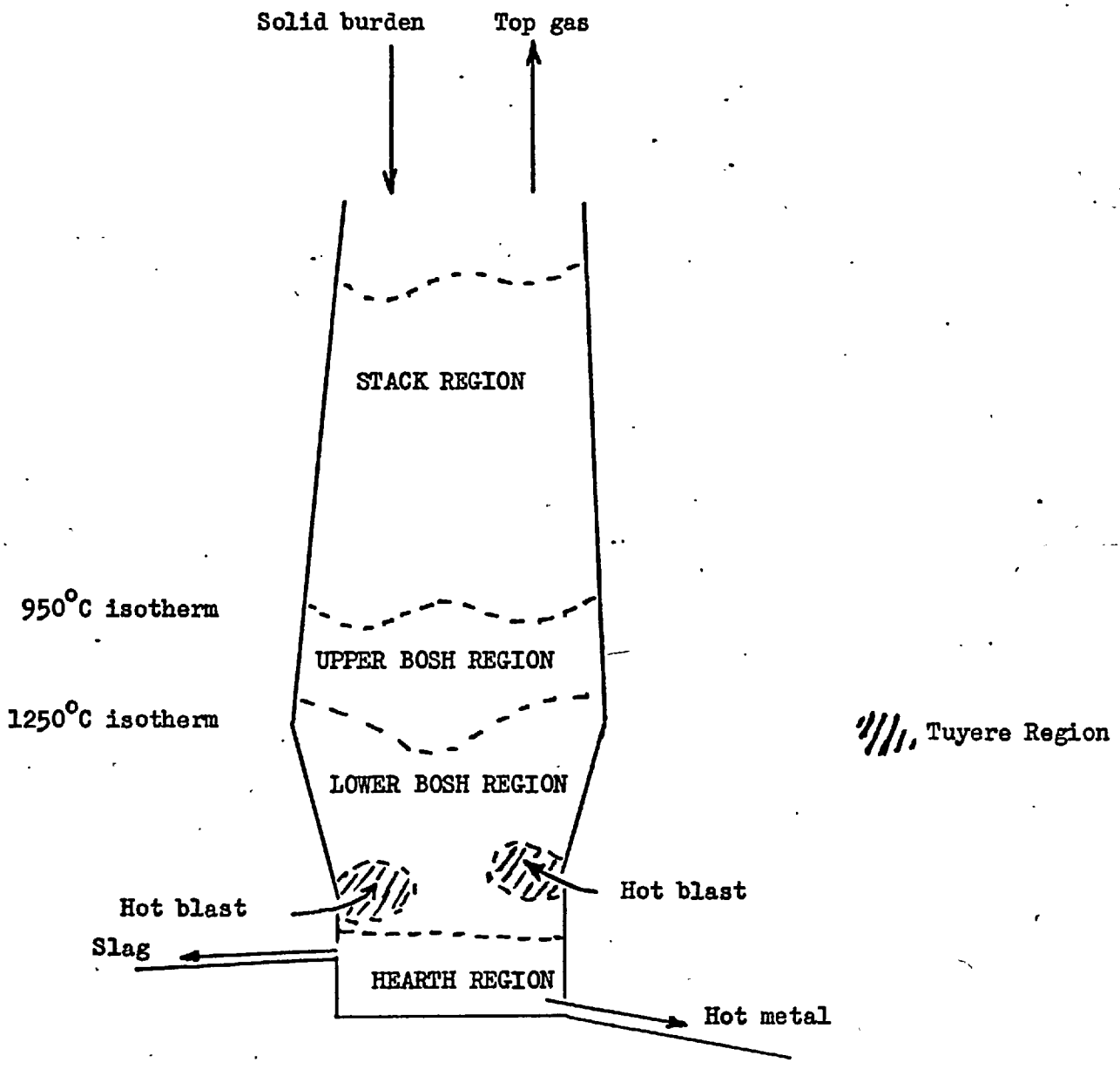


Fig. 3.1 The Chemical Sub-division of the Furnace

The process chemistry is to date not completely understood and is still the subject of research. Current theory does, however, suggest the major functions in these regions.

A very large number of functions are involved and their selection and parameterisation is non-trivial. In what follows the basic considerations used to determine these functions are outlined and invoke basic theory, experimental results and physical argument.

3.2.1 Reduction of iron oxides

To produce iron from natural iron ores, oxygen must be removed. In the blast furnace about 30% of the total weight of oxygen is removed in the Stack and Upper Bosh regions. The major reduction sequence, termed as Indirect Reduction is thought to be as follows:-

Below 570°C

Hematite → Magnetite → Iron

Above 570°C

Hematite → Magnetite → Wustite → Iron

The reactions are:-

$$3Fe_2O_3 + CO \rightleftharpoons 2Fe_3O_4 + CO_2$$

$$Fe_3O_4 + CO \rightleftharpoons 3FeO + CO_2$$

$$Fe_3O_4 + 4CO \rightleftharpoons 3Fe + 4CO_2$$

$$FeO + CO \rightleftharpoons Fe + CO_2$$

Although these are consecutive steps in the reduction of iron oxides to metallic iron in the blast furnace the zones of occurrence of the various iron oxides overlap to a considerable extent. Theoretically this reduction sequence should begin as soon as the ore is charged to the furnace. In practice, however, the reactions are not significant until a temperature of about 400°C is reached and so the function of

the upper part of the Stack is simply to dry the charge.

At temperatures above 950°C, while the ore is still in a solid form, i.e. in the Upper Bosh region, the indirect reduction sequence continues at increasing rates. But the carbon dioxide formed is unstable in the presence of coke and so the highly endothermic reaction

$$CO_2 + C \rightarrow 2CO$$

termed as 'carbon solution loss', occurs, which regenerates reducing gas.

Pure iron melts at 1,537°C, but in the blast furnace this melting point is lowered to about 1,150°C, by the presence of elements such as silicon and lime. As the temperature of the solids approaches 1,150°C, a very viscous slag is formed, which coats the particles of ore and thus impedes the gaseous reduction reactions until, by the temperature of 1,250°C, they practically cease. From this point onwards, that is in the Lower Bosh region, the final reduction is achieved via direct contact with the coke. The reaction, termed Direct Reduction, is

$$FeO_{slag} + C_{coke} \rightarrow Fe_{hot\ metal} + CO$$

One effect of injecting fuel oil or steam into the hot blast is to produce hydrogen in the gas leaving the tuyere region. At temperatures above 820°C hydrogen is a more efficient reducing agent than carbon monoxide (Ref. 28) and so the following reductions are also possible:-

$$Fe_3O_4 + H_2 \rightleftharpoons 3FeO + H_2O$$

$$FeO + H_2 \rightleftharpoons Fe + H_2O$$

Some of the water vapour formed will react with carbon monoxide or in the Lower Bosh with carbon:-

$$H_2O + CO \rightarrow H_2 + CO_2$$

$$H_2O + C \rightarrow H_2 + CO$$

In developing the reaction rate equations for the reduction sequence described above, it is important to note that, from data describing only the hot blast and the top gas, one cannot differentiate between reduction by carbon monoxide and that by hydrogen with the appropriate regeneration. The full sequence of reactions can, therefore, be considered as follows:-

Stack Region:-	$Fe_xO_y + CO \rightarrow Fe_xO_{y-1} + CO_2$	(a) *
	$H_2 + CO_2 \rightarrow H_2O + CO$	(b)
Upper Bosh Region:-	$Fe_xO_y + CO \rightarrow Fe_xO_{y-1} + CO_2$	(c)
	$C + CO_2 \rightarrow 2CO$	(d)
	$H_2 + CO_2 \rightarrow H_2O + CO$	(e)
Lower Bosh Region:-	$Fe_xO_y + C \rightarrow Fe_xO_{y-1} + CO$	(f)
	$H_2 + CO \rightarrow H_2O + C$	(g)

where hydrogen has a catalytic effect in reactions (a) and (c).

The concentration of iron oxides is large when compared with those of the gaseous components and so the indirect reduction reactions, via either carbon monoxide or hydrogen (a) and (c), are considered as pseudo first order opposing reactions. The rate equation takes the form:-

$$-\frac{dFe_xO_y}{dt} = a_1 (CO - K_1 CO_2) + a_2 (H_2 - K_2 H_2O)$$

where a_1, K_1, a_2 and K_2 are factors which depend on the temperature and the particular oxide level concerned. Values for the various equilibria can be found in Ref. 29 and take the form:-

* This includes reduction by both hydrogen and carbon monoxide

$$Ln(K_1) = 3580/T - 4.6$$

for the Fe_3O_4/FeO equilibrium.

The results of Schurman (Ref. 30) using vertical probes to measure the gas composition profiles, suggest possible simplifications. Consider an equation of the form:-

$$-\frac{dFe_xO_y}{dt} = a\,(CO - KCO_2)$$

where a = constant (to be identified from top gas data)

K = CO/CO_2 ratio of top gas

Integrating this over the Stack region an expression for the carbon monoxide profile can be found:-

$$CO(x) = \left\{CO(o) - \frac{K}{1+K}\,B\right\} \exp\left(-\frac{a}{v}(1+K)\,x\right) + \frac{K}{1+K}\,B$$

where a = constant

v = gas velocity

x = height in Stack above the 950°C isotherm

B = $\%CO + \%CO_2$, a constant for the Stack region

Using the top gas analysis from Schurman's curve to evaluate a,

$$CO(x) = 15 \exp\,(-0.205x) + 25$$

is the solution given the assumed rate equation; values calculated using this equation are shown together with measured values in Fig. 3.2. The calculated CO and CO_2 values display a close fit to the experimental curves, and suggest that this simplified approach gives a satisfactory description of the indirect reduction sequence under these particular conditions.

However, as conditions in the Stack change so the constants (and thus the top gas analysis) must also change. The equation can be extended to cover variations in the heat level of the Stack and Upper Bosh regions by introducing the Arrhenius effect, and changes in the amount of hydrogen in the gas:-

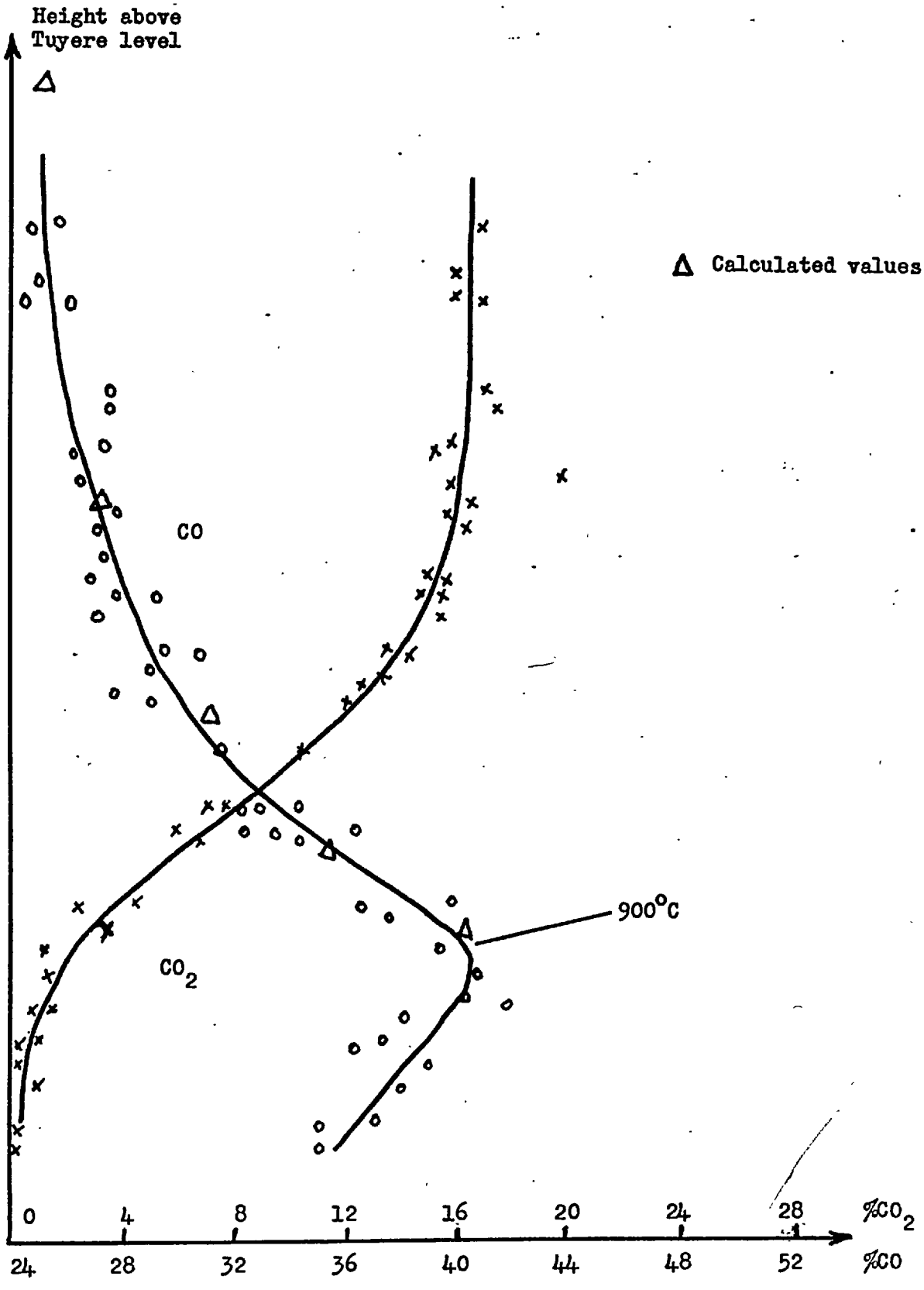


Fig. 3.2 Composition profiles as measured by E. Schurman

$$-\frac{dFe_xO_y}{dt} = a(1+ g_1H_2)\,(CO - KCO_2)\exp(-E/RT)$$

where a = rate constant (evaluated from top gas data)

K = $\%\,CO/\%CO_2$ in top gas

E, g_1, R = constants

T = temperature ^oK

The laboratory results of Flierman and Van Langen (Ref. 26) make it possible to extend this equation to the lower oxide levels of the Upper Bosh region. They evaluate the relative dependence of a and K on the oxygen/iron ratio of the ore. An advantage with this simplification is that the use of the O/Fe ratio averts the need to tract individual oxide levels.

Flierman (Ref. 26) also develops an equation describing carbon solution loss (d) of the form:-

$$-\frac{dc}{dt} = K_m\, g_c\, [CO_2]$$

where K_m = the coke reactivity $Ncm^3/g.sec.$

g_c = wt. of carbon

$[CO_2]$ = concentration of CO_2 $Mols/Ncm^3$

K_m is corrected for variations in temperature by the Arrhenius term:

$$K_m = g \exp(-E/RT)$$

where g, E and R are constants.

To describe direct reduction, (f), one can assume that the rate at which the iron oxide in the primary slag is reduced is proportional to the area of contact between it and the coke. This in turn is proportional to the amount of oxide unreduced, and so the following equation suffices:-

$$-\frac{dFeO}{dt} = g.O$$

where g = the rate constant

O = the weight of unreduced oxide

The shape of the hydrogen distribution has again been measured using vertical probes (Ref. 30) and is shown in fig. 3.3. This is assumed to remain unchanged and can be approximated by three linear sections; the gradients indicate the relative proportions of reactions (b), (e) and (g). Further examination of these results shows that 80% of the regeneration occurs in the Lower Bosh region and 20% in the Upper Bosh and Stack regions.

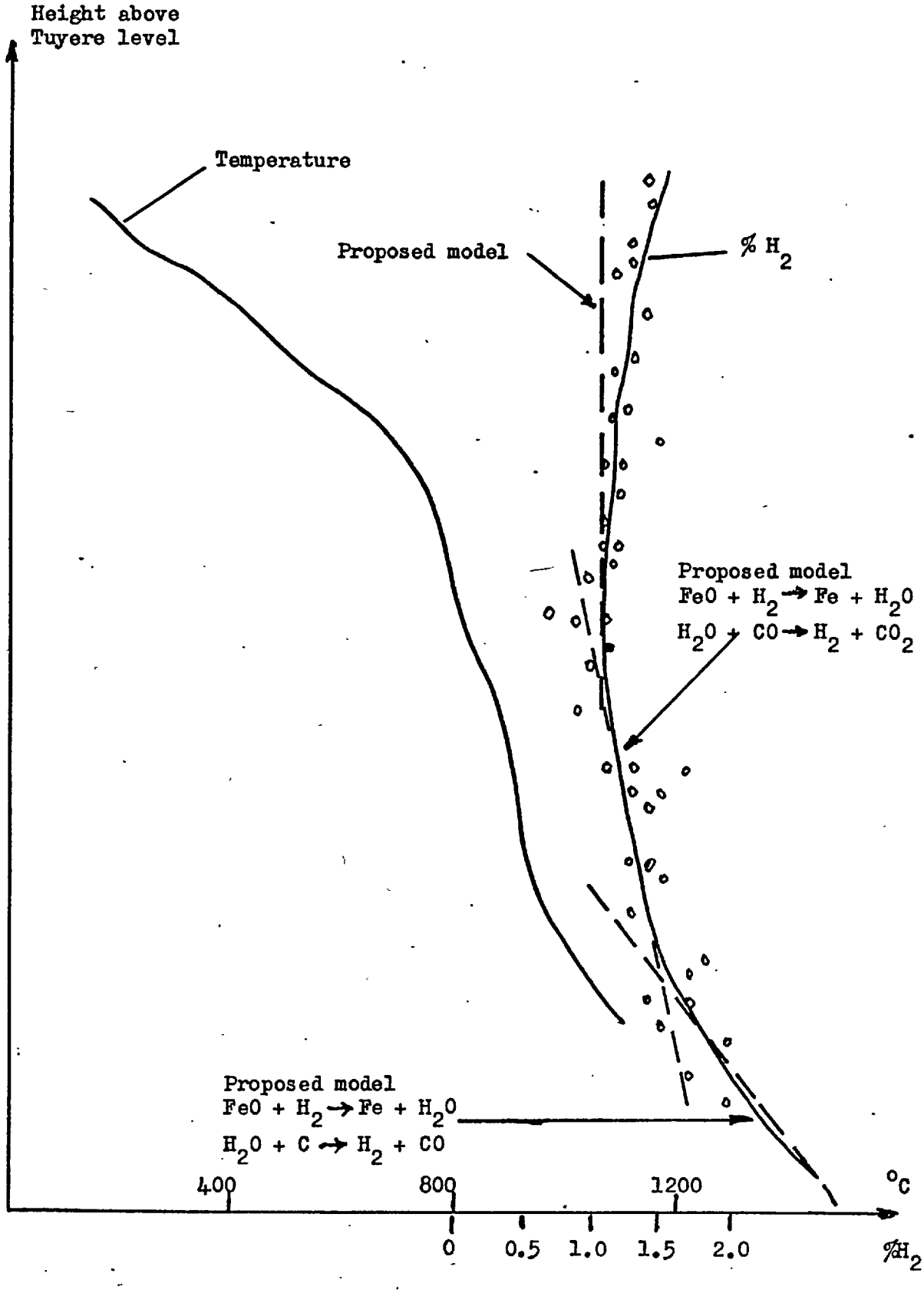
To calculate the total amount of these reactions (b, e and g) use is made of the hydrogen utilisation factor, i.e. the ratio of the difference in the hydrogen input and output levels to the input level. This factor can be calculated continuously from blast and top gas data, and can, therefore, be used as an input to the model in its online environment. Furnace data spanning one weeks operation shows that the hydrogen utilisation factor has mean of 33% and a standard deviation of 7%.

3.2.2 Reduction of Metalloids

The hot metal produced in a blast furnace is not pure iron but a metal almost saturated with carbon and containing various trace elements such as silicon, manganese, phosphorus and sulphur. Little is known, either from the theoretical or experimental viewpoints, about the reduction mechanisms involved. Several theories have been proposed, but have yet to be substantiated with experimental results. The theory examined by Bodsworth (Ref. 31) serves as an outline of the problem.

The reduction of metalloids is split into three distinct processes:-

Fig. 3.3 Composition profiles as measured by E. Schurman



(1) The transfer of elements into the hot metal as the droplets of metal and slag pass through the bed of coke in the Lower Bosh region.

(2) Further transfers of elements into the metal as it descends through the slag bath in the Hearth region.

(3) Partitioning of the solute elements between the hot metal and slag in the Hearth region.

Measurements taken from the experimental furnace in Liege (Ref. 32) generally support this approach and show that about 80% of the silication, carburisation and manganese transfer occur prior to the tuyere level and that all of the phosphorus is absorbed into the metal by this level. The reactions taking place are:-

$$SiO_2 + 2C \rightarrow Si + 2CO$$

$$MnO + C \rightarrow Mn + CO$$

$$P_2O_5 + 5C \rightarrow 2P + 5CO$$

The rate constants for these reactions are small while the iron is solid and so the reactions can be considered to start as the primary slag is formed.

It is assumed that the transfer of silicon can be described by an equation of the classical form

$$\frac{dSi}{dt} = g\,(N_{SiO_2} - K\,N_{Si})\ \exp\ (-E/RT)$$

where g, E, R = constants

N_{SiO_2}, N_{Si} = mole fractions of silica and silicon.

T = temperature (^oK)

The classical equilibrium constant K' is defined and tabulated as

$$K' = \frac{a_{Si} (P_{CO})^2}{a_{SiO_2} (a_C)^2}$$

where a_{SiO_2} a_{Si} a_C = activities of silica, silicon and carbon

P_{CO} = partial pressure of CO

In the Bosh region $P_{CO} = 1 + 0.85 \times P_B$

where P_B = Blast pressure

K can be related to K' as follows:-

$$K = \frac{\gamma_{Si} P_{CO}^2}{\gamma_{SiO_2} (a_C)^2} K'$$

where γ_{Si}, γ_{SiO_2} = activity coefficients for silica and silicon.

Taylor (Ref. 33) gives data regarding K', γ_{Si}, γ_{SiO_2} and a_C from which the following are fitted:-

$$\log_{10} K' = - 28634/T + 16.28$$

$$\log_{10} \frac{N_{Si}\gamma_{Si}}{\%Si} = 0.08 (\%P + \%Si) + 0.25\%C - 0.05$$

$$\log_{10} N_{SiO_2} \gamma_{SiO_2} = (.001 \frac{R + .13}{150}) (1400 - T) - .00025R - .0026$$

where $R = \%CaO + \frac{1}{2}\%Al_2O_3 + \frac{1}{3}\%MgO - \%SiO_2$

$$\log_{10} \frac{a_C}{\%C} = 0.17 \%C - 0.07 \%Si - 0.06$$

The importance of silicon lies in its relation to furnace control. Manganese, phosphorus, carbon and sulphur on the other hand, are included simply to complete the thermal and material balances for the Lower Bosh and Hearth regions. Thus a considerably simplified approach is acceptable for such elements.

Transfer of manganese is described by

$$\frac{dMn}{dt} = g(N_{MnO} - K N_{Mn})$$

where $\log_{10} K = 15020/T - 8.884$

g = rate constant

The reduction of phosphorus pentoxide is by direct contact and is assumed to be proportional to the amount of unreduced oxide

$$\therefore \frac{dP}{dt} = (1 - h K) P_2O_5$$

where h = height above the tuyere level

K = rate constant

P_2O_5 = the amount of unreduced oxide.

The major part of the sulphur present in the coke is released in the Tuyere region during combustion, in gaseous form i.e. S_2, COS, S, CS_2, H_2S and SH. As these gases counterflow with the molten materials the sulphur is absorbed by the hot metal. Samples of molten materials at the Tuyere level have a high sulphur content in relation to the cast metal, Ref. 32, and so suggest that the majority of the desulphurisation occurs while the metal is accumulating in the Hearth region. The reaction mechanism is discussed in Ref. 34, where the following is suggested:-

$$CaO + FeS \rightarrow CaS + FeO$$

$$FeO + C \rightarrow Fe + CO$$

$$FeO + \tfrac{1}{2}Si \rightarrow Fe + \tfrac{1}{2}SiO_2$$

Using equations fitted to data in Ref. 34

$$\frac{dFeS}{dt} = g\,(\%S_{slag} - K\,\%S_{metal})$$

where g is a rate constant and

$$\text{Ln } K = \text{Ln } CaO + c_1Si + c_2Mn + c_3SiO_2 + c_4Al_2O_3 + c_5MgO + c_6$$

The equations describing carburisation are somewhat different. The column of coke - sometimes referred to as the coke reserve - extends through the slag layer and probably to the bottom of the furnace. Metal awaiting tapping in the Hearth region, being in

contact with this coke becomes saturated with carbon. The final carbon content of the hot metal can be determined from a solubility equation. Turkdogan (Ref. 35) gives the following

$$\log_{10} (N_c + .84\, N_p + .71\, N_{Si} - .01\, N_{Mn} + N_S) = -.375 - 560/T$$

where N_c, N_p, N_{Si}, N_{Mn}, N_S = respective mole fractions

T = temperature ^oK

These mole fractions are dependent on the %C in the hot metal and so an iterative method is used, at each cast, to determine the carbon content of the metal.

3.2.3 Heat Transfer

The heat transfer mechanisms governing flows of heat between the gas and solid streams and within the solid stream are assumed to be convection and conduction respectively, and so the following equations apply

$$H_1 = a\,\alpha(T_g - T_S)$$

$$H_2 = -\beta \frac{dT}{dx}$$

where H_1 = heat flow from gas to solids K cals/m^3s

H_2 = heat flow within the solids K cals/m^2s

a = effective area for convection/unit volume

α = heat transfer coefficient K cals/$m^2 s\,^oC$

β = thermal conductivity K cals/m^2s (^oC/m)

3.2.4 Reactions in the Tuyere region

Air at approximately 900^oC is blown into the furnace at the tuyeres. This immediately reacts with coke; the resulting combustion forming the main source of heat in the furnace. Firstly, the oxygen

combines with carbon i.e. $O_2 + C \rightarrow CO_2$

Moving away from the tuyeres the oxygen concentration decreases to the point when the carbon dioxide reacts to form carbon monoxide.

$$CO_2 + C \rightarrow 2CO$$

These effects are shown in Fig. 3.4.

The air injected at the tuyeres normally contains varying amounts of fuel oil and steam, and can be enriched with oxygen. These additions react as follows:-

$$H_2O + C \rightarrow H_2 + CO$$

$$(nC + H_2) + \frac{n}{2} O_2 \rightarrow H_2 + nCO$$

where n is the carbon/hydrogen ratio of the fuel oil. These reactions are complete and so the analysis and temperature of gas leaving this region can be found via material and heat balances.

3.2.5 Heat and Material balances

In 3.1 the general form of the differential equations is established and in 3.2 rate equations describing the various mechanisms are derived. The differential equations for the process can now be assembled using heat and materials balances to give the driving functions in the general equations.

The equation relating gas temperature in the Lower Bosh region to space and time is discussed as an example. The basic equation is

$$W_g \left(\frac{\partial T_g}{\partial t} + V_x \frac{\partial T_g}{\partial x}\right) = G_{H_g}$$

where c_i = concentration of i^{th} component in gas

S_i = specific heat of i^{th} component

V_x = component of gas velocity in the x direction

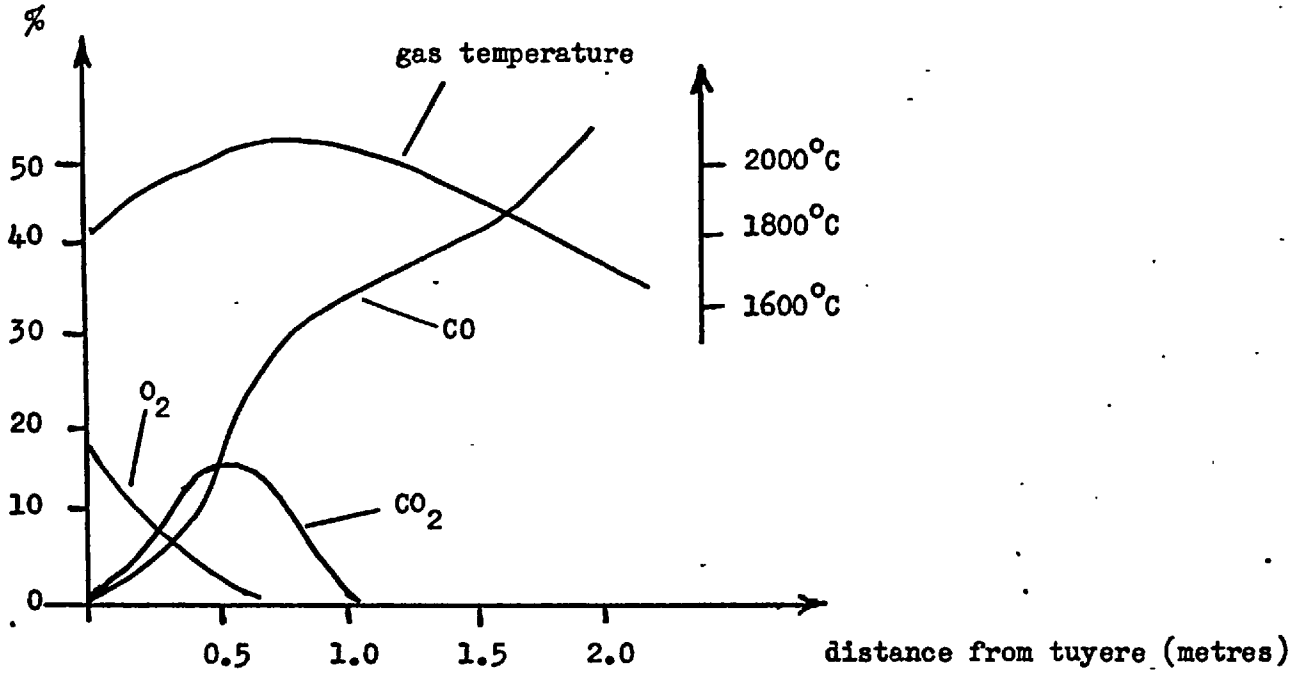


Fig. 3.4 The gas composition and temperature distribution in the tuyere region (Ref. 28)

T_g = gas temperature

G_{H_g} = amount of heat generated in the gas per unit vol. per sec.

$W_g = \Sigma S_i c_i$

A heat balance gives

$$(\Sigma S_i c_i)\left(\frac{\partial T_g}{\partial t} + v_x \frac{\partial T_g}{\partial x}\right) = -H_l - h_{Mn}\frac{dMn}{dt} - h_{Si}\frac{dSi}{dt} - h_p\frac{dP}{dt} - h_{DR}\frac{dFeO}{dt} - HL - HS$$

where H_l, $\frac{dMn}{dt}$, $\frac{dSi}{dt}$, $\frac{dP}{dt}$, $\frac{dFeO}{dt}$ are defined in 3.2 and

HL = heat loss per unit vol. per sec.

HS = heat loss due to changes of state

h_{Mn}, h_{Si}, h_p, h_{DR} = heats of reactions

Earlier, the use of oxygen/iron ratio was proposed to avoid calculation of the reactions at each oxide level. Here the need to calculate the water equivalent W_s for the solids arises. This involves a knowledge of the oxide levels and so an assumption of binary mixtures is made, which makes it possible to calculate the constituent oxide levels from the overall oxygen/ iron ratio. An example is shown in fig. 3.5.

The differential equations relating to each of the 21 elements can be established in this way.

3.3 A numerical solution

The initial ideas behind this simulation are discussed in Ref. 36 and were based more on intuition than on rigorous analysis. The burden was divided into a number of horizontal slices about 1 metre thick, with a stepwise approximation to the counter current motion. To avoid the small step length associated with the high

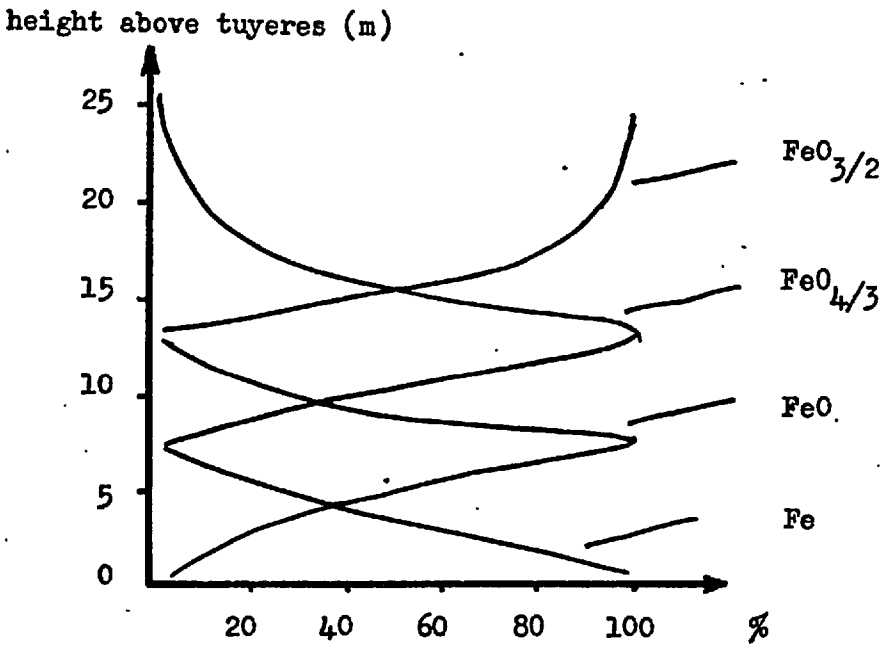


Fig. 3.5 Oxide levels given a binary mix

gas velocity - the gas residence time in each slice is approximately 0.2 secs. - a trial gas slice was tracked through the furnace and the result used to make a time increment of 1 minute in the burden state vector.

To investigate this type of numerical solution further and to seek the most efficient implementation and maximum step length, the method is now put on a more rigorous mathematical basis.

In sections 3.1 and 3.2 the equations relating the concentration of materials and their temperatures to space and time are developed and are summarised here:-

$$\frac{\partial c_i}{\partial t} + \frac{\partial}{\partial x}(V_x c_i) = G_i \qquad i = 1 \ldots m \tag{1}$$

$$W_s \left(\frac{\partial T_s}{\partial t} + V_x \frac{\partial T_s}{\partial x}\right) = G_{H_s}$$

$$W_g \left(\frac{\partial T_g}{\partial t} + V_x \frac{\partial T_g}{\partial x}\right) = G_{H_g}$$

with boundary conditions as follows:-

(i) $c_i(x,o)$ is given for $o \leq x \leq h$ $\quad i = 1 \ldots m$

(ii) $T_s(x,o)$ and $T_g(x,o)$ are given for $o \leq x \leq h$

(iii) $T_s(o,t)$ and $T_g(h,t)$ are given for $t > o$

(iv) $c_i(x,t)$ is given for $t > o$ at either $x = o$ or $x = h$ as appropriate

The first step in the development of the numerical solution is to assume that the gas and solid velocities are known functions of x and t. The system then reduces to

$$\frac{\partial c_i}{\partial t} + V_x \frac{\partial c_i}{\partial x} = G_i - c_i \frac{\partial V_x}{\partial x} \tag{2}$$

$$\frac{\partial T_s}{\partial t} + V_x \frac{\partial T_s}{\partial x} = G_{H_s} / W_s$$

$$\frac{\partial T_g}{\partial t} + V_x \frac{\partial T_g}{\partial x} = G_{H_g} / W_g$$

and can be classified as 'semi-linear'. This suggests a method based on 'characteristics'.

Consider the fundamental differential relations

$$dc_i = \frac{\partial c_i}{\partial t}\, dt + \frac{\partial c_i}{\partial x}\, dx$$

Comparison with (2) shows that if the increments dx and dt are chosen so that

$$\frac{dt}{1} = \frac{dx}{V_x} \tag{3}$$

then

$$\frac{dc_i}{G_i - c_i \frac{\partial V_x}{\partial x}} = \frac{dt}{1} = \frac{dx}{V_x} \tag{4}$$

Now (3) can be identified with the ordinary differential equation

$$\frac{dx}{dt} = V_x$$

and so, subject to the restrictions placed on V_x by the requirements of the existence theorm for such equations, there will be a unique solution passing through any point $P(x_o,t_o)$; this solution is termed a characteristic curve of system (1) and on such a curve

$$\frac{dc_i}{dt} = V_x \frac{dc_i}{dx} = G_i - c_i \frac{\partial V_x}{\partial x} \qquad i = 1 \ldots m$$

$$\frac{dT_s}{dt} = V_x \frac{dT_s}{dx} = G_{H_s} / W_s \tag{5}$$

$$\frac{dT_g}{dt} = V_x \frac{dT_g}{dx} = G_{H_g} / W_g$$

The boundary conditions suggest that these equations are considered in two sets:-

(5a) those equations relating to gases

(5b) those equations relating to solids

For system (5a) the characteristic curves are given by

$$\frac{dx}{dt} = V_{x_g}$$

and for system (5b)

$$\frac{dx}{dt} = V_{x_s}$$

In practice little is known about the variation of gas and solid velocities with height in the furnace, and so these are assumed to be constant. In an on-line environment these constants may be estimated from the stock line velocity and the blast volume. However, in the short term the characteristic curves are sets of parallel lines (Fig. 3.6.)

On a gas characteristic

$$\frac{dc_i^g}{dt} = G_i - c_i \frac{\partial V_{x_g}}{\partial x} = G_i^1 \quad (\vec{c}^g, \vec{c}^s)$$

Expanding the function G^1 in terms of values for solid concentrations on the initial line one has

$$\frac{dc_i^g}{dt} = G_i^1 \left\{ \vec{c}^g (P), \vec{c}^s (P^1) \right\} + \sum_j \frac{\partial G_i^1}{\partial c_j^s} \, dc_j^s + \ldots$$

$$= G_{i_{pp^1}}^1 + \sum_j \frac{\partial G_i^1}{\partial c_j^s} \, G_j^1 \, \Delta t + \ldots$$

where $G_{i_{pp^1}}^1$ is evaluated using solid concentrations at point P^1 (i.e. $\vec{c}^s (P^1)$) and gas concentrations at point P (i.e. $\vec{c}^g (P)$). Thus, if Δt is chosen such that $\left| G_j^1 \, \Delta t \right|$ is small then

$$\frac{dc_i^g}{dt} = G_{i_{pp^1}}^1 (1 + E_i) \tag{6}$$

where

$$E_i \approx \frac{1}{G_{i_{pp^1}}^1} \sum_j \frac{\partial G_i^1}{\partial c_j^s} \, G_j^1 \, \Delta t$$

Consider next the equation, dropping the E_i component

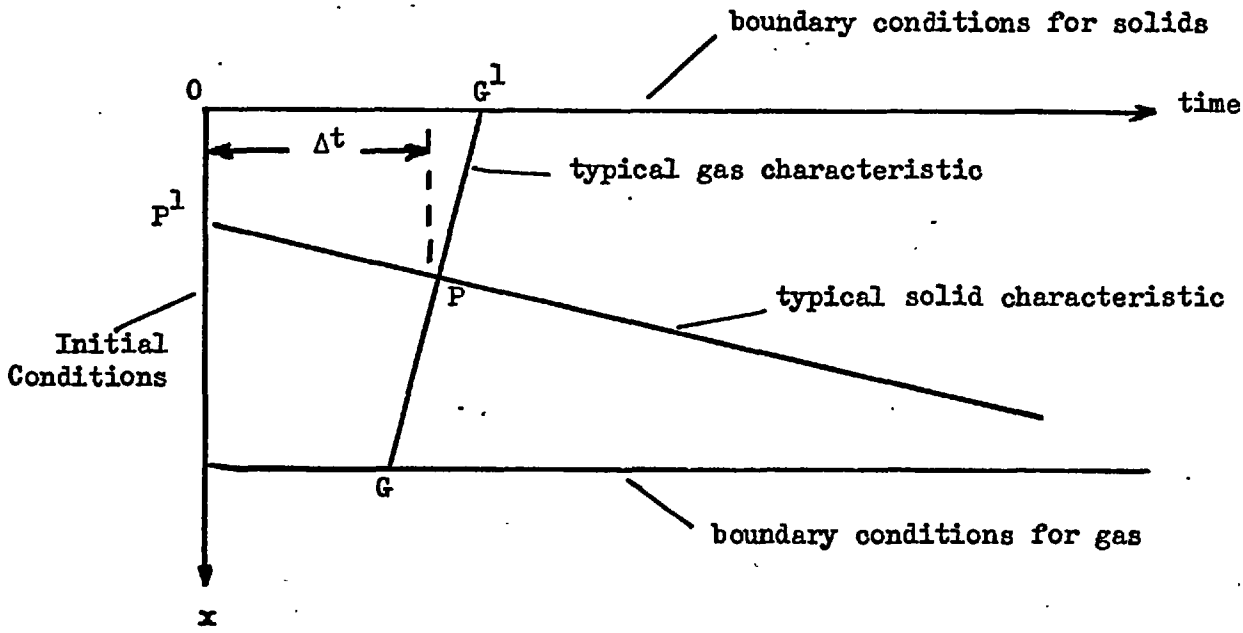


Fig. 3.6 The characteristic curves for the system of equations (4)

$$\frac{dc_i^{g*}}{dt} = G_{i_{pp}}{}^{l}$$

This equation can be integrated along the typical gas characteristic GG^l under marching conditions from the point G, using one of the many finite difference methods. In this case the forward Euler Method was chosen because firstly it is the most simple and secondly the truncation error can be kept under control by using a small step length.

Now integrating (6) yields

$$c_i^g \leq (1 + E_i max)\int_{t_o}^{t} G_{i_{pp}}{}^{l} dt$$

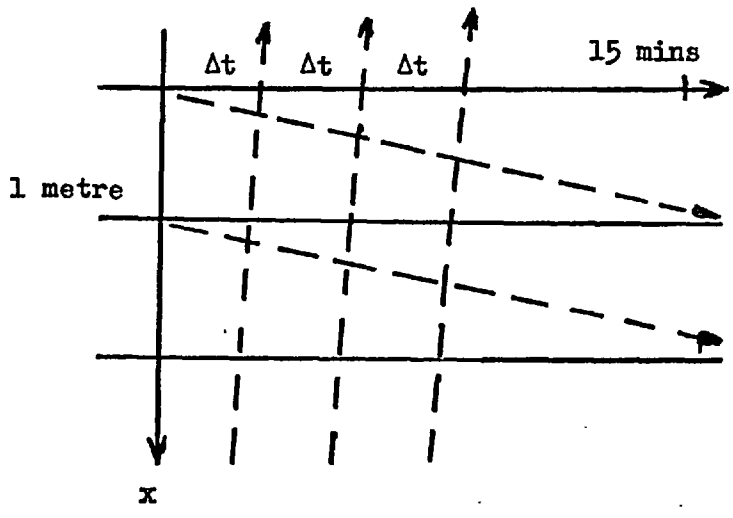
where $E_i max = \max E_i$ for points on GG^l

$$\therefore (c_i^g - c_i^{g*})/c_i^{g*} \leq E_i max$$

Thus if c_i^{g*} is used to estimate c_i^g, the % Error - introduced because values of $\vec{c}^s$ are taken at P^l and not from the gas characteristic concerned - is $100E_i$ max.

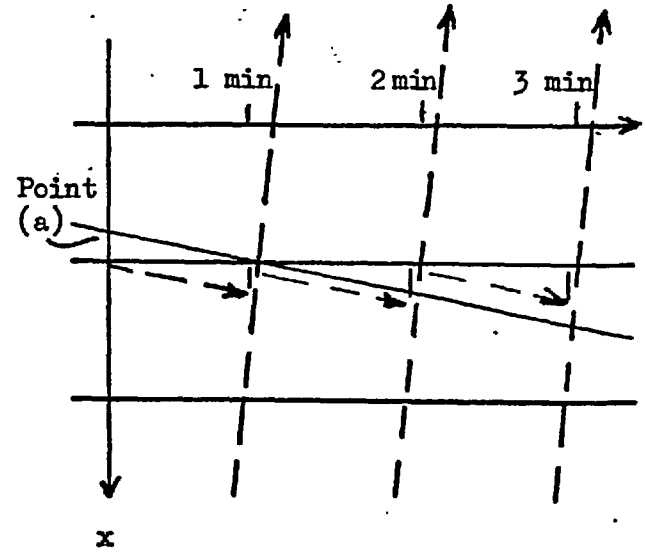
Examples of these calculations are given in Appendix 2.

Systems (5a) and (5b) have in effect been decoupled and so having calculated values for $\vec{c}^g$ on the gas characteristic these can be used together with $\vec{c}^s$ on the initial line to calculate the values of the gradient of $\vec{c}^s$ for subsequent use in the integration along the solid characteristics. Several techniques have been used to carry out this integration along the solid characteristics, the aim being to minimise the number of gradient calculations and to lengthen the time step that can be used for the solids before inaccuracy sets in. Schematic diagrams of several methods, showing the integration paths, make up fig. 3.7. Here the solid lines represent the mesh and the dotted lines the integration path along the characteristic curves.



$$c_i(x+\Delta x, t+\Delta t) = c_i(x,t) + G_i^1 \Delta t$$

Method 1



$$c_i(x,t+1) = c_{i_{(a)}}(t) + G_{i_{(a)}}^1$$

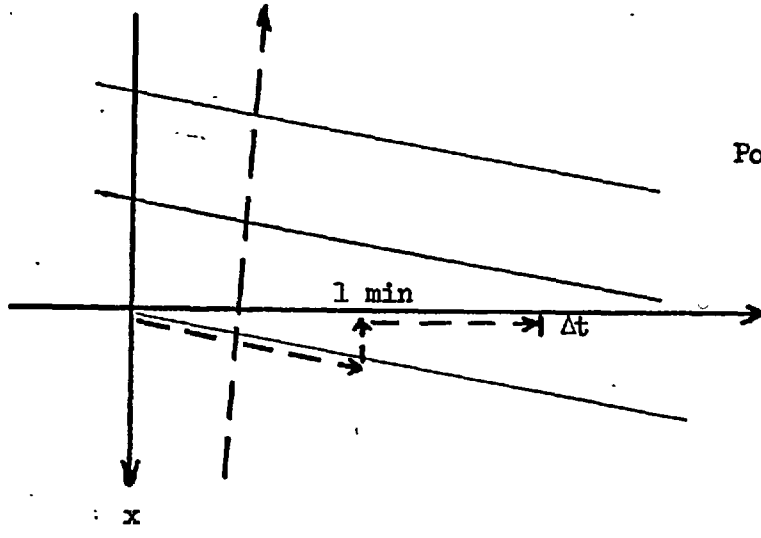
where

$$c_{i_{(a)}}(t) = (1-V)c_i(x,t) + Vc_i(x-\Delta x,t)$$

$$G_{i_{(a)}}^1 = (1-V)G_i^1(x,t) + VG_i^1(x-\Delta x,t)$$

Method 2

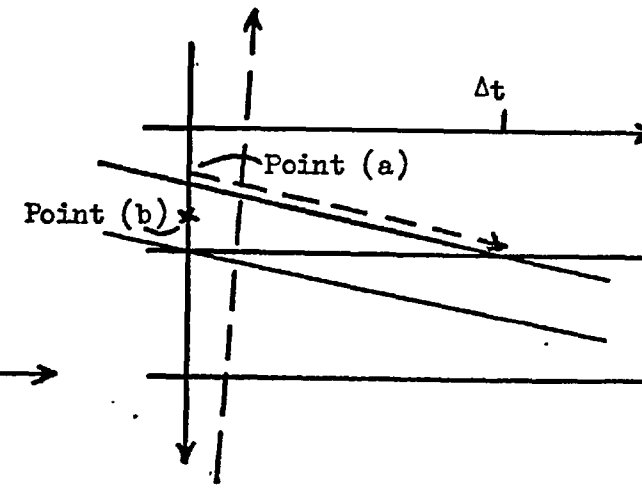
Fig. 3.7 Various Integration Procedures



$$c_i(t+\Delta t) = (1-\Delta t)c_i(t) + \Delta t c_i(t+1)$$

where $c_i(t+1)$ is given in Method 2

Method 3



Method 4

— — — — integration paths

The first method simply integrates along the initial gas characteristic and then down each solid characteristic - the maximum time step being $\Delta t = 1$ minute. Problems with this method are

(i) that the state vector can only be interrogated every fifteen minutes or so when the solid characteristics cut the original mesh,

(ii) that the initial gradients G_s^1 are not typical of those for following steps (even in steady conditions) and must, therefore, be recalculated for each step.

In the second method interpolation is used to establish the burden state vector at the mesh points after each step. Here experimentation using the initial gradients for consequent time steps shows that this can be done for 2 or 3 time steps without serious loss of accuracy.

In the third method the first one minute step to establish $\vec{c}_s\ (x, t + 1)$ for $x = 1\ 2\ \ldots$ is as in Method 2. Then linear interpolation is used to give $\vec{c}_s\ (x, t + \Delta t)$ as follows:-

$$\vec{c}_s\ (t + \Delta t) = (1 - \Delta t)\ \vec{c}_s\ (t) + \Delta t\ \vec{c}_s\ (t + 1)$$

The final method is the logical generalisation of the above. Here the first step is the integration along the initial gas characteristic followed by the calculation of the gradient vector $\vec{G}_s^1$ at the initial mesh points. Linear interpolation is then used to establish the solid state vector and the gradient vector at points (a) and (b) respectively. Finally integration along the solid characteristic from (a) on to the mesh point proceeds in a single step. The formulae are as follows:-

$$c_i\ (x, t + \Delta t) = c_{i_{(a)}}\ (t) + d\ \Delta t$$

where

$$c_{i_{(a)}}(t) = (1 - v\,\frac{\Delta t}{\Delta x})\,c_i(x,t) + v\,\frac{\Delta t}{\Delta x}\,c_i(x - \Delta x, t)$$

$$d = (1 - \lambda v\,\frac{\Delta t}{\Delta x})\;G_i^1(x,t) + \lambda v\;\frac{\Delta t}{\Delta x}\;G_i^1(x - \Delta x, t)$$

Successive application of the above allows the complete solution of the original system to be generated. Trial calculations on a typical equation, say

$$\frac{dFeO}{dt} = K\;FeO$$

indicate that the last method is best in terms of accuracy and stability whilst also being straightforward to implement. In practice operation with $\lambda = \frac{1}{2}$ and $\Delta t = 3$ mins. has provided a successful simulation of transient operation.

When implementing the integration along the initial gas characteristic particular care must be taken on the boundaries between regions and when discontinuities such as melting occur. Generally these boundaries do not lie on mesh points and so linear interpolation has been used to include relative proportions of reactions from both regions. To increase the accuracy at these points the forward Euler method is replaced by a Predictor-Corrector method.

CHAPTER 4

Some simulation and trial results

In this chapter some comments are made on the more practical problems associated with setting up and running the proposed model for a particular furnace and practice. The results of both off-line and on-line modelling exercises are then presented and discussed.

As with other large industrial simulations the problem of parameter tuning arises and this is complicated if the model is non-linear in the parameters. To make progress here it is usually better to start by adjusting the parameters manually according to a logical assessment of steady state levels and having regard for the fundamentals of the process. When checking the dynamics of the model any misfit may well indicate that the form of the driving function is incorrect in addition to the parameters. An example is the silicon/steam injection response which is discussed later and highlights the need for an understanding of the plant behaviour.

4.1 The problem of initial parameter estimates

The model proposed in Chapter 3 takes the form of a simulation. Information regarding the burden, the blast and the burden descent rate is fed to the model (as boundary conditions) at regular intervals (Fig. 4.1), together with a set of thermodynamic and chemical parameters specifying the process. A convenient interval for these calculations is one large bell dump (approximately 6 minutes). The result is

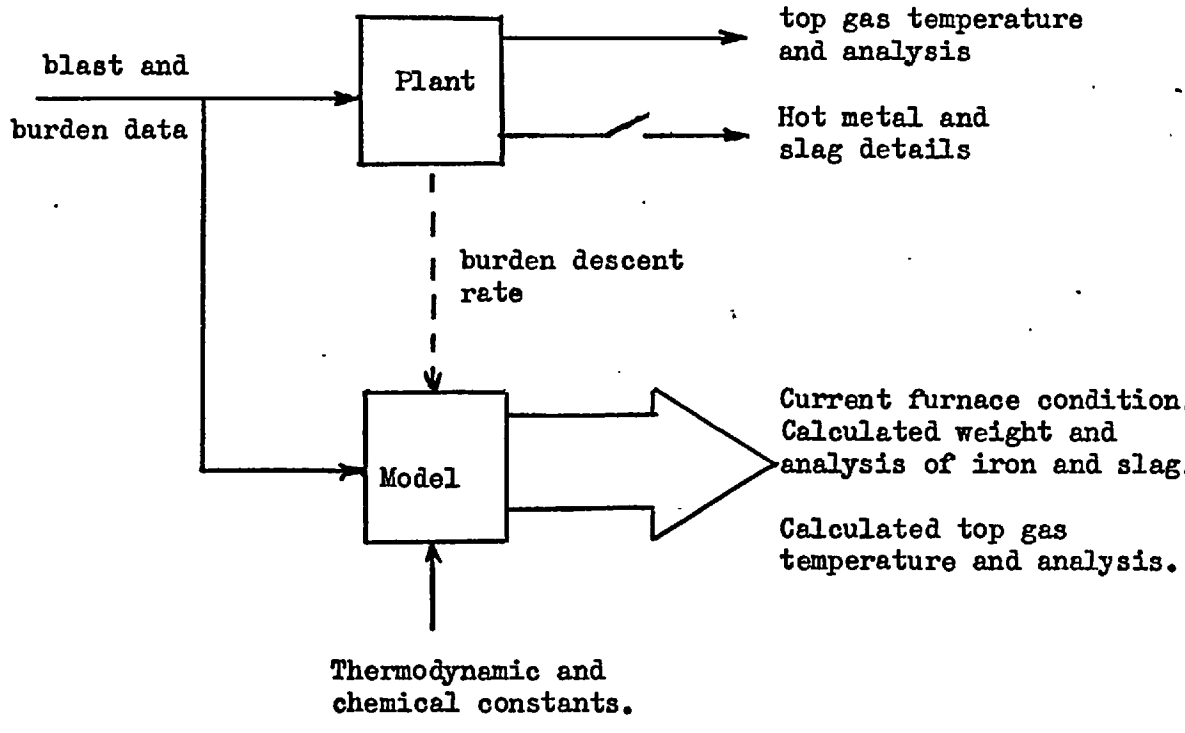


Fig. 4.1 The online simulation

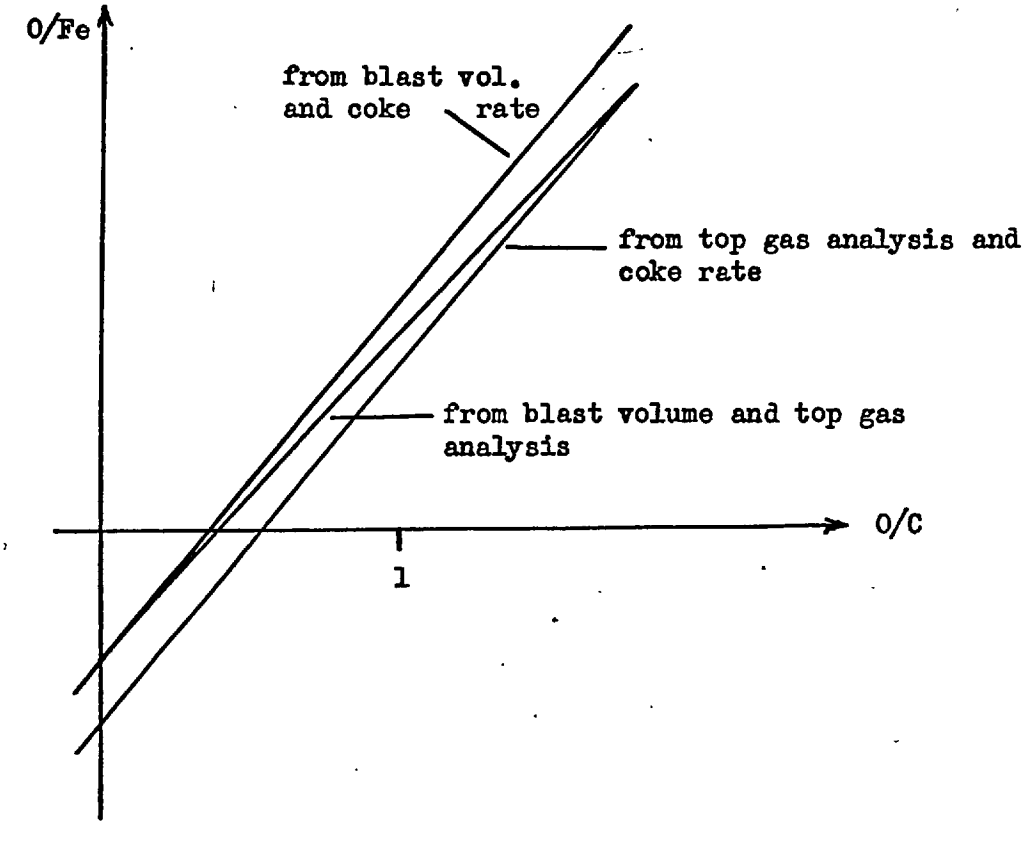


Fig. 4.3 Various 'operating' lines

(i) an up-to-date estimate of the composition and temperature of burden and gas throughout the furnace,

(ii) an estimate of the amount and analysis of hot metal and slag in the furnace hearth,

(iii) a calculated top gas analysis and temperature.

The kinetic constants depend on operating conditions and burden characteristics and, therefore, have to be estimated initially and then corrected during furnace operation. To keep the number of parameters requiring attention to a minimum a rather elementary analysis of the process chemistry was proposed in Chapter 3 and this introduces the following parameters:-

Reduction of iron ores

rate constants for indirect reduction (Stack and Upper Bosh)

equilibrium constant for indirect reduction

rate constant for carbon solution loss

rate constant for direct reduction

Heat transfer

solid/gas heat transfer coefficient

effective areas for heat transfer (Stack/Upper Bosh and Lower Bosh)

heat loss

Silicon

rate constant for $SiO_2 + 2C \rightarrow Si + 2CO$

Miscellaneous

rate and equilibrium constants for manganese reduction

Hearth heat loss

hydrogen utilisation

where the important constants as far as tuning the model to a particular practice is concerned are those in the first three groups.

Averaged plant input and output data can be used to provide the initial parameter values and for this a thorough understanding of the type of equation used to describe phenomena such as direct and indirect reduction or heat transfer is necessary. This is backed up by a set of parameter step responses (Figs. 4.2.1 - 5). Bearing in mind the general features of the composition profiles (from probe experiments), such as the s shaped temperature profile, the parameters are gradually tuned so that the temperature and analysis of hot metal, slag and top gas from the model agree with those from the plant. Of course, some of the parameters, such as the rate for carbon solution loss, affect the shape of the profiles but not the actual outputs and so the final estimates are not unique.

Before commencing the parameter fitting it is important to check that the data balances. That is for example, that the amount of carbon in the top gas plus that in the hot metal balances with the total amount charged. A useful check here is to draw the three 'Rist' operating lines (Chapter 2) by permutating blast volume, top gas analysis and coke rate (Fig. 4.3). The closeness of the three lines indicates whether or not the data balances.

A certain amount of trial and error is unavoidable in this procedure, but further reference to the parameter step responses, and the use of the operating line to assess the degree of misfit, suggests how this can be kept to a minimum. Consider each parameter step change in turn and its effect on the operating line.

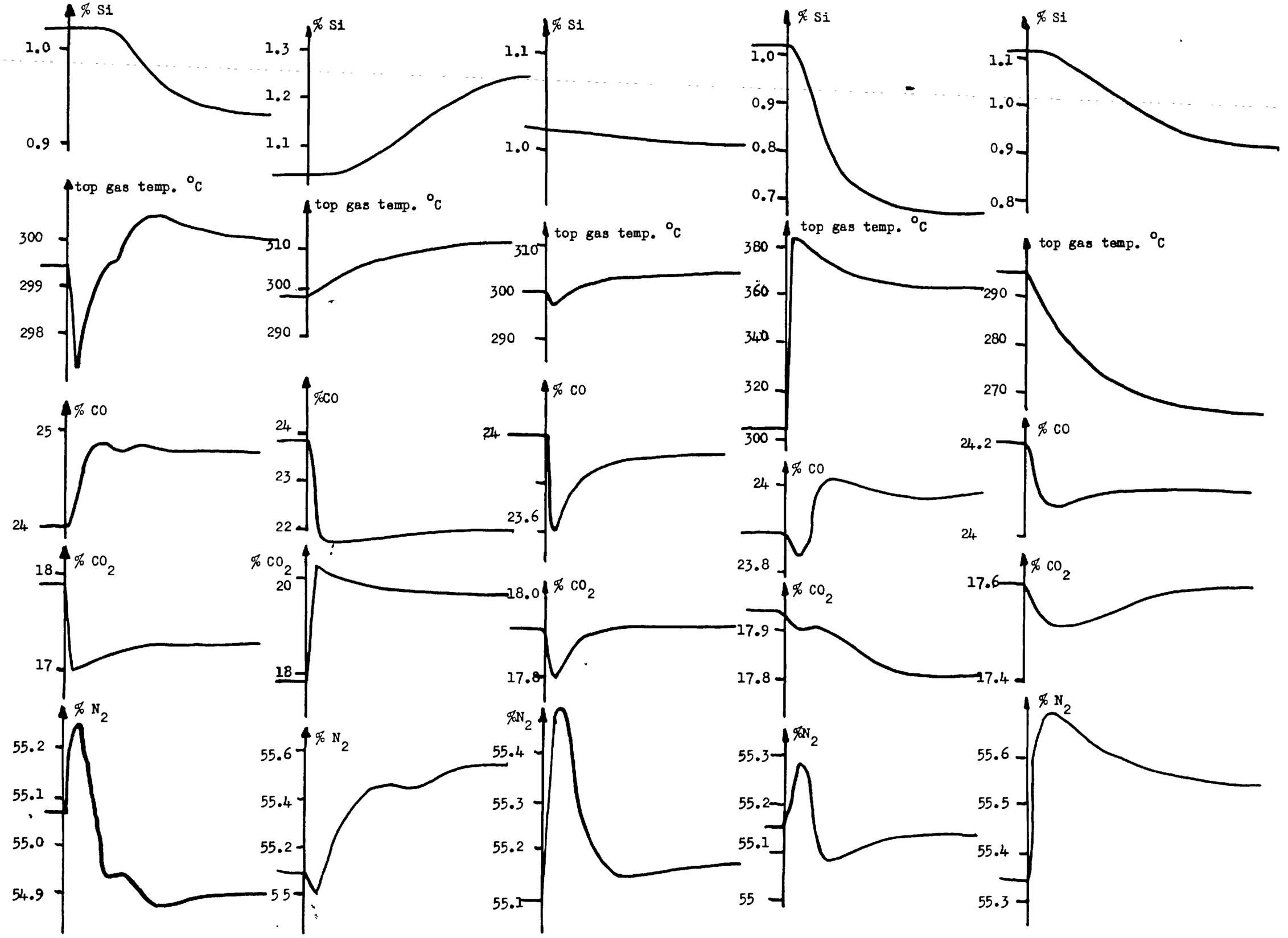


Fig. 4.2.1 30% drop in the IR. rate coefficient

Fig. 4.2.2 30% drop in the IR. equilibrium coefficient

Fig. 4.2.3 25% drop in the solution loss rate

Fig. 4.2.4 30% drop in the heat transfer coefficient

Fig. 4.2.5 0.3% increase in the heat loss coefficient

(i) the I.R. equilibrium constant, the I.R. rate constants and the D.R. rate constant simply vary the proportions of direct and indirect reduction. This represents a pivot of the operating line about the intercept A, (Fig. 4.4), the resulting variation in silicon only slightly affects this intercept,

(ii) the rate for carbon solution loss leaves the operating line unchanged,

(iii) parameters associated with heat transfer and the silicon rate only marginally affect the operating line; the intercept tends to move vertically in proportion to the silicon content whilst the upper end of the line remains practically unchanged. This results in a pivot about B in Fig. 4.4.

An example of this latter case is the increased heat loss. Initially the 1250°C isotherm moves towards tuyere level and the isothermal region contracts causing a severe drop in the amount of direct reduction, less reducing gas in the Stack and thus less indirect reduction, and explains the rise in % N_2. Then as the comparatively unreduced ore reaches the Lower Bosh the amount of direct reduction increases and the balance tends to be restored.

Bearing these points in mind parameter tuning can be resolved into four stages:-

Stage 1

Set the indirect reduction equilibrium constant K to the top gas CO/CO_2 ratio minus 0.1 and the hydrogen utilisation. This value

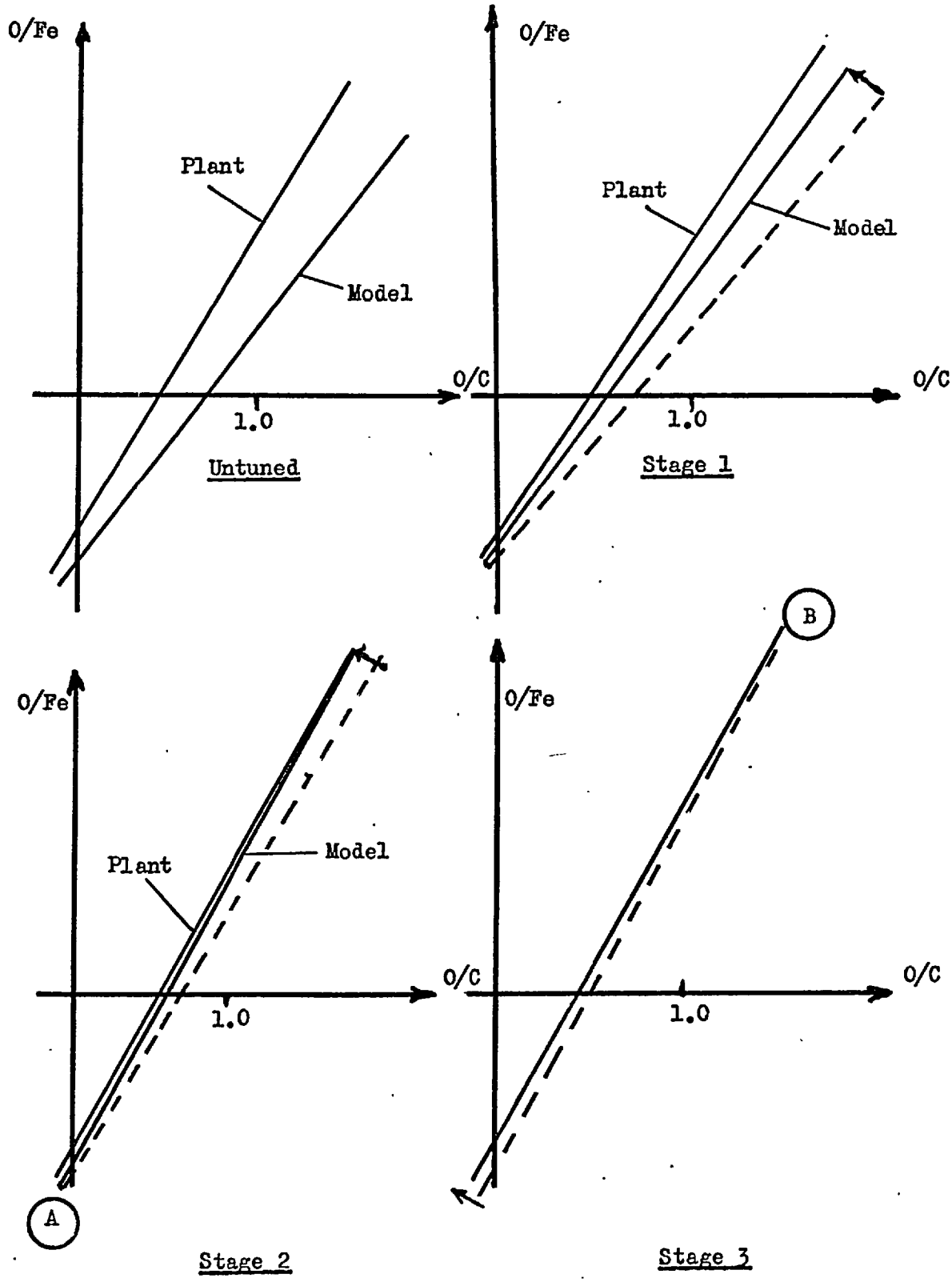


Fig. 4.4 Stages in tuning the parameters

for K ensures that the plant top gas is not beyond the equilibrium value and generally brings the computed and actual top gas analyses closer together.

Stage 2

Tune the model to have the correct O/C ratio for the top gas. Firstly, tune the rate for direct reduction to give the correct amount of FeO in the slag. Then use proportionate changes to the rate constants for indirect reduction.

Stage 3

Correct the top gas temperature. The choice between the heat loss or heat transfer parameters depends on the silicon level. If both the top gas temperature and the silicon level are high use the heat loss. Then correct the silicon level using the silicon rate constant.

Stage 4

Tune the miscellaneous parameters.

The effect of each stage on the plant and model operating lines is shown in Fig. 4.4. The application of these rules serves as a course tuning, and re-application of Stages 2 and 3 is generally required to correct any slight interaction.

Typical steady state results from the tuned model are shown in Table 3. The small differences between the top gas and slag analyses, and particularly $\%H_2$, %CaO, $\%Al_2O_3$ and % MgO, point to errors in the overall material balances. This is discussed further in Chapter 6.

TABLE 3

Measurement	Model Input	Model Calculation	Operational Data	Unit
Furnace Data				
Hearth diameter	6.096	-	6.096	m_3
Effective volume	727.78		727.78	m^3
Effective working height	19.66		19.66	m
Charge				
Sinter	74.3		74.3	%total burden
Scrap	17.0		17.0	%total burden
Carbonates	0.24		0.24	%total burden
Coke Ash	10.55		10.55	%total coke
Coke Carbon	83.58		83.58	%total coke
Burden charge rate	40.32		40.32	t/h
Coke charge rate	13.75		13.75	t/h
Coke consumption	547.5		547.5	kg/t pig iron
Blast				
Hot blast volume	37000		37000	m^3/h
Hot blast temp.	800		800	^oC
Hot blast moisture	4.74		4.74	g/m^3
Injected oil	0		0	g/m^3
Oxygen content	21		21	% total blast
Top Gas				
Temperature		216	192	^oC
CO_2		16.45	16.30	%total volume
CO		24.50	24.70	%total volume
H_2		1.07	1.00	%total volume
N_2		57.98	57.98	%total volume
Pig iron				
Temperature		1500	1450	^oC
Output		24.85	25.13	t/h
C		4.20	4.20	%total weight
S		0.042	0.042	%total weight
Mn		1.50	1.20	%total weight
Si		0.75	0.75	%total weight
P		0.30	0.31	%total weight
Slag				
Temperature		1525	1500	^oC
Volume		314.0	315.5	kg slag/t iron
FeO		0.36	0.40	%total weight
SiO_2		33.42	33.00	%total weight
Al_2O_3		16.60	17.22	%total weight
CaO		40.64	42.69	%total weight
MnO		1.71	1.07	%total weight
MgO		4.83	4.36	%total weight
S		1.08	1.07	%total weight

A selection of composition profiles for two practices, one using predominently a rich Hamersley ore and the other 60% sinter, are shown in Figs. 4.5.1 to 4 and can be compared in general terms with the profiles in Figs. 2.3, 3.2 and 3.3. The general characteristics are indeed displayed by curves from the model and this suggests that the analysis of the process chemistry is adequate. The curves underline certain facets of blast furnace behaviour:-

(i) a 'Preparation Zone' in which the charge is preheated and dried; and

(ii) a 'Thermal Reserve Zone' in which the gas and solid temperatures are approximately equal and relatively steady,

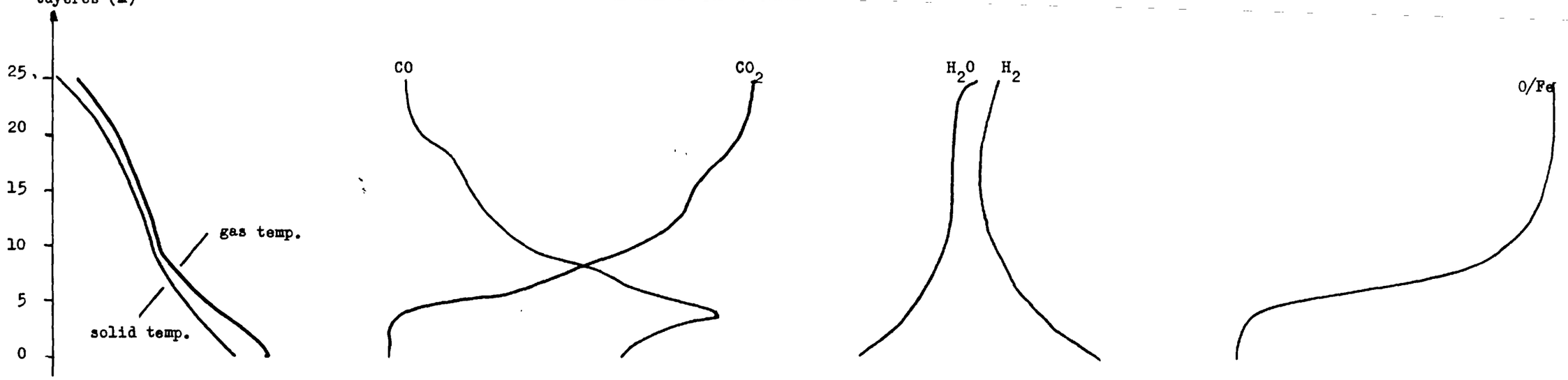
but no evidence is apparent in the oxidation profile of a 'Chemical Reserve Zone'.

The profiles also suggest an interpretation of how the process develops. As gas leaves the tuyere level direct reduction of the liquid primary slag rapidly increases the proportion of carbon monoxide. When the gas encounters solid ore lumps (at temperatures below 1250^{o}C) gaseous indirect reduction occurs, with carbon solution loss regenerating reducing gas for use in the Stack. At temperatures below 950^{o}C indirect reduction proceeds alone and any limestone present decomposes. Below 400^{o}C the constancy of the profiles suggests a complete lack of chemical activity.

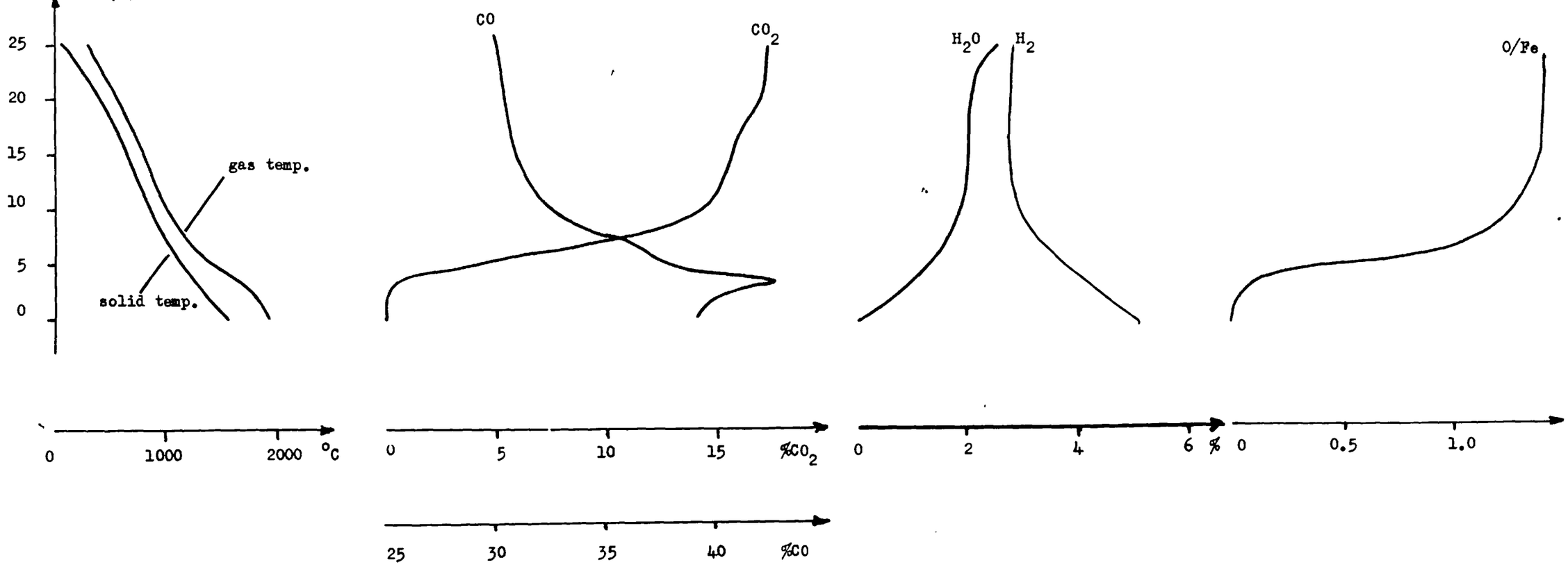
4.2 An assessment of certain dynamic responses

The next useful step in the verification of the dynamic model is to examine and compare the results of input step tests with published results (Table 4). The following step responses are

Rich Hematite Practice



60% Sinter Practice



Steady State Profiles from Simulation Studies

Fig. 4.5.1

Fig. 4.5.2

Fig. 4.5.3

Fig. 4.5.4

TABLE 4

Plant Transfer Functions

Author	Steam Injection	Blast Temperature	Coke Rate	Oil Rate	% Oxygen
	Grains/ft.^{3}	^oC	kgms/t ore	g/Nm^3	
The proposed model	$-\frac{.058}{1 + 2.8s}$	$\frac{.0052}{1 + 6s}$	$\frac{.014e^{-8s}}{1 + 8s}$	$\frac{.028e^{-2s}}{1 + 11s}$	$\mp\frac{.05}{1 + 3.5s}$
Vidal (Ref. 16)	$\frac{-.021}{1 + s} + \frac{.007e^{-8s}}{1 + 1.5s}$	$\frac{.004}{1 + 6s}$	$\frac{.015e^{-12s}}{(1 + 4.3s)^2}$		
Barbieri (Ref. 18)	$\frac{-.053}{1 + 3.4s}$	$\frac{.0025}{1 + 6.2s}$	$\frac{.015e^{-8s}}{1 + 16s}$		
Staib (Ref. 15)	$\frac{-.023}{1 + 2s}$	$\frac{.002}{1 + 14s}$	gain = .016	$\frac{.02e^{-14s}}{1 + 14s}$	
Rebeko (Ref. 7)			$\frac{.016e^{-4.5s}}{1 + 7.5s}$		$\frac{.03}{1 + 2.25s}$
D. Bulter (Ref. 37)		$\frac{.003e^{-4s}}{1 + 9s}$		$\frac{.017e^{-4s}}{1 + 16s}$	

shown in Figs. 4.6 - 10:-

Steam injection + 3.4 grains/ft.^{3}

Blast temperature + 50^{o}C

Coke rate + 16 kgms/tonne of ore

Oil injection 6 kgms/Nm^3

Oxygen enrichment 2%

These tests were carried out on the assumption that the gas velocity is held constant at 5m/sec and that the movement of the burden is in proportion to the carbon burning rate at the tuyeres. The solid velocity is, under these conditions, a linear function of blast volume, steam injection, oil injection and oxygen enrichment.

4.2.1 Steam injection

This causes quite a rapid cooling of the Hearth. The dissociation of the steam lowers the flame temperature and increases the carbon burnt at the tuyeres (and, therefore, production). For this response fixed constants are used for the indirect reduction rate terms and so no account is taken of the more efficient reduction in the Stack, a consequence of more hydrogen in the gas. So far only Vidal (Table 4) has attempted to quantify this effect. If more conclusive information becomes available the rate terms can be made linear functions of the % hydrogen in the gas.

The response is modelled accurately by a 1st order linear system with a time constant of 2.8 hours. However, further step changes of different sizes show that this time constant can vary considerably as the silicon level changes (Fig. 4.11).

Step Responses from the Simulation

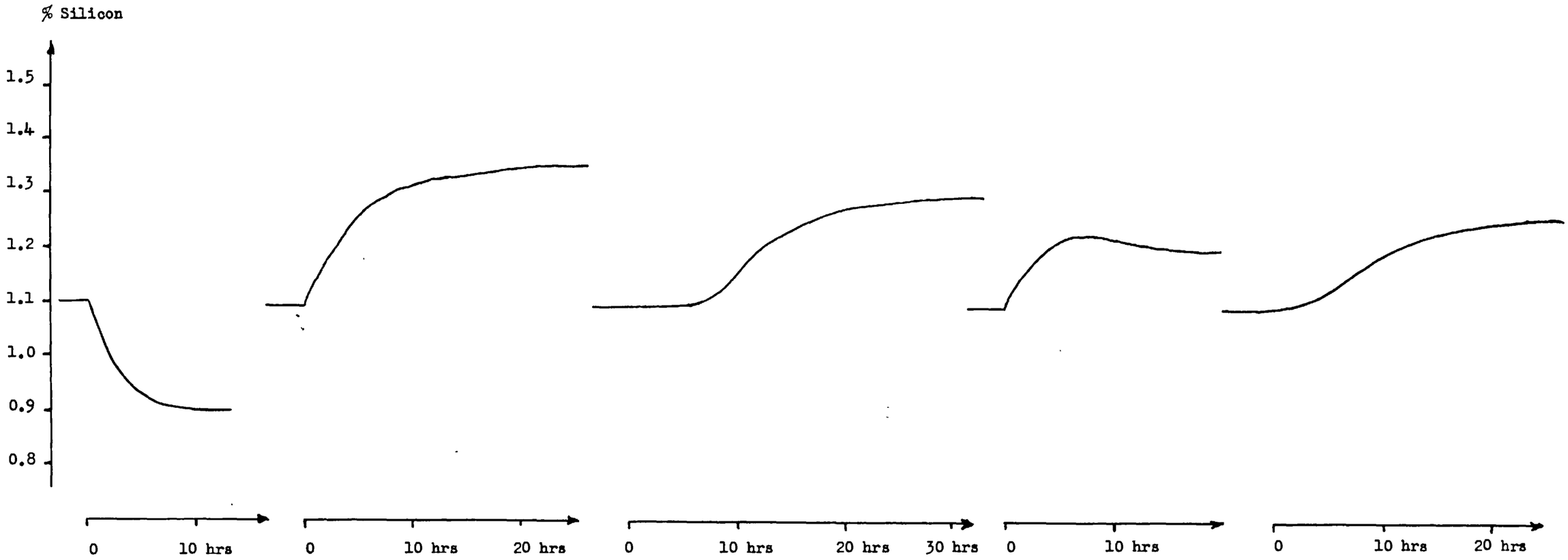


Fig. 4.6 Step change of + 3.4 grs/cu. ft. in the Steam Injection Rate

Fig. 4.7 Step change of + 50°C in the Blast Temperature

Fig. 4.8 Step change of + 16 kgms/tonne of ore in the coke rate.
(Implemented by decreasing the amount of ore charged)

Fig. 4.9 Step change of 2% in the Blast Oxygen Content.
(This includes a 10% increase in production)

Fig. 4.10 Step change of 6 kgms/Nm^3 in the Oil Injection Rate.
(This includes a 2.4% decrease in production)

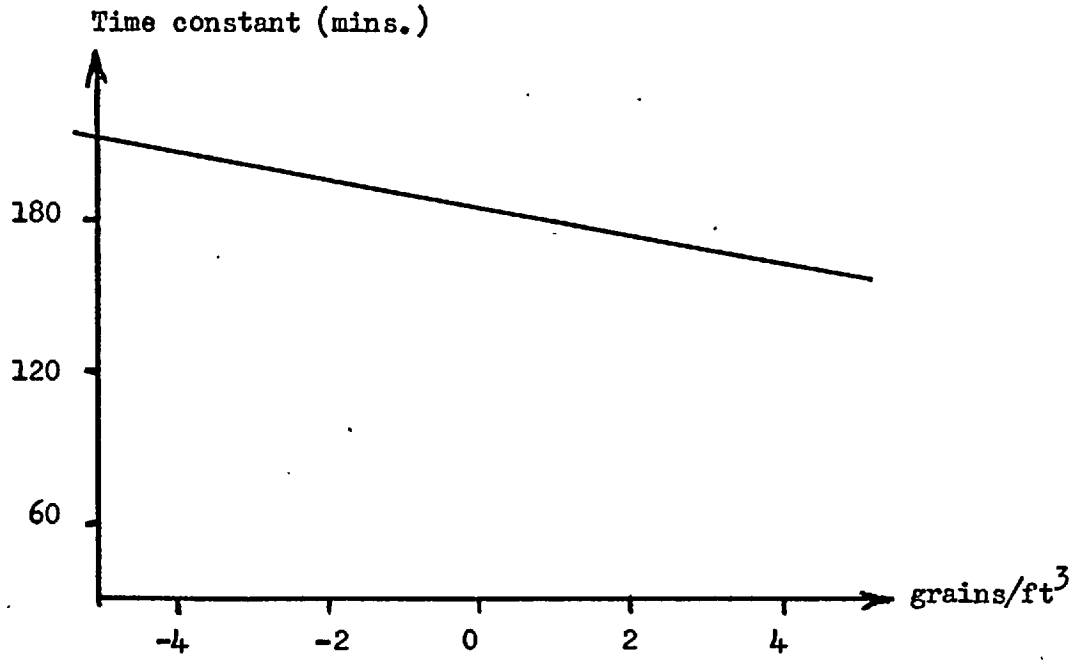


Fig. 4.11 The time constant for a change in Blast Humidity

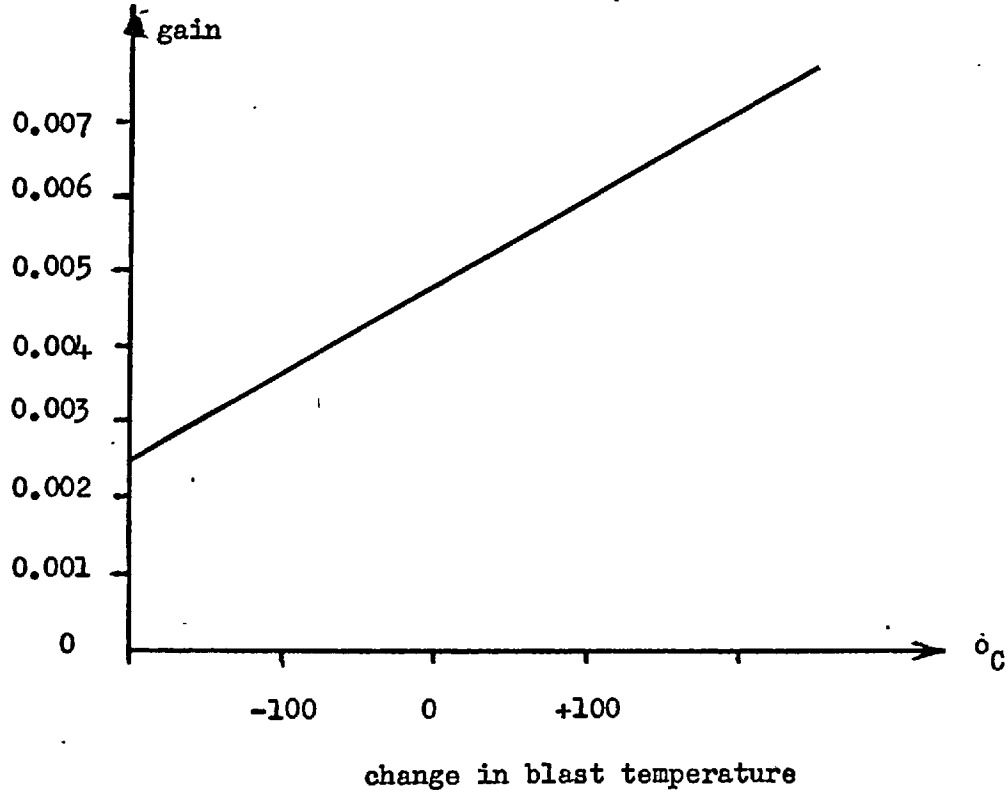


Fig. 4.12 Gain factor for Blast Temperature

4.2.2 Blast temperature

This response reflects the increased heat input and is again characterised by a 1st order linear system with a time constant of 6 hrs. This response is slower than that for the equivalent change in steam injection. In the latter case a greater rise in flame temperature occurs and the water equivalent of the gas is reduced. This means that any additional heat transfer occurs nearer to the tuyeres and, therefore, affects the silicon earlier.

Further step tests indicate that the gain can vary from 0.0052 by as much as 30% (Fig. 4.12). This appears to be a non-linearity inherent in the silicon equilibrium factor and so these variations in gain are likely on each of the channels affecting silicon.

4.2.3 Coke rate

In this case the total iron charged was decreased, which decreases the thermal load - hence the increased silicon. The response is characterised by a dead time of 8 hours and a single time constant of approximately 8 hours.

4.2.4 Oil injection

Here the injection of carbon tends to reduce the furnace drive and results in increased silicon despite the extra thermal requirement of preheating the oil. The response has a 2 hour dead time and a time constant of 11 hours.

4.2.5 Oxygen enrichment

This causes an immediate increase in production. The higher flame temperature due to increased combustion per unit blast tends

to increase the silicon level slightly.

The conclusions from this discussion are:-

(1) In general terms the responses calculated using the dynamic model agree with published results, although some differences in gains and time constants are apparent. Figs. 4.11 and 4.12 suggest that different input levels and in particular the silicon level are possible reasons for this. Also the dead time involved may well be dependent on furnace size and on the blowing rate.

(2) With reservations about the parameters, the responses can be described by a single time constant together with in some cases a dead time. Figs. 4.11 and 4.12 show that these parameters vary such that the furnace cools faster than it can be heated and that the effect of the controls becomes less as the furnace cools. Operators experiences generally back this up.

(3) The principle of superimposition appears to hold for normal operation.

4.3 A simulation of normal furnace working

The accuracy with which the model can predict the plant silicon values can only be established by direct comparisons with plant operating data. Such comparisons are shown in Fig. 4.13.

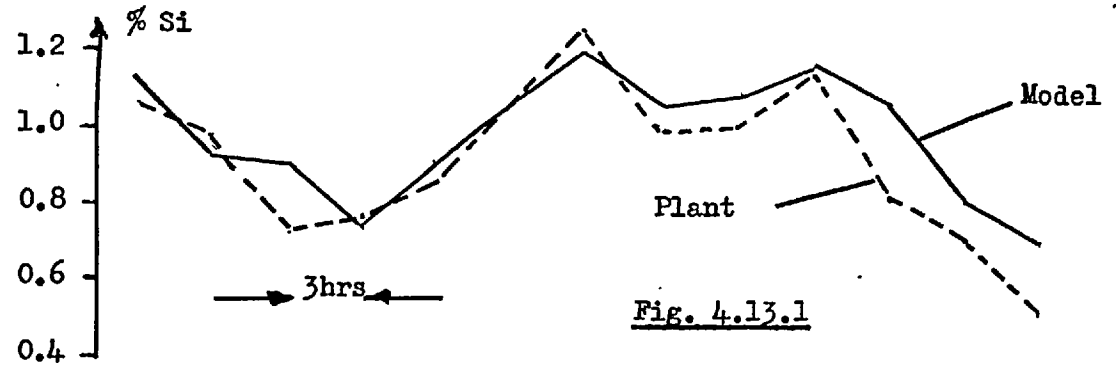


Fig. 4.13.1

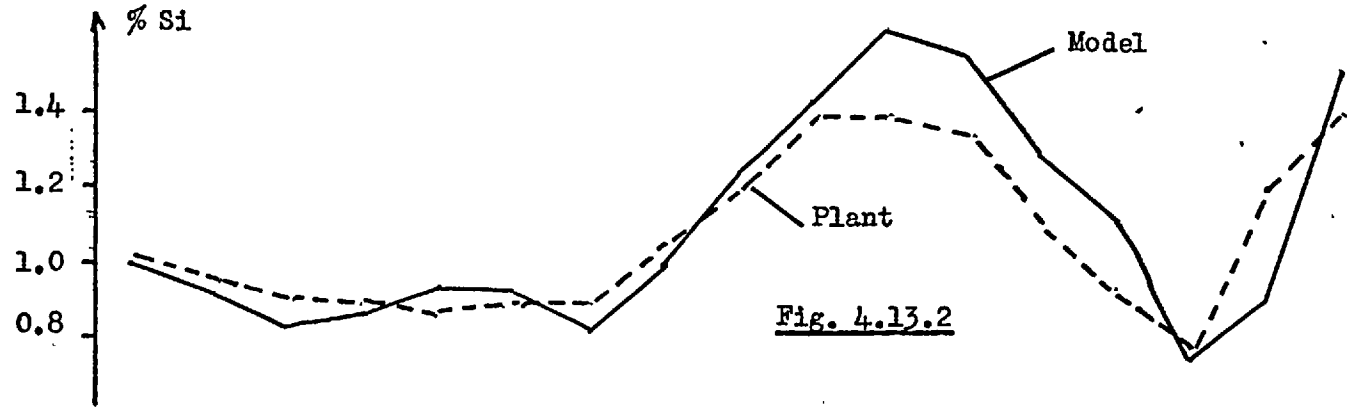


Fig. 4.13.2

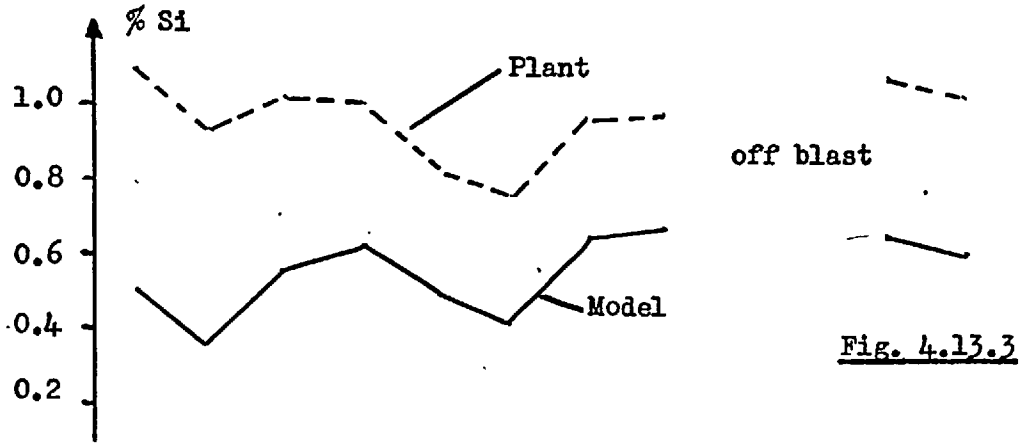


Fig. 4.13.3

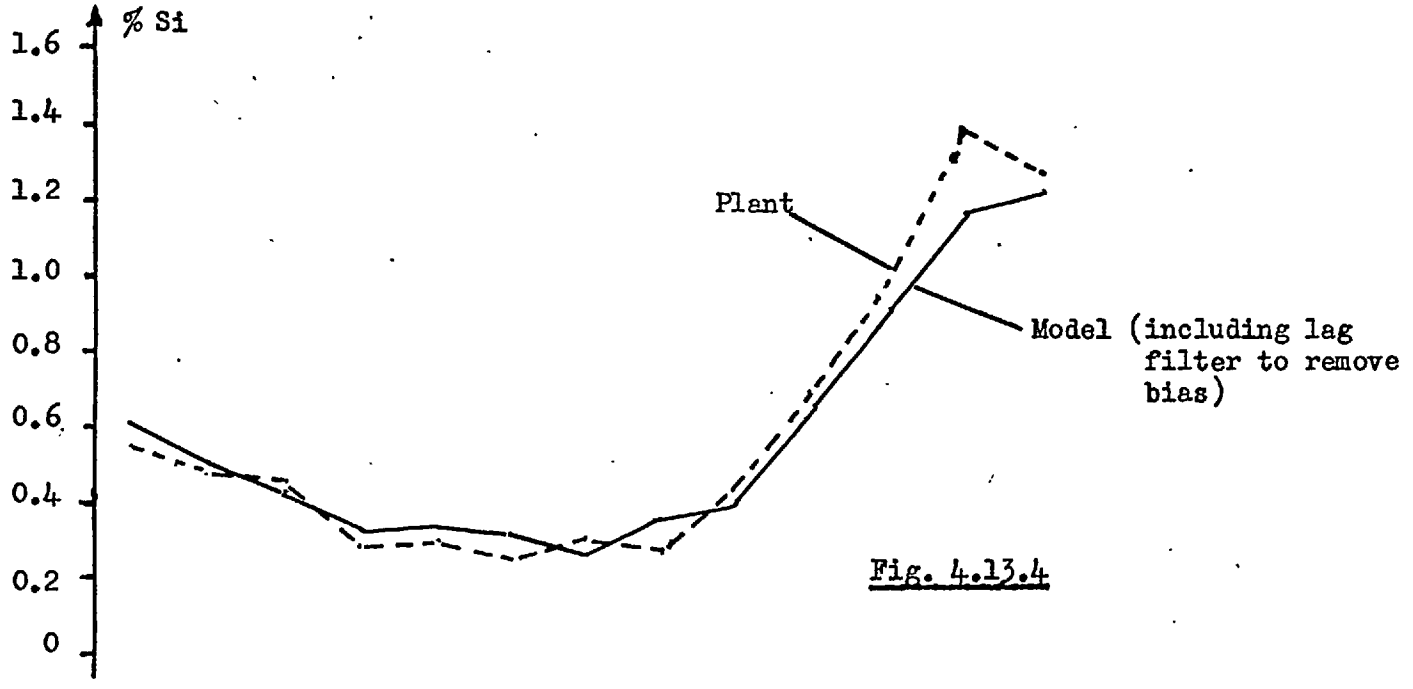


Fig. 4.13.4

The model has been programmed in Fortran to run on an Argus 500 process control computer at British Steel Corporation's Port Talbot Works as part of an automation project. The model is segmented to occupy 8K of core store and runs at 1/16 of real time. For the purpose of this comparison the model is fed with data regarding the blast and charge and a measured stock descent rate (Fig. 4.1).

The use of information regarding the rate of descent of the stockline has been the subject of much experimentation. Initially the burden velocity throughout the furnace was assumed to be proportional to that at the stockline. However, it soon became apparent that during irregular driving conditions the movement of the stockline did not reflect movement in the Bosh and Hearth or vice versa. The method which gives the best simulation of both normal and irregular driving conditions is to calculate a burden velocity at the tuyeres, in proportion to the rate at which carbon is burnt, and one at the stockline. The velocity at any particular height is then found by linear interpolation.

The degree of correlation between plant and model silicon levels, which can be achieved over periods of one or two days when the parameters have been correctly estimated and then held constant, is shown in Fig. 4.13. Between 30% and 70% of the variation in silicon is explained by the model output. If past silicon values from the plant are used as they become available as a new starting point more of the silicon variation is explained.

These results again suggest that the representation of the process chemistry is adequate.

Fig. 4.13.3 shows that, at times, a bias exists between plant and model, indicating parameter drift. The results discussed so

far are based purely on measurements of the charge and blast - no use is made of the plant top gas, one of the critical variables in other schemes (Chapter 2). Methods for improving the accuracy of the model on-line, by using top gas and cast analyses are discussed in Chapter 6.

CHAPTER 5

Methods of control using the simulation

In Chapters 3 and 4 a simulation of the blast furnace process is developed which allows transient behaviour to be followed. In this chapter this model is used to examine certain control system design problems, and indeed becomes an integral part of the plant control systems.

At first sight the plant input/output diagram, Fig. 5.1, suggests a complicated multivariable control situation. In practice this is not the case. Control can be broken down into three practically independent areas:-

(i) control of the thermal balance

(ii) control of the Hearth chemistry

(iii) control of the production rate

Control of the Hearth chemistry is implemented by burden preparation (to establish the consistency of materials) and by accurate proportioning of materials into the furnace. This latter item is the subject of local control loops correcting for weighing errors and variations in the material analyses. Levels of production are limited by furnace size and are approximately proportional to the amount of carbon burnt in front of the tuyeres. Thus, blast volume and oxygen enrichment serve to regulate production. Operators are, therefore, left with steam injection, blast temperature, oil injection and coke rate with which to establish and regulate the silicon content of the hot metal - this is equivalent to control of the thermal balance if the Hearth chemistry is stabilised.

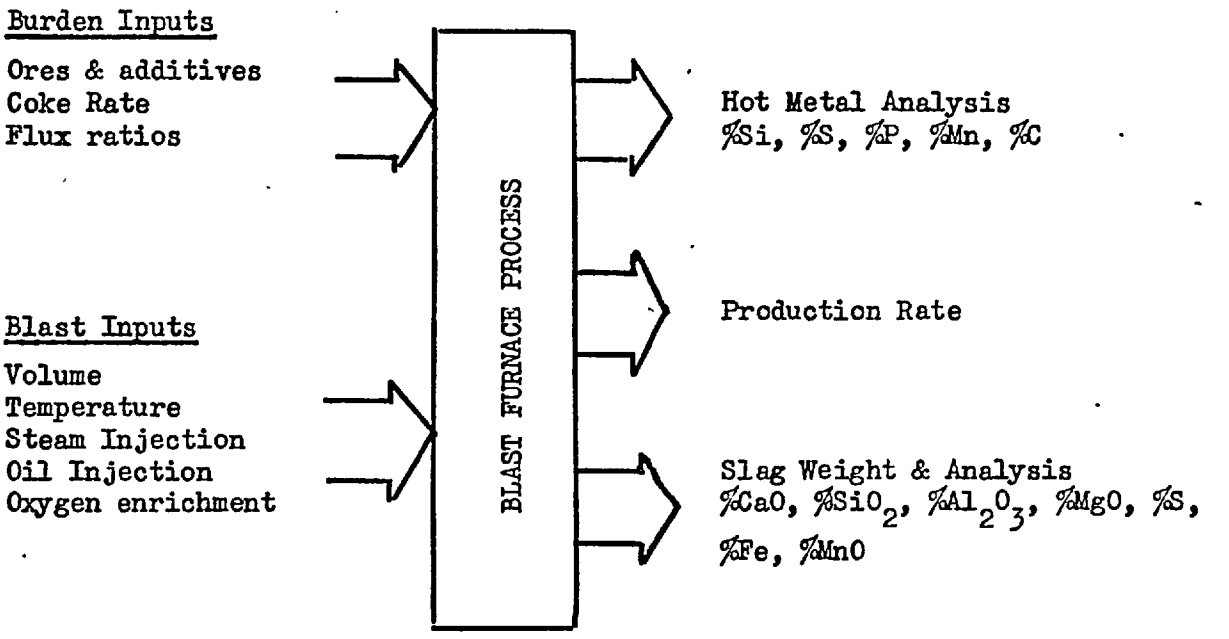


Fig. 5.1 Plant Input/Output Diagram

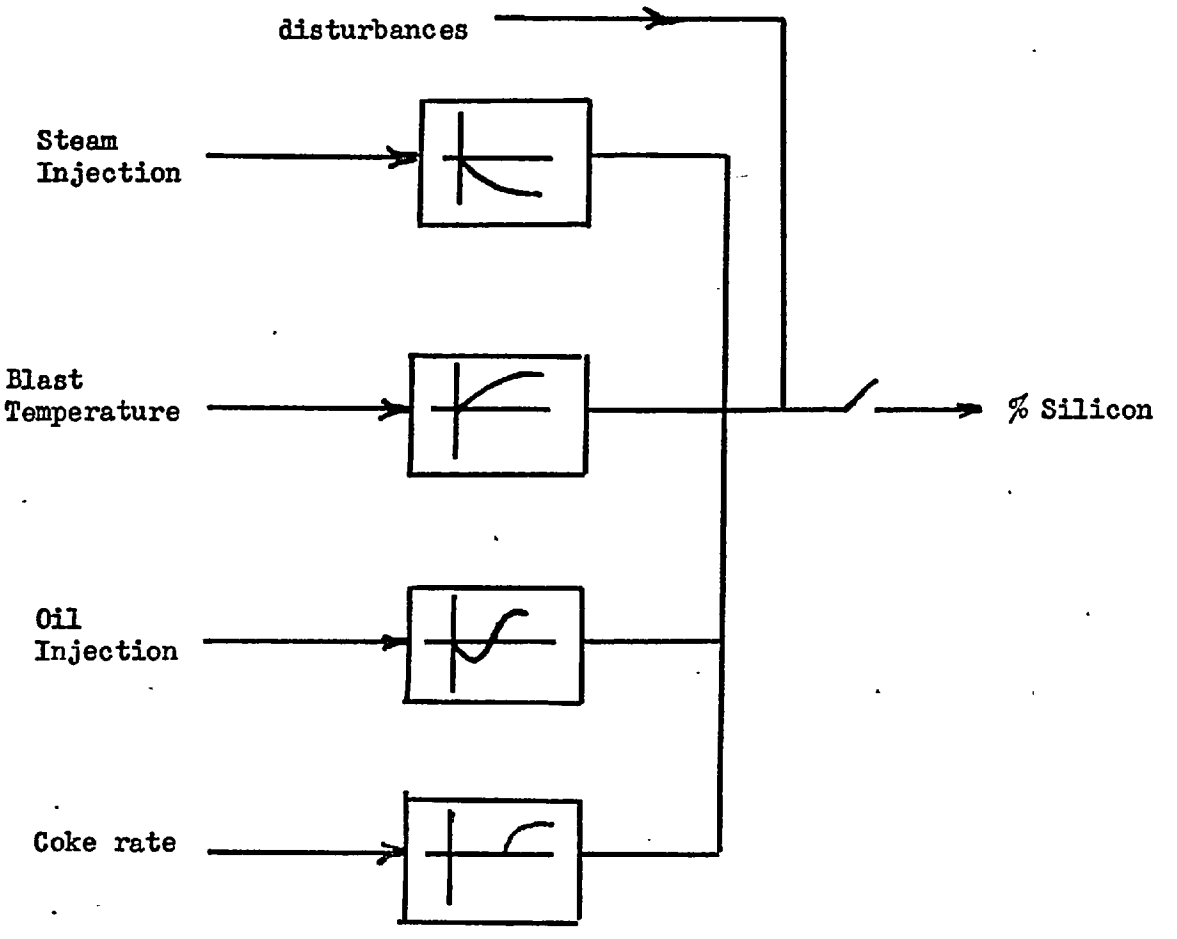


Fig. 5.2 Block Diagram for the Simplified System

The importance of blast furnace coke rate on costs is paramount since it is the largest single item of conversion cost in an integrated steelworks. The problem uppermost in operators' minds is, then, to choose levels for the blast inputs which serve to control the silicon content and minimise the coke rate.

In view of the long and widely different furnace responses that are involved, operators wisely choose to use a single input (generally steam injection or blast temperature) for silicon control and then gradually tune the other input variables towards their most economic levels, making perhaps one or two changes per day. Apart from the problem of exceeding the practical limits on furnace inputs there is little to justify the extra complication in using simultaneously two or more inputs for short term silicon control and so two areas particularly warrant further investigation

(i) control of silicon using a single input

(ii) attainment of the most economic operation.

5.1 Control of silicon using a single variable

From the description in Chapter 1 it can be seen that the main factor limiting the performance of manual control is the very low frequency at which information becomes available. Here the use of the simulation as an observer transforms the system into effectively a continuous one and widens the scope for feedback, optimal and predictive control techniques.

It is by no means apparent which of these techniques is best suited to the particular problem of silicon control and the non-linear differential equations are difficult to use directly for design purposes. However, the step tests carried out using

the model, and discussed fully in Chapter 4, and the results of other researchers' experiments on plant (Refs. 13, 15, 16, 18) suggest that the important input/output relationships from the control point of view, i.e. silicon/steam injection, silicon/blast temperature and silicon/coke rate, are fairly well behaved (Fig. 5.2) and that superimposition holds over a reasonable range. By replacing both the plant and the observer by first order linear systems, and an additional transport delay where coke rate is concerned, the transition from one silicon reference value to another can be studied and some insight gained into the respective systems.

Two single input/single output models will be used

$$\dot{Si} + 0.358\ Si = 0.478 - 0.021u$$

and

$$\dot{Si} + 0.166\ Si = -0.537 + 0.000835\ \theta$$

where

θ = blast temperature

u = steam injection rate.

The degree of fit between the non-linear model and the first order systems is shown in Fig. 5.3.

In analysing the various systems the initial condition is

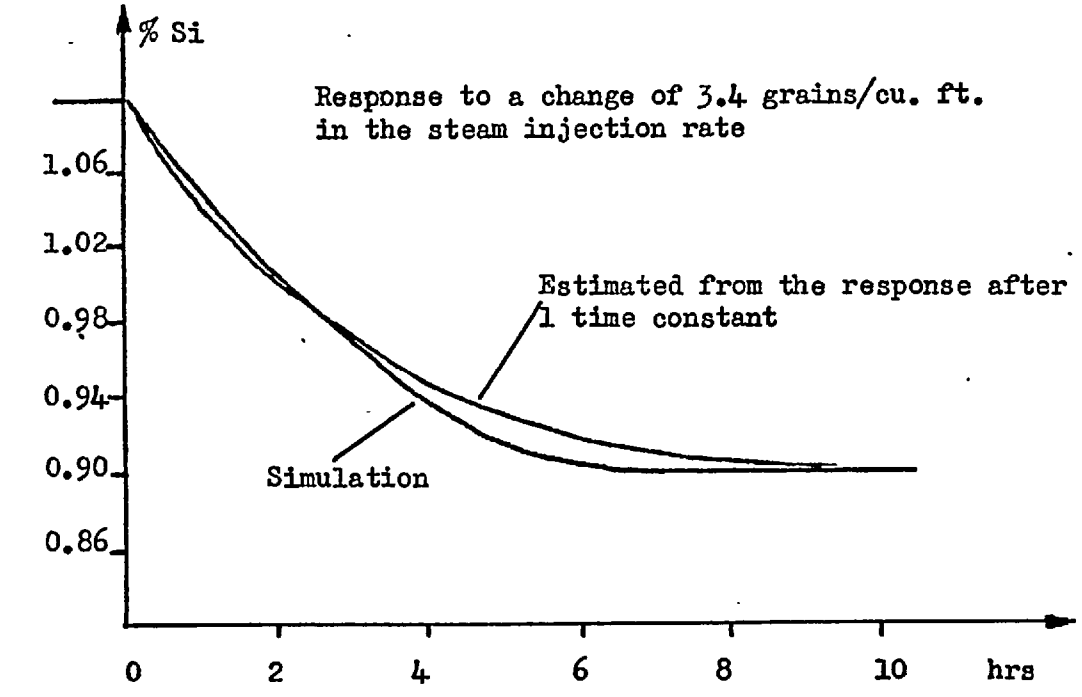
$Si\ (o) = 1.1$ i.e. $u = 4.0$, $\theta = 868.0$ $t < o$

and

$Si\ ref = 0.65\ \%$

5.1.1 Manual control

In order to establish comparisons, two manual systems are included. The first, Fig. 5.4 (a), is a completely feedforward system in which the new input is that corresponding to a steady



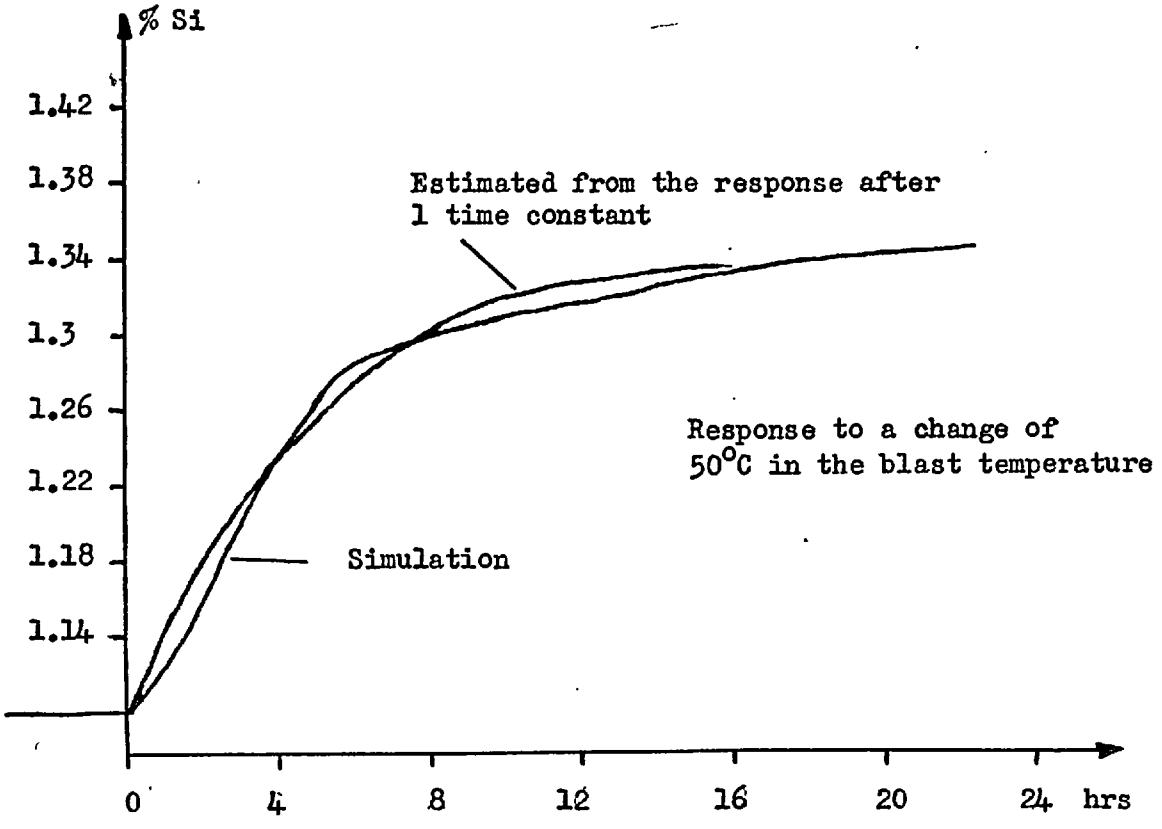
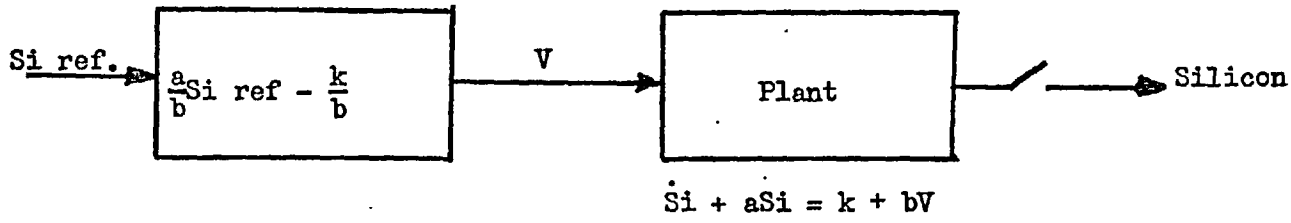
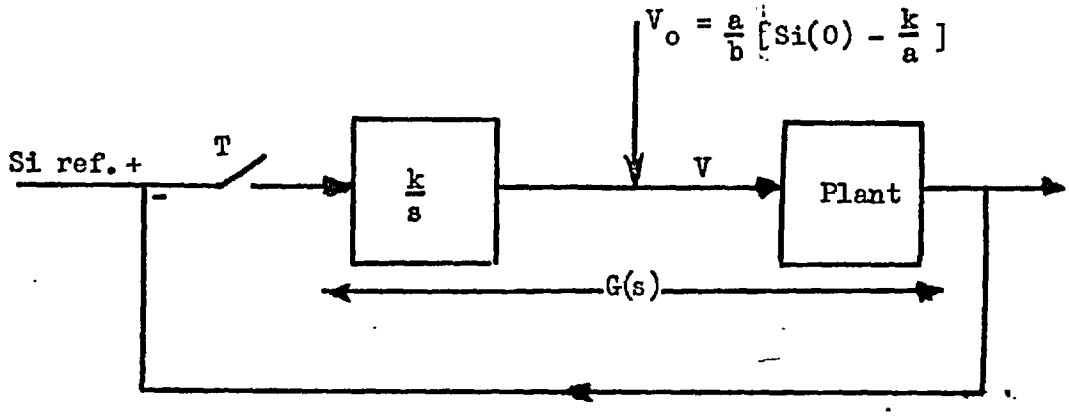


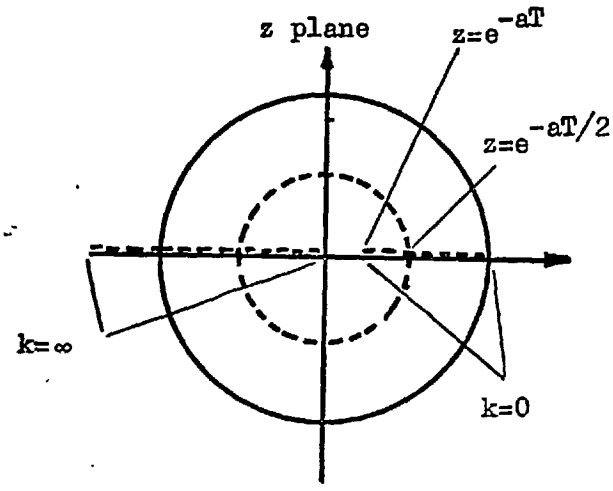
Fig. 5.3 Model fitting using simulated step inputs



(a) Feed forward



(b) Closed Loop



Root Locus for system b

Fig. 5.4 Manual Control Systems

output level, Si ref. The system response is quickly established

$$Si\ (t) = 0.65 + 0.45\ e^{-at}$$

but with the noise levels associated with the blast furnace process the system is seldom of use.

The second system, Fig. 5.4 (b), uses proportional feedback and an integrator in the forward path, the sampling interval being every cast. The open loop transfer function is

$$G(s) = \frac{Kb}{s\ (s + a)}$$

and so

$$G(z) = \frac{Kb\ (1 - e^{-aT})\ z}{a(z-1)\ (z-e^{-aT})}$$

The closed loop transfer function is, therefore,

$$\frac{K\ b\ (1 - e^{-aT})z^2}{a\ (z - z_1)(z - z_2)(z - 1)}$$

where z_1 and z_2 are the poles of the closed loop transfer function. Use of the 'Complex Inversion Formula' yields the time response of the system.

Responses using both steam injection or blast temperature as the control input are shown in Figs. 5.5.1 and 5.5.2 where K is chosen to give both an underdamped and a critically damped response. The continuous output response of the sampled data system is estimated by connecting the discrete output sequence by a smooth curve; this can be justified because the sampling frequency is substantially higher than the natural frequency.

5.1.2 Systems using the model as an 'observer'

The next logical step is to include the non-linear model in the feedback loop as shown in Fig. 5.6 (a); in this way the constraint on sampling every cast can be avoided.

Fig. 5.5.1 System Responses using Steam Injection as the Control

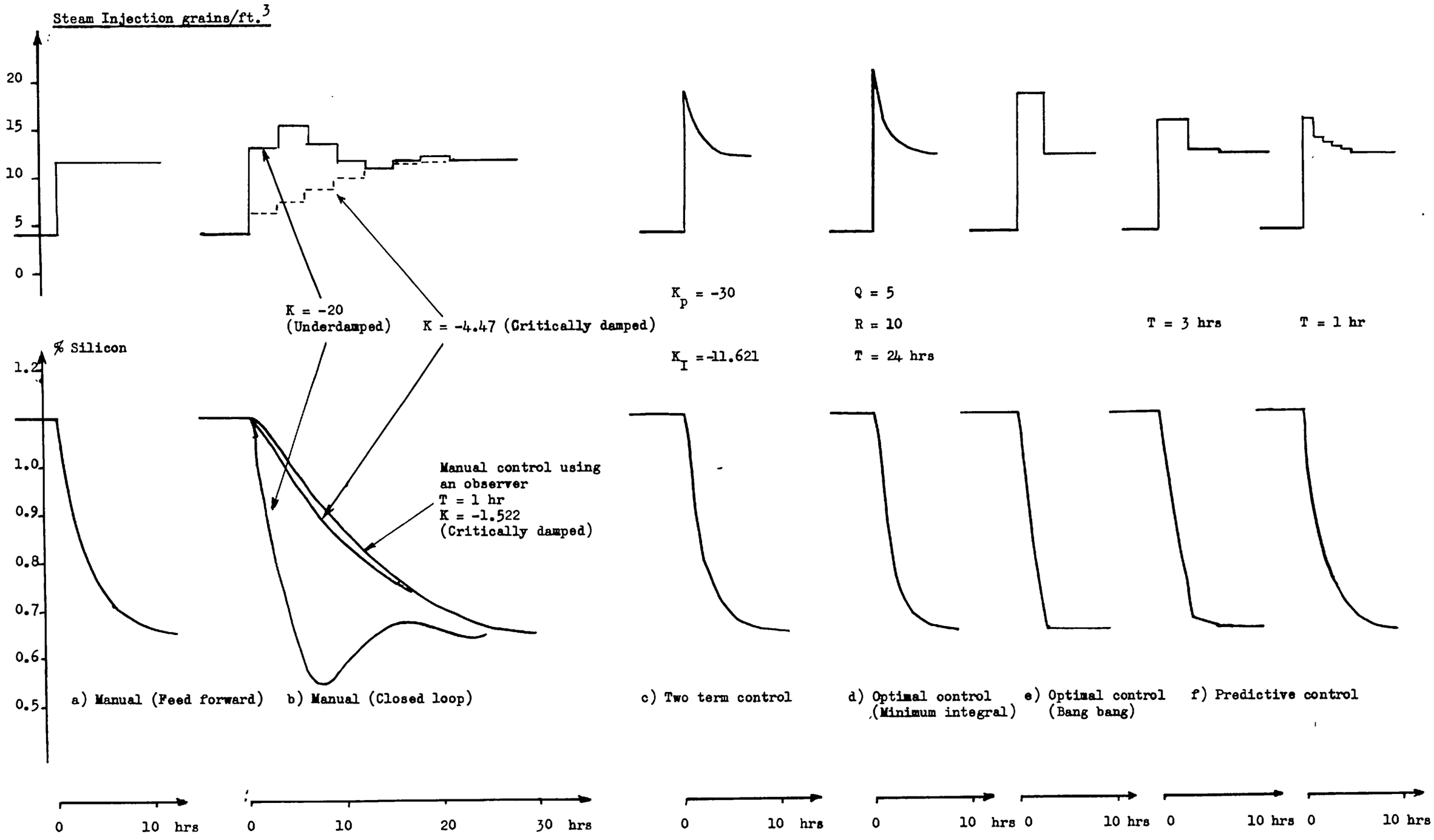
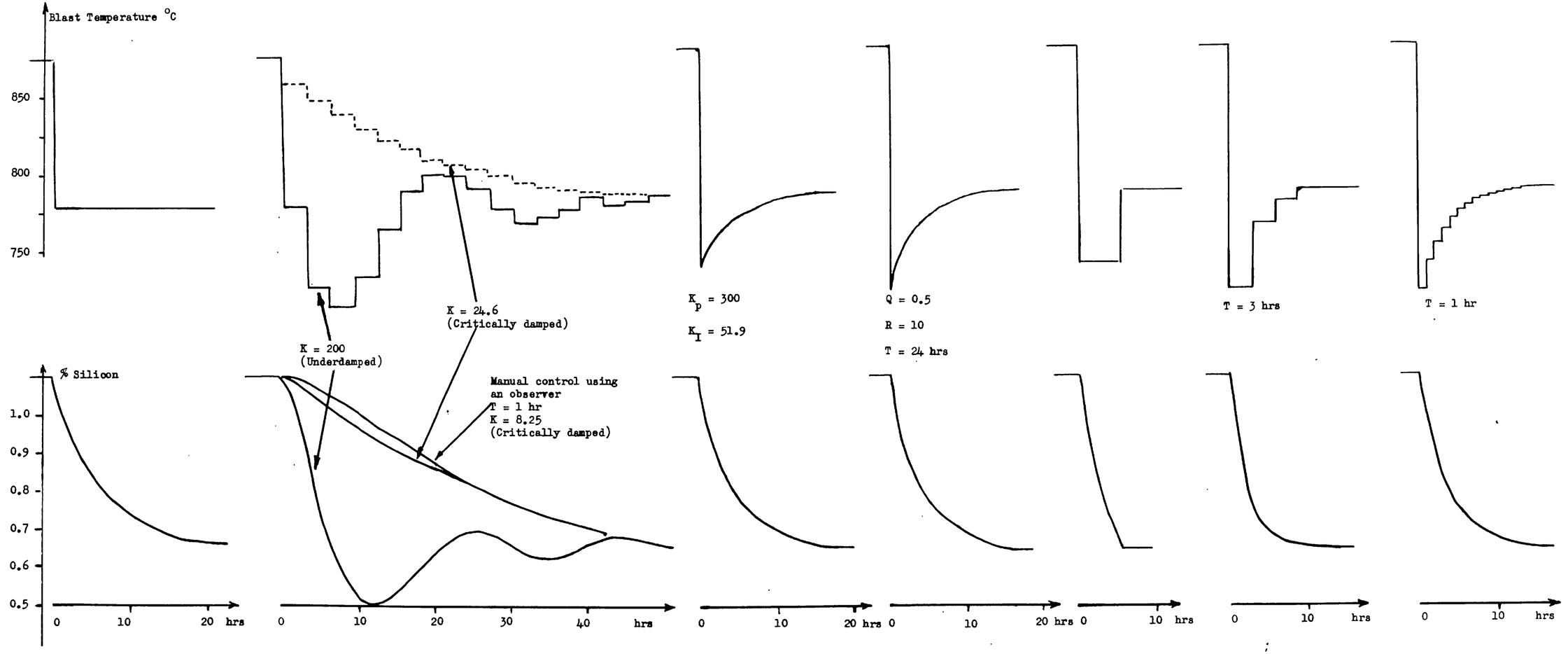


Fig. 5.5.2 System Responses using Blast Temperature



a) Manual (Feed forward)

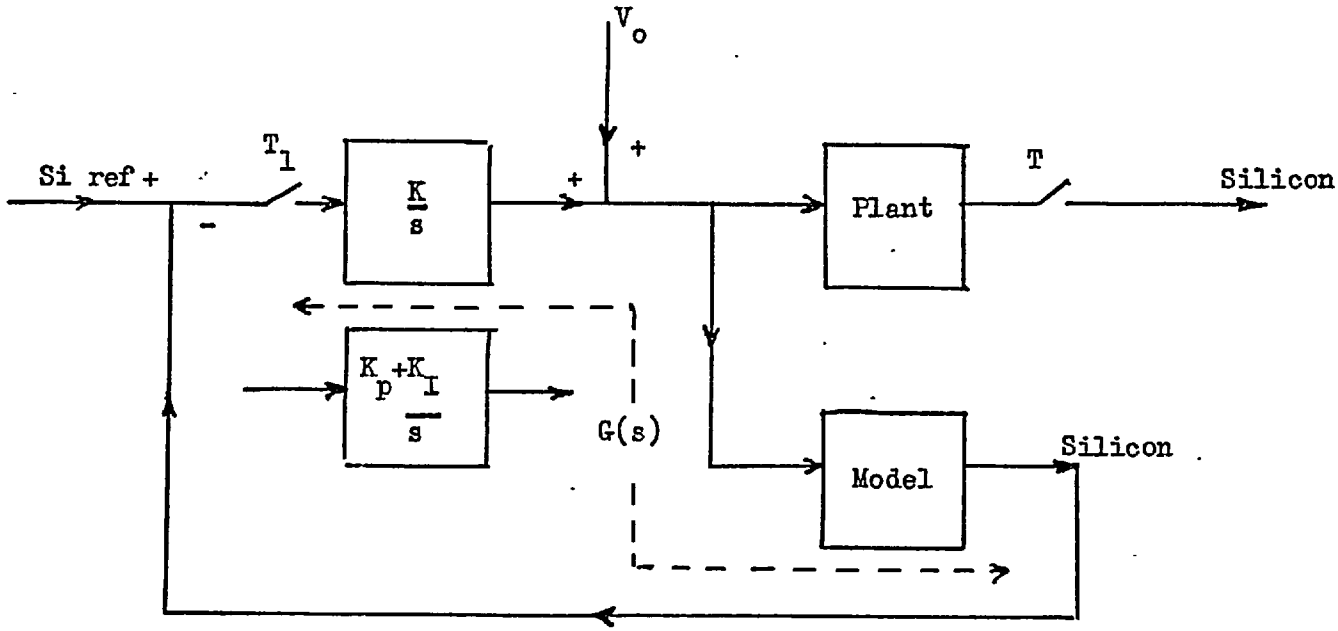
b) Manual (Closed loop)

c) Two term control

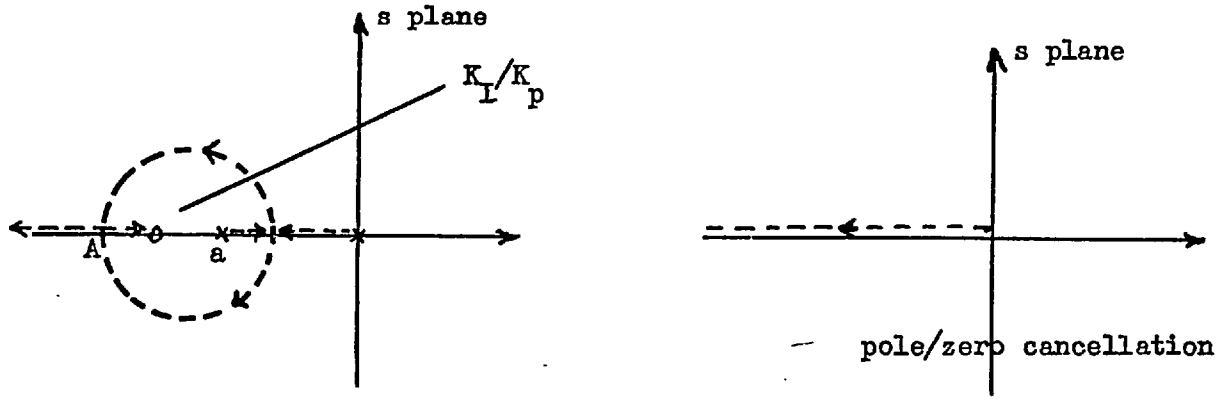
d) Optimal control (Minimum integral)

e) Optimal control (Bang bang)

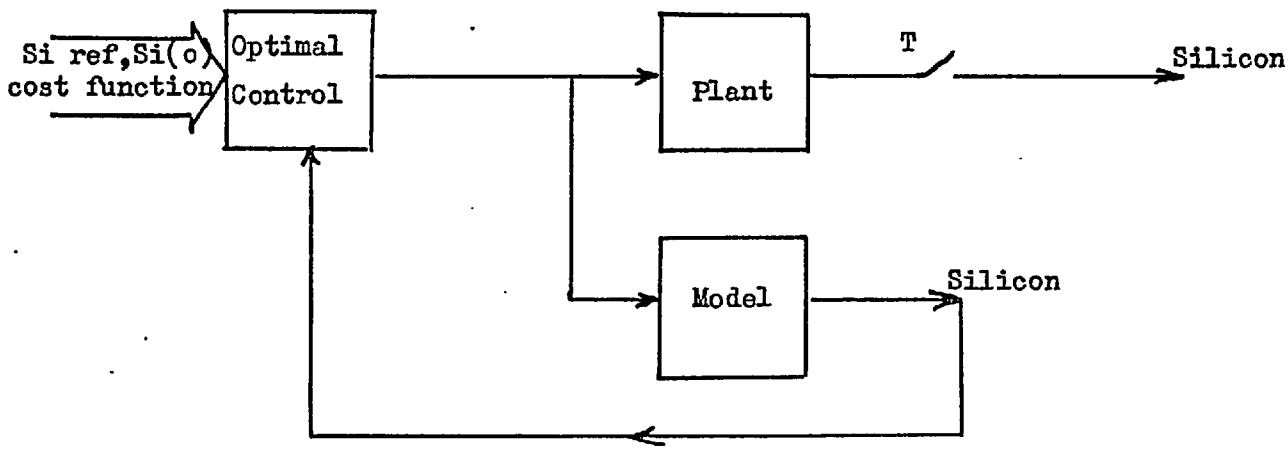
f) Predictive control



(a) Single term feedback



Root Loci for the 2 term controller



(b) An optimal controller

Fig. 5.6 Systems using the model as an observer

Firstly, from the critically damped responses shown in Figs. 5.5.1(b) and .2(b) it can be seen that the use of a faster sampling rate with the second manual system yields hardly any improvement in response. To make further improvement continuous control must be introduced. A single proportional term yields an offset and so a proportional/integral controller is the obvious starting point.

The closed loop transfer function is

$$G(s) = \frac{(sK_p + K_I)\, b}{s(s + a) + (sK_p + K_I)b}$$

Using the no overshoot condition

$$(a + K_p b)^2 = 4K_I b$$

to relate K_p and K_I, controller design reduces to finding a value for K_p which yields input values which are realistic in terms of practical limits. System responses are again shown in Figs. 5.5.1 c and .2 c and show a considerable improvement over manual control. This design procedure moves the zero of the open loop transfer function and thus the working point A (Fig. 5.6) along the negative real axis. An alternative approach is pole zero cancellation.

To judge whether any further improvement is possible with this type of system consider next optimal control based on the 'LQP' problem. To simplify the algebra introduce x(t) and v(t) such that

$$x(t) = Si(t) - Si\ ref.$$

and

$$\dot{x} + ax = - aSi\ ref. + aSi^{o} + bu = v$$

Defining the cost function as

$$s(T) = \int_0^T \left(Q\, x^2(\tau) + Rv^2(\tau) \right) d\tau$$

then the solution of 'Bellmans Equation'

$$-\frac{\partial s}{\partial t} = \underset{v(t)}{\text{Min}} \left\{ Qx^2(t) + Rv^2(t) + (v(t) - ax(t)) \frac{\partial s}{\partial x} \right\}$$

where

$$s(x(t), t) = \underset{v(t)}{\text{Min}} \int_t^T (Q\ x^2(\tau) + R\ v^2(\tau))\, d\tau$$

yields the function $v(t)$ which minimises s. This generally reduces to the solution of a Riccati differential equation with boundary values at $t = o$ and $t = T$. Fortunately, in this example an analytic solution is possible (Ref. 38) and these are shown in Figs. 5.5.1 d and .2 d, values of Q and R being chosen by trial and error to give satisfactory performance.

Another slightly different problem can be posed by constraining the input variable rather than, as in the last example, including it in the cost function. In this case the control objective is to minimise

$$s(u) = \int_o^T (Si - Si\ ref.)^2\, dt$$

subject to the constraint $\|u - \bar{u}\| \leq \delta$, $\delta > o$

Again introducing new variables to simplify the algebra

$$u = \bar{u} + v$$

$$Si = x_1 + \frac{k + b\bar{u}}{a}$$

the augmented system becomes

$$\dot{x}_1 = -ax_1 + bv$$

$$\dot{x}_2 = x_1^2$$

The 'Maximum Principle' expresses the optimality conditions for such systems in terms of a Hamiltonian function

$$H(\lambda, x, v) = \Sigma \lambda_i\ x_i$$

where

$$\dot{\lambda} = -\frac{\partial H}{\partial x}$$

with

$$\lambda(T) = \begin{Bmatrix} 0 \\ 1 \end{Bmatrix}$$

According to the Principle the function u(t) which maximises $x_2(T)$ also minimises $H(\lambda, x, v)$

Therefore

$$v^* = -\delta \text{ sign } (b_1 \lambda_1^*)$$

where

λ_1^* is the solution of

$$\dot{x}_1 = -ax_1 + bv^*$$

$$\dot{\lambda}_1 = a\lambda_1 - 2x_1$$

and given

$$x_1(o) \text{ and } \lambda_1(T) = o$$

Again, for this relatively straightforward example a numerical solution is unnecessary; one can argue that v will initially be at $\pm \delta$, depending on $x_1(o)$ and will switch to zero as $x_1(t)$ becomes zero.

The system responses are plotted in Figs. 5.5.1 e and .2 e and suggest that the performance of the PI system can only marginally be improved by optimal techniques.

5.1.3 Feedforward Predictive Control

Powell (Ref. 39) has discussed a predictive control technique with reference to analogue and hybrid systems which uses a future trajectory of the system error and gives a piecewise constant control action. Several reasons suggest that this type of system is ideally

suited to silicon control:

(i) One feels instinctively that continuous controllers are somewhat of a luxury on systems with extremely long time constants and that operators would be much happier with systems which keep the inputs constant for reasonable periods of time.

(ii) One feature of the blast furnace process is that some of the transfer functions such as silicon/steam injection or silicon/blast temperature are reasonably well behaved while others such as silicon/burden basicity are much more difficult to handle and involve long and variable time delays. With predictive control the full non-linear model can be used to handle disturbances on the more difficult channels while a much simpler linear model is used on the control input channel to simplify the optimisation.

(iii) Many of the disturbances affecting the process originate in furnace inputs e.g. unavoidable changes to the blast variables or variations in the burden material analyses, and are often known in advance. Systems in which such disturbances are fed forward have the advantage that the control is applied earlier and is therefore, smaller in magnitude. Such systems will also make better use of the

severely limited amount of fast acting control that is available, that is without recourse to a burden change, and are less likely to come up against the input constraints.

To develop feedforward predictive control consider Fig. 5.7. Here the non-linear simulation is run in real time in parallel with the plant in order to estimate the current furnace condition. This is then used as the starting point for the fast version of the simulation, running with constant blast inputs, which gives the future silicon trajectory.

The control u(t) is given by

$$J = \underset{u(t) \in \Omega}{\text{Min}} \int_0^T \frac{1}{2} \left[\text{Si ref.} - \text{Si}\ (t + \tau / u(t)) \right]^2 d\tau$$

Now introducing a simplified linear model for the control input

$$\text{Si}\ (t + \tau / u) = \text{Si}\ (t + \tau / u_o) + \int_t^\tau (u(s) - u_o)\ W(\tau - s)\ ds$$

where $W(\tau)$ is the impulse response and Si $(t + \tau / u_o)$ is given by the fast dynamic model.

Knowing that the control u(t) will be recalculated at regular intervals the problem can be simplified further by seeking the best constant level for u(t). In this case

$$\text{Si}\ (t + \tau / u) = \text{Si}\ (t + \tau / u_o) + h(\tau)\ (u - u_o)$$

where $h(\tau)$ is the step response.

Now $$\frac{\partial J}{\partial u} = \int_0^T \left[\text{Si ref.} - \text{Si}\ (t + \tau / u) \right] h(\tau)\ d\tau$$

and

$$u = u_o + \frac{\int_0^T \left[\text{Si ref.} - \text{Si}\ (t + \tau / u_o) \right] h(\tau)\ d\tau}{\int_0^T h(\tau)\ h(\tau)\ d\tau}$$

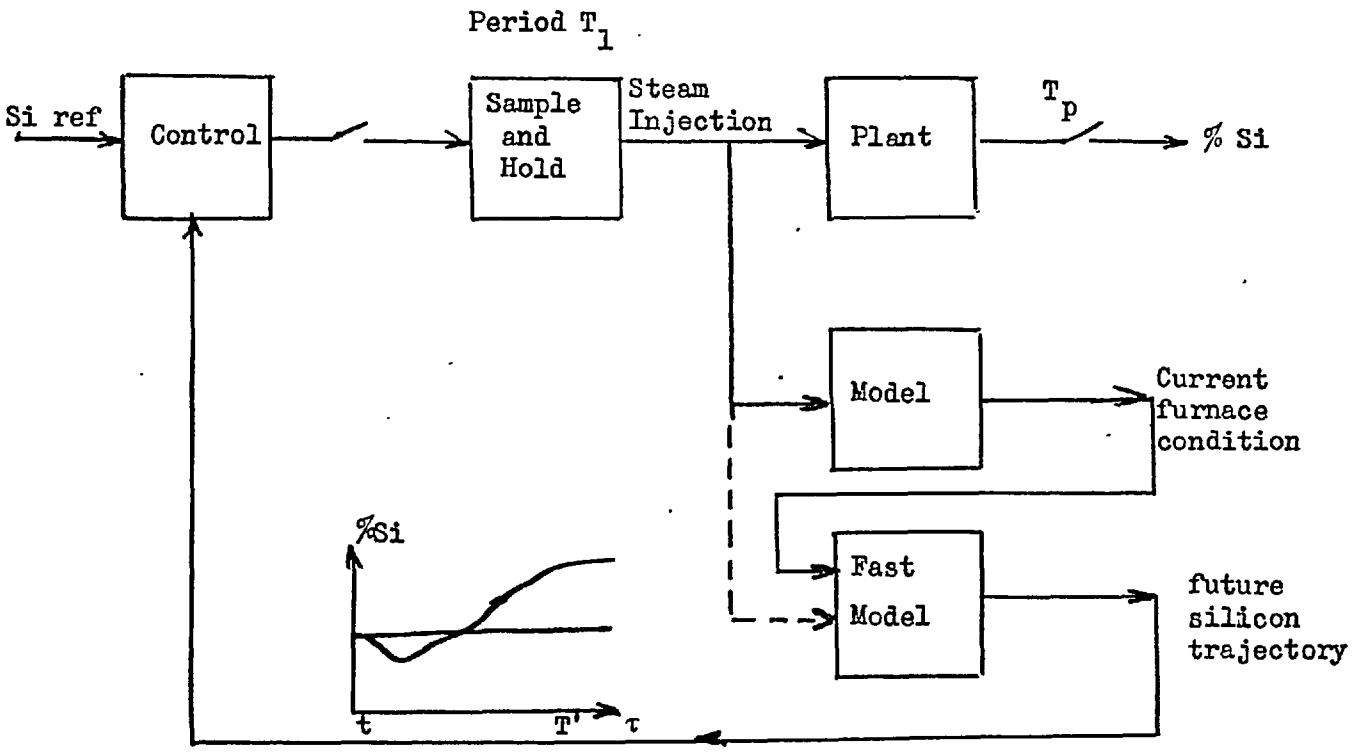


Fig. 5.7 A Predictive Controller

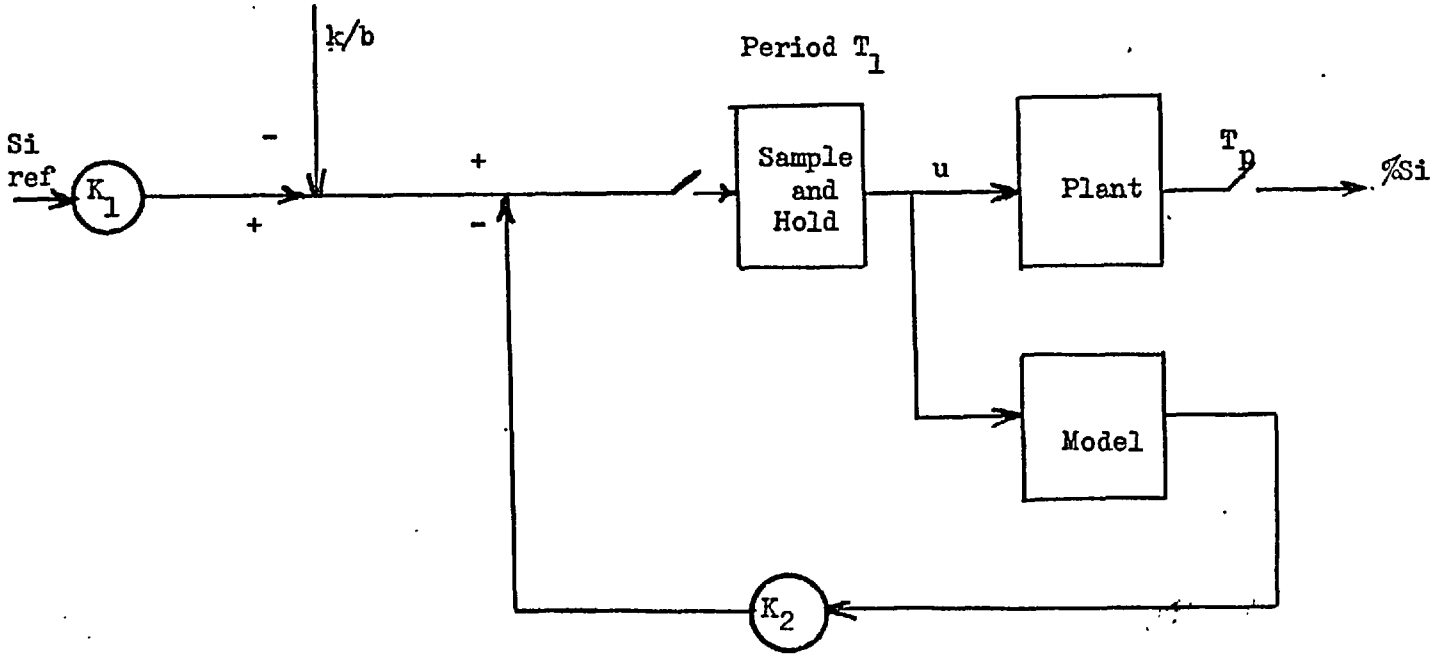


Fig. 5.8 Equivalent Linear System for the example

$$K_1(T) = \frac{\int_0^T h(\tau)\, d\tau}{\int_0^T h(\tau)\, h(\tau)\, d\tau}$$

$$K_2(T) = \frac{\int_0^T h(\tau)\, e^{-a\tau} d\tau}{\int_0^T h(\tau)\, h(\tau)\, d\tau}$$

In order to gain some insight into the performance of the system and to establish values for the prediction time T and the frequency of control, both the plant and the dynamic models are replaced by the simplified linear model.

$$\dot{Si} + a\,Si = k + bu$$

If $u_o = -k/b$

and the simplified model and the non-linear simulation are identical then

$$Si\,(t + \tau/u_o) = Si\,(t)\,e^{-a\tau}$$

Now

$$u = u_o + Si\ ref. \frac{\int_o^T h(\tau)\,d\tau}{\int_o^T h(\tau)h(\tau)\,d\tau} - Si(t)\frac{\int_o^T h(\tau)e^{-a\tau}d\tau}{\int_o^T h(\tau)h(\tau)\,d\tau}$$

and the response is

$$Si\,(t) = Si\ ref. + (Si(o) - Si\ ref.)\,e^{-A(T)t}$$

The response of this system is limited only by constraints on the plant inputs. Performance is satisfactory with T = 6 hours, and no stability problems occur if a value for T below this is used.

When the sample and hold is introduced the open loop transfer function is

$$\frac{(1 - e^{-sT_1})}{s}\ \frac{bK_2(T)}{(s + a)}$$

and the closed loop transfer function becomes

$$Si\,(z) = \frac{bK_2(T)\,(1 - e^{-aT_1})/a}{z - e^{-aT_1} + b\,K_2(T)\,(1 - e^{-aT_1})/a}$$

Consideration of the denominator shows that the system can be unstable if T_1, the sampling rate is large with respect to T the prediction time. Satisfactory performance is given with T_1 = 3 hrs

and T = 6 hours.

The response of this system to the usual initial conditions is shown in Figs. 5.5.1 f and .2 f and compares favourably with the continuous systems.

Notice that this gives a linear control law which can be realised by the diagram of Fig. 5.8. However, if the simplified linear model and the complex simulation do not give the same predicted behaviour then Si $(t + \tau/u_o)$ must be set equal to the time function predicted by the simulation and the control law is non-linear and cannot be represented as in Fig. 5.8.

5.1.4 Comments on the above systems

The important assumption upon which this discussion of silicon control is based is that of linearity. In particular both the plant and the observer are described by a first order linear system. In view of this some comment must be made regarding possible errors in the model used as the observer.

In Chapter 4 the accuracy of the non-linear dynamic model is discussed and the success or failure of any of the schemes depends heavily on this. The conclusions in Chapter 4 were that an extremely high degree of correlation exists between plant and model, although at times some offset is apparent. Such offsets will be transmitted through the controller and must, therefore, be estimated and removed, by regular comparisons between plant and model. With predictive control a particularly convenient procedure is to initiate the calculation of the future silicon trajectory at the start of each cast, and then wait and fix its relative level when the cast analysis is known, before calculating the control.

The feedback systems have been conservatively designed and so any variation in the gain and time constant on the control channel is unlikely to seriously affect the system performance. In the predictive controller a little more care is necessary and it is advisable to update the linear model regularly by running the non-linear simulation with a step input.

The following conclusions are drawn from Fig. 5.5.1 and 2

(i) Considerable benefit is likely with model based silicon control systems, although to achieve this it is not sufficient to simply ask operators to make more frequent control actions using their normal procedure and based on the output from the model.

(ii) The bang-bang type of optimal control gives the best response in the test case, but this is only marginally better than that of the two term controller which is more straightforward to implement. Bang-bang control, however, has the advantage that the controls can conveniently be made by an operator.

(iii) Predictive control is particularly well suited to silicon control and allows the plant inputs to be held steady from cast to cast.

5.2 Control of silicon using a blast variable and the coke rate

A problem touched upon earlier in this chapter is the limited amount of fast acting control, that is steam injection or blast temperature, available at any particular time. On many plants

disturbances in the burden are so great that alterations also have to be made, in the short term, to the coke rate in order to stabilise thermal conditions. This type of system can be organised so that the primary loop uses one of the systems described in 5.1 with blast temperature or steam injection, whilst a secondary loop uses the coke rate to centralise the primary input within its working range.

An insight into the design of the secondary loop can be gained by the application of Z transform theory to the example in 5.1 and again adopting a linear representation of the plant. Where processes with dead time are involved the 'Q' method suggested by Higham (Ref. 40) is useful.

Consider Fig. 5.9. Predictive control is used in the primary loop with blast temperature as the control. Control is given by

$$\frac{1}{2} \underset{u(t)\in\Omega}{\text{Min}} \int_0^{t_f} [\text{Si ref.} - \text{Si}\,(t + \tau/u(t))]^2 \, d\tau$$

It was shown in 5.1.3 that for the linear plant and model the control u(t) is proportional to Si(t).

The coke rate control is to be designed so that the overall response is as in Fig. 5.10. The closed loop transfer function is therefore

$$\frac{z^{-3}\,Q}{1 - (1 - Q)z^{-1}}$$

where Q is a parameter to be tuned during commissioning.
Now if D(z) G(z) is the open loop response then

$$\frac{D(z)\,G(z)}{1 + D(z)\,G(z)} = \frac{z^{-3}\,Q}{1 - (1 - Q)z^{-1}}$$

$$\therefore \quad D(z) = \frac{1}{G(z)} \quad \frac{Q\,z^{-3}}{1 - (1 - Q)z^{-1} - Qz^{-3}}$$

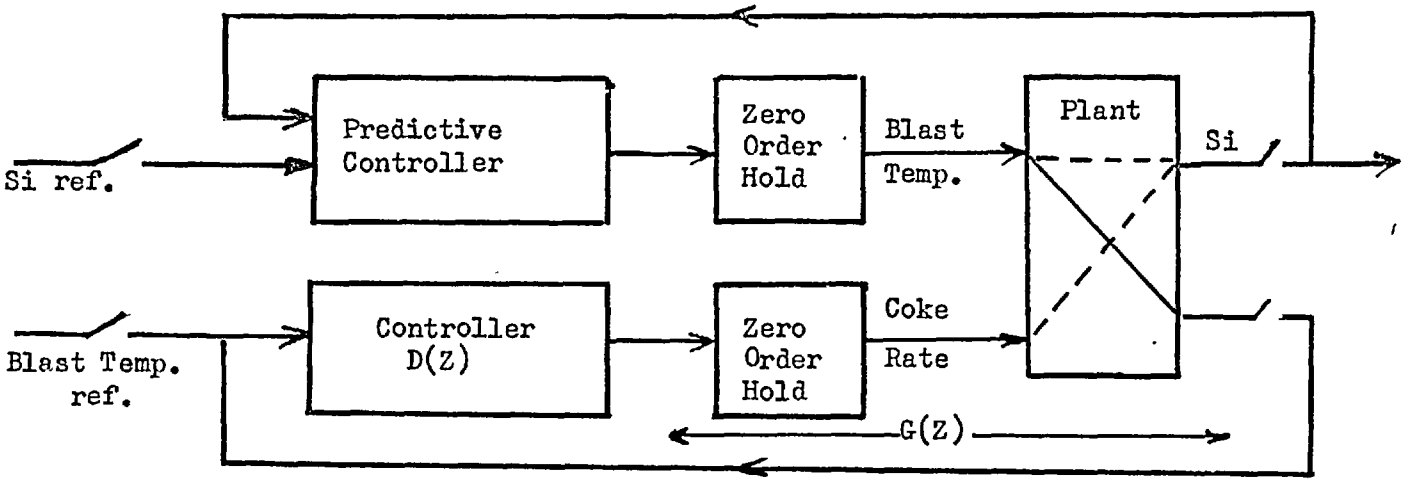


Fig. 5.9 Control using blast temperature and the coke rate

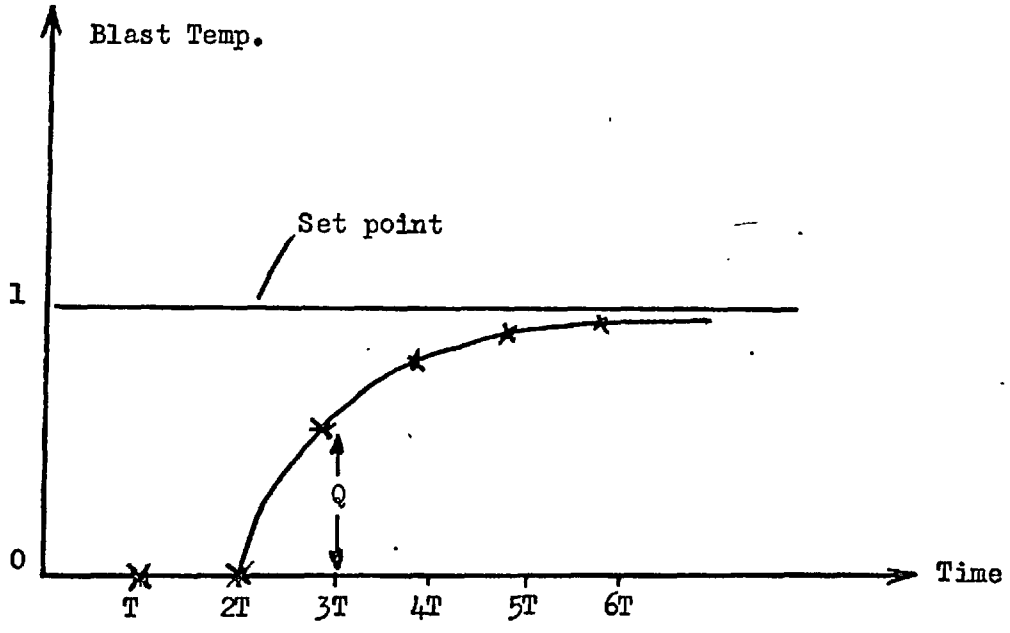


Fig. 5.10 The desired closed loop system response

In this example G(s) is of the form

$$G(s) = K \left(\frac{1 - e^{-sT}}{s}\right) \frac{g_c}{1 + sT_c} \quad e^{-2sT}$$

where g_c and T_c are the gain and time constant of the silicon/coke rate channel and T is the sampling interval i.e. 1 cast (3 hrs approximately).

and so

$$G(z) = Kg_c \left(1 - e^{-T/T_c}\right) \frac{z^{-3}}{1 - e^{-T/T_c} z^{-1}}$$

Following the algebra through the change in the controller output is given by

$$\Delta D(z) = \frac{Q \left(1 - e^{-T/T_c} z^{-1}\right)}{K g_c \left(1 - e^{-T/T_c}\right) \left(1 + Qz^{-1} + Qz^{-2}\right)}$$

This equation fixes the current change to be made to the coke rate in terms of the current and past blast temperature differences and past coke rate changes. The controller is, therefore, fully specified and implementation within the computing system is fairly straightforward.

5.3 Attainment of efficient operation

Opinion amongst ironmakers regarding the most economic levels for the blast inputs tends to vary from plant to plant and often depends on the current state of equipment etc. Many agree, however, that in order to minimise the coke rate and yet still maintain a reasonable degree of silicon control

(i) blast temperature should be held at its maximum subject to a reserve to guard against sudden chilling of the furnace hearth

(ii) oil injection should be at the highest level that can usefully be burnt at the tuyeres

(iii) steam injection should be sufficient to give short term silicon control.

Having fixed these operating standards operators are faced with the problem of establishing them following stoppages or slack blast periods. Because changes to the coke rate are involved this is often a time consuming process and is one in which use of the non-linear simulation can help considerably.

As with silicon control, the use of hill climbing routines with the large and complex non-linear model is not a practical proposition. One solution, which presupposes that simplified models are available for the control channels, is to extend the ideas of predictive control.

The main difference between plant set up and silicon control is the time scale. With silicon control a single step change for steam injection or blast temperature is calculated perhaps once every 3 hours. For plant set up coke rate changes are involved and with the associated time delay can take up to a day to be fully effective. Because this response is so completely different from those of the blast variables a sequence of step changes is considered.

With this in mind consider firstly finding u(t) to minimise

$$J = \frac{1}{2}\int_0^T [Si_c - Si(t/u)]^2 dt + \frac{1}{2}\int_0^T K\,(u - u^*)^2 dt$$

where u^* is the operational standard and the form of u(t) is shown in Fig. 5.11.

Introduce a linear model for the control channel

$$Si(t/u) = Si(t/u_o) + h(t)\,(u_1 - u_o) + h(t - \Delta T)\,(u_2 - u_1) + \ldots$$

where h(t) is the step response and $Si(t/u_o)$ is calculated using the non-linear model.

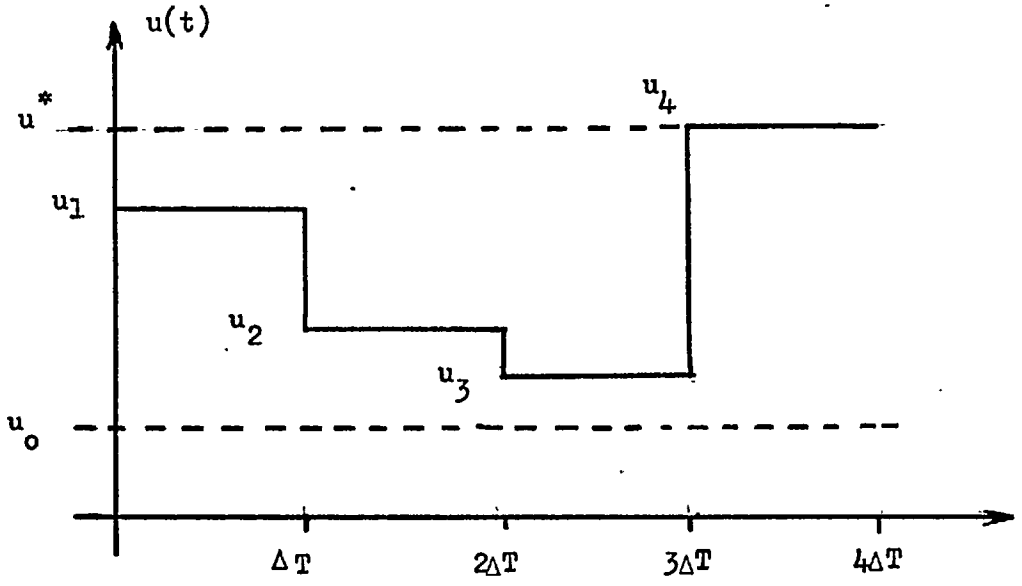


Fig. 5.11

Then

$$\frac{\partial J}{\partial u_1} = \int_o^T [Si_c - Si(t/u)][\, h(t) - h(t - \Delta T)\,]\ dt + K\Delta T\ (u_1 - u^*)$$

$$\frac{\partial J}{\partial u_2} = \int_o^T [Si_c - Si(t/u)]\,[h(t - \Delta T) - h(t - 2\,\Delta T)\,]\,dt + K\Delta T\ (u_2 - u^*)$$

$$\frac{\partial J}{\partial u_3} = \ldots\ldots$$

and these reduce, after substituting for Si(t/u) and re-arranging, to a set of linear algebraic equations yielding u_1, u_2 . . . u_n.

Now extending this to the multi-input case $\vec{u}(t)$ must minimise

$$J = \frac{1}{2}\int_o^T [\, Si_c - Si(t/\vec{u})\,]^2 dt + \frac{K_1}{2}\int_o^T (u_1 - u_1^*)^2\ dt + \frac{K_2}{2}\int_o^T (u_2 - u_2^*)^2\ dt$$

$$+ \frac{K_3}{2}\int_o^T (u_3 - u_3^*)^2\ dt + K_4\int_o^T u_4\ dt$$

where u_1 = steam injection

u_2 = blast temperature

u_3 = oil injection rate

u_4 = coke rate

K_1, K_2, K_3, K_4 = respective cost constants

u_1^*, u_2^*, u_3^* = respective operational standards

Using the method developed for the single input situation the problem again reduces to the solution of a set of linear algebraic equations. The solution of these equations, with careful choice of the cost constants, gives a sub-optimal (and hence reasonably efficient) schedule for re-establishing the operational standard

input levels and a minimum coke rate, following disturbances to production.

Initial studies of this procedure suggest two step changes to the coke rate at t = o and t = 18 hrs, step changes every 6 hrs for steam injection, blast temperature and oil injection and a value for T of 36 hrs.

If constraints are introduced then the problem becomes one of constrained optimisation. Certain techniques are available but the implementation is by no means straightforward. One possibility when an input constraint is not satisfied is to fix this particular input at its constrained value and then resolve the linear equations for the remaining controls.

5.4 Concluding remarks

The use of the non-linear simulation has been discussed in three areas:-

1. Silicon control using a single blast input
2. Silicon control using a blast input and the coke rate
3. Plant set up.

In each case linear approximations, based on both simulation and plant experiments, have been made to simplify controller design procedures, and in each case a control configuration is proposed.

Calculations shown in Figs. 5.5.1 and 2 suggest that the benefits in terms of better silicon control are quite large. But it must be remembered that the final performance of these systems is very much dependent on correct predictions from the on-line simulation and so any final evaluation must await on-line plant trials.

CHAPTER 6

Methods for improving simulation accuracy in an on-line environment.

In Chapter 5 several methods of controlling silicon content, using an on-line process simulation as the basis, are discussed. Any subsidiary calculations which for example estimate the current efficiency of the process and which can be fed back to improve the accuracy of the simulation are likely to be of direct benefit in terms of the overall system performance.

Here three such systems, which are easily implemented, are examined, one estimating the bias between plant and simulation silicon levels, another correcting the materials input to the simulation and a third varying chemical and physical parameters in the simulation to correct the calculated top gas analysis and temperature.

6.1 Estimating the silicon bias

The numerical simulation running from data regarding the blast, charge and stock velocity, and a particular parameter set gives unique operation, whereas the plant can be affected by a host of other normally slowly varying factors. For example, the blend of ores and the type of coke used, physical and chemical properties of the burden materials or the charging pattern. In the simplified analysis of the process and the resulting equations, given in Chapter 3, these effects are lumped into the unknown physical, chemical and thermodynamic parameters. As long as their variation is reasonably slow such disturbances show themselves as an offset

between plant and simulation. This type of effect is shown in Fig. 6.1, where on-line plant and simulation results are plotted for thirteen casts.

To avoid the fairly lengthy re-application of parameter tuning as described in Chapter 4 whenever an offset exists, the offset can be estimated using a simple lag filter. The result is also shown in Fig. 6.1 and generally represents a significant improvement in accuracy. In practice at Port Talbot manual re-adjustments to parameters is now necessary only when major changes to practice occur.

6.2 Correction of material flow

A major problem associated with material balances for the blast furnace process is accuracy. The process environment and the vast quantities of material involved are such that one has extreme difficulty in obtaining correct material weights and representative analyses. The situation is further complicated by the considerable and varied time delays involved as materials pass through the ironworks area. In view of this an iron balance can easily show errors of up to 5% and balances for the trace elements considerably higher.

The numerical simulation is founded on material balancing and so any error in the chemical element weights charged will be transmitted through the simulation and into the calculated hot metal and slag analyses.

Before discussing a system to correct for these errors it is important to note that at least on No. 5 furnace at Port Talbot, the errors vary slowly in relation to the fundamental sampling rate (1 cast). For example, the percentage errors in a weekly Al_2O_3

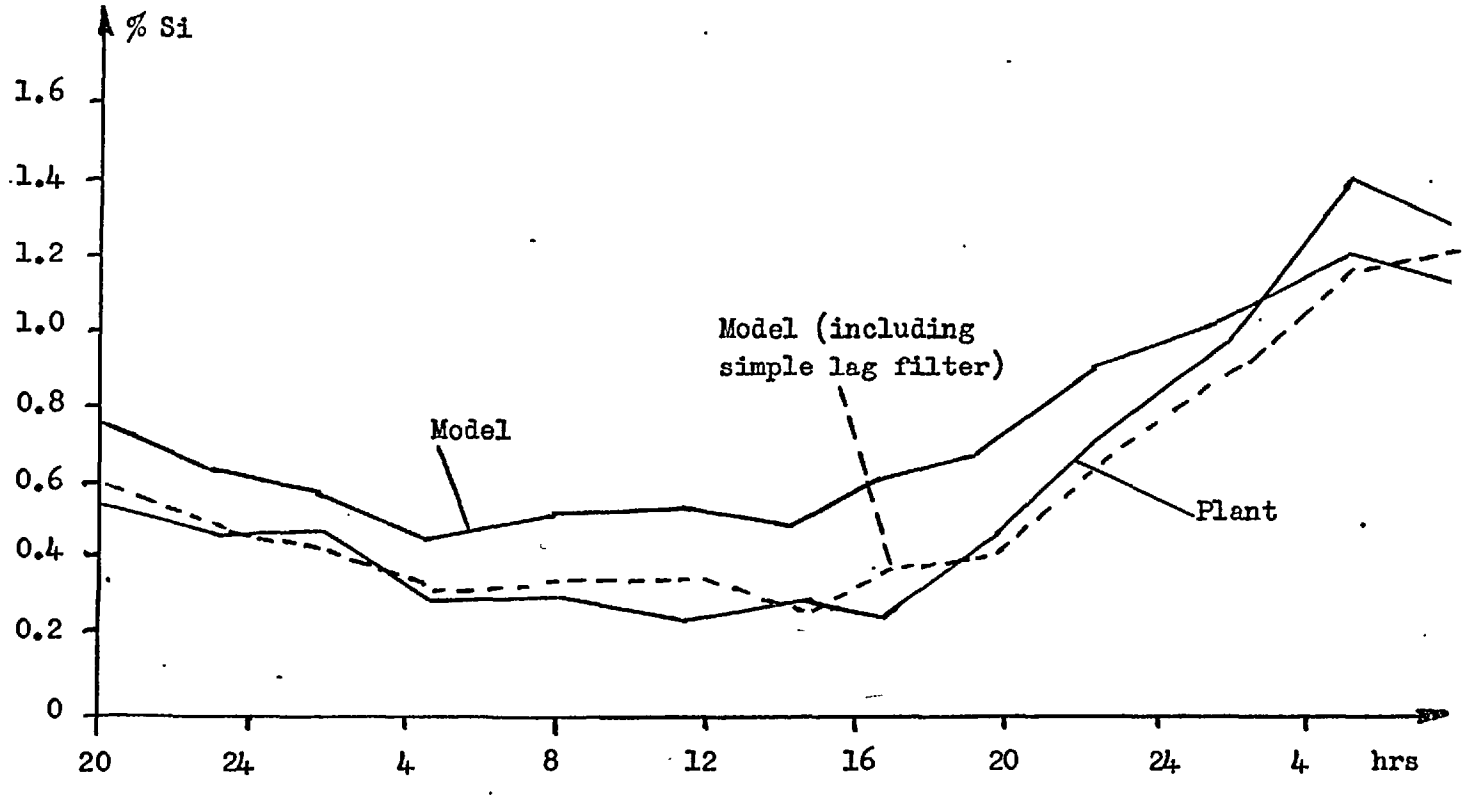


Fig. 6.1 Estimation of the Silicon bias

balance were

	5.41	8.67	11.73	9.08
and	8.24	7.99	5.79	5.45

for two four week periods and more generally the errors are often of the same sign for periods of 2 or 3 weeks. It is, therefore, in order to consider the system in Fig. 6.2.

Rather than make a direct comparison of plant inputs and outputs and thus neglecting the considerable transport delay, a comparison is made between the output of the simulation and the plant after each cast and corrections fed back on to the simulation inputs.

Allowing for some mixing as the burden passes through the furnace, the plant (and simulation) can be described for design purposes as

$$\frac{1}{1 + sT_m} \quad e^{-2sT}$$

where T_m is the time constant associated with mixing (approximately 1 hour) and T is the cast interval. The design procedure suggested by Higham (Ref. 40) and used in 5.2 is again applicable and yields

$$\Delta D(z) = \frac{Q\,(1 - \exp(-T/T_m)\, z^{-1})}{(1 - \exp(-T/T_m))\,(1 + Qz^{-1} + Qz^{-2})}$$

This relates the change in correction to immediate past changes and errors, and is easily implemented.

The technique can be applied to all elements in the hot metal and slag with the exception of carbon. That is

SiO_2, Al_2O_3, Mn, CaO, MgO, S, P.

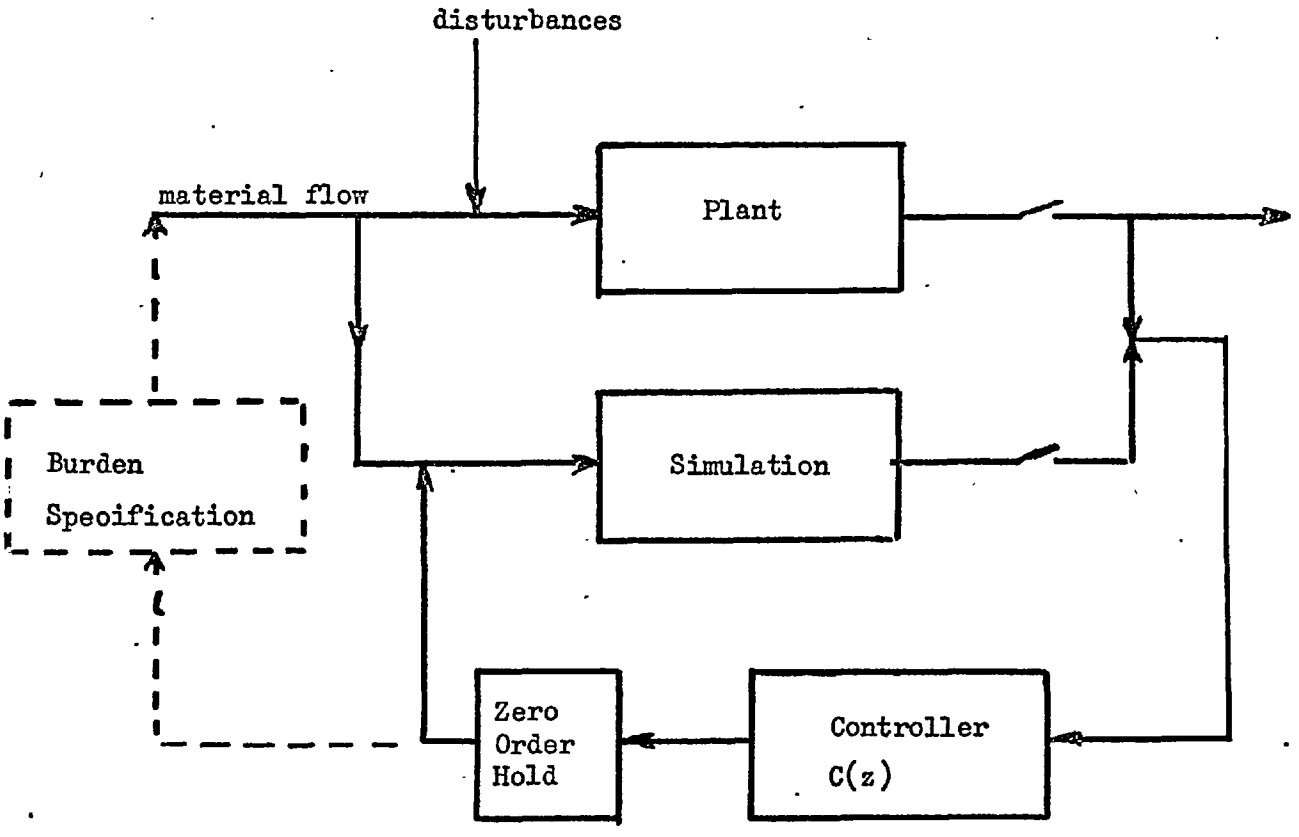


Fig. 6.2 System for correcting the material flow

The carbon balance is affected by uncertainty regarding the hot blast volume and is subject to accumulation in the coke reserve. It is also important to note that the corrections cannot be absolute, because the weight of slag produced by the plant is generally not known.

Initial on-line tests show that a typical correction is

SiO_2	Al_2O_3	Mn	CaO	MgO	S	P
- .0442	- .1093	- .0199	- .0721	.0079	- .0181	- .0018

cwts/ton hot metal

and to put these figures into perspective they have been converted into percentages of the total element inputs

SiO_2	Al_2O_3	Mn	CaO	MgO	S	P
- 2.1%	- 14%	- 9.2%	- 3.5%	1.2%	- 19.8%	- 6.3%

In closed loop operation the error in corrected output rates from the simulation can normally be held at less than 1½%.

It is also interesting to note that these corrections have been fed back into the static balance used in specifying burdens and this has also resulted in a significant improvement in accuracy.

6.3 Measurements from the top gas

The residence time of gas within the furnace is such that continuous measurements of top gas analysis and temperature give up to date information on processes occurring within the furnace as a whole. In particular the effects of variations in the reduction phenomena or in the heat transfer, caused say by a change in the radial gas distribution or the properties of the charge, can be immediately detected.

The most natural use of this information is to specify additional boundary conditions associated with gas at the furnace top i.e.

$$\vec{c}^{g}(o, t) \text{ for } t > o$$

in the notation of Chapter 3. To satisfy these additional conditions an iterative process must be introduced in which the integration along the initial gas characteristic is repeated with various sets of parameters until agreement is reached with measurements from the furnace top.

Although possible in theory, problems with timing in the on-line environment make the approach impractical and so a second somewhat less accurate approach is suggested. Here the idea of controlling the simulations top gas using the parameters is developed.

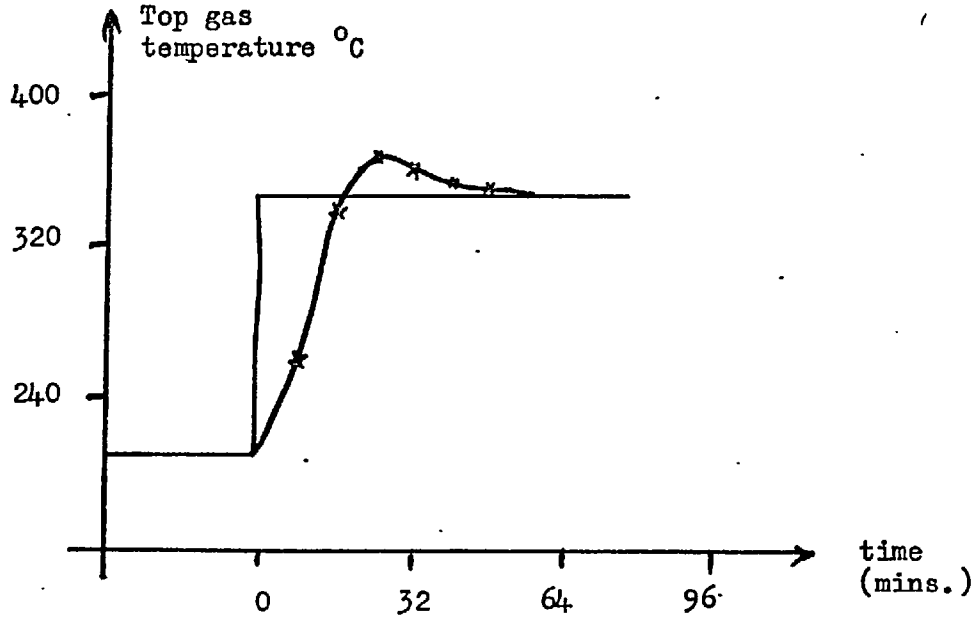
Consider the parameter step changes in Figs. 4.2.1 to 4.2.5 . The rate and equilibrium constants mainly affect the gas analysis, whilst the heat transfer coefficient and the heat loss affect the temperature distribution. These responses are practically complete after about one hour. This non-interaction and the shape of the responses suggest that integral feedback will be sufficient.

The calculated nitrogen content in the top gas is highly sensitive to measurement error in the hot blast volume and so any attempt to control this under such circumstances would introduce an incorrect reduction sequence.

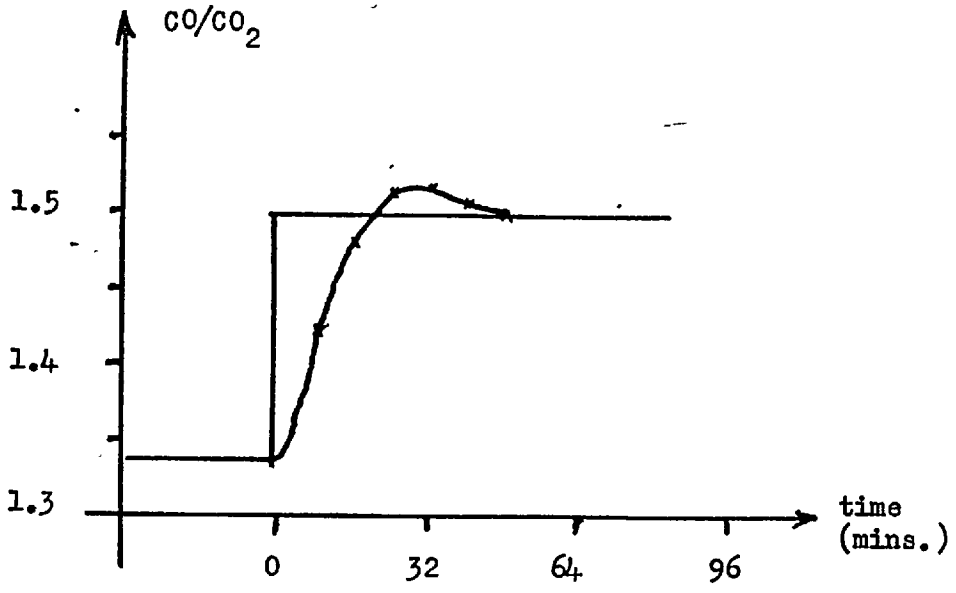
In view of this, two controllers are evaluated, one using the heat transfer coefficient to control top gas temperature, the other using the rate constant for indirect reduction to correct the CO/CO_2 ratio. Remembering that the top gas gives no indication of

the source of the disturbance, this choice of parameters spreads control throughout the furnace rather than concentrating on a single region.

The responses, when these closed loop calculations are added to the simulation, to changes in the demanded top gas temperature and CO/CO_2 ratio are shown in Fig. 6.3, and are satisfactory. It has not been possible to evaluate any improvements in the accuracy of the on-line simulation resulting from these calculations, but their use will undoubtedly extend the range of operation that can be simulated without recourse to manual parameter changes.



Correction of Top Gas Temperature using the heat transfer coefficient



Correction of CO/CO_2 using the indirect reduction rate constant

Fig. 6.3 Correction of the top gas using parameters

CONCLUSIONS AND FUTURE RESEARCH

This thesis first attempts a systematic classification of the very vast amount of literature on blast furnace modelling and control, and identifies the importance of understanding furnace dynamics and of making more information regarding the current furnace condition available to the operator.

With this in mind a numerical simulation intended specifically for use in plant control is developed and discussed in depth. In particular emphasis is placed on a simplified, but practical, analysis of the process and is based on both theoretical argument and experimental results.

The method of solution must be considered an improvement on others published to date. Both steady state and transient operation can be simulated directly and the method is manageable in terms of computer time and core storage. The simulation has been coded in Fortran and run off-line on both an IBM 360/40 and an ICL 1905, and runs in 1/60 th of real time. In an on-line environment at Port Talbot the simulation is segmented into 8K blocks and runs on an Argus 500 computer in 1/16th of real time.

Manual parameter tuning is discussed in depth and has been reduced to a sequence of logical operations.

The validity of the simulation is considered in three areas:-

1. Steady operation
2. Responses to test input signals
3. A simulation of normal operation

In the first two of these good agreement is shown between the model and both published experimental results and the operator's experiences.

A necessary prerequisite to complex modelling of this type is accurate and reliable information from instruments and weighing systems, and adequate facilities for sampling and analyses of raw materials. To date one or two important sources of information, such as coke moisture levels, have not been available. However, the initial on-line simulation results presented in Chapter 4 display a high level of correlation with plant silicon values and suggest that considerable benefit is likely when the proposed simulation is used for silicon control. The importance of maintaining this data base must be stressed as any corruption of the furnace state vector often takes several hours to die away.

Several systems aimed at controlling silicon using the simulation as an observer are considered in Chapter 5. Predictive control is particularly suited to the process - the inputs are held steady between casts and because control is applied earlier the system is less affected by the shortage of fast acting control. For continuous control a two term controller gives near optimal results.

The final performance of this type of system is very much dependent on the performance of the simulation on-line, and a final evaluation must await lengthy on-line trials.

In retrospect the major problem and effort was concerned with developing the right form of equations and in understanding the complex behaviour in physical terms. Once these are accomplished the design of the controls is relatively straightforward. This feature seems to be common in the field of process control and is precisely the position outlined in Ref. 41 with regard to Cold Mill control.

Turning to future research the problem of plant set up where input constraints are present could well be the subject of a further simulation exercise.

As more detailed information becomes available from test rigs and pilot plant regarding the process and its rate equations the proposed numerical technique would form the ideal base for more fundamental investigations into technological aspects such as burdening and the use of auxiliary fuels.

REFERENCES

(1)	K. H. GEE	Iron and Steel Engineer, July, 1964.
(2)	D. J. SHELLENBERGER & T. A. POWELL	Journal of Metals, March, 1968.
(3)	G. H. McCLESKEY	Instrumentation Technology, July, 1969.
(4)	N. A. ROBINS	Iron and Steel Engineer, December, 1967.
(5)	K. KATSURA & T. YAMAMOTO	Journees Internationales de Siderurgie, 1965, Amsterdam, Paper B9.
(6)	G. B. SPALLANZANI et al	Journees Internationales de Siderurgie, 1965, Amsterdam, Paper B8.
(7)	A. F. REBEKO et al	Stal in English, August, 1969, P692-695.
(8)	C. STAIB et al	Journees Internationales de Siderurgie, 1965, Amsterdam, Paper B4.
(9)	P. JOURDE et al	Journees Internationales de Siderurgie, Amsterdam, 1965, Paper B5.
(10)	A. POOS et al	Journees Internationales de Siderurgie, Amsterdam, 1965, Paper B6.
(11)	P. DUMITRASCO et al	Journees Internationales de Siderurgie, Luxembourg, 1970, Paper B103.
(12)	A. N. POKHVISNEV	Teoriya i Praktika Metallurgii, 1939, p15 - 19.
(13)	W. RINGELBAND et al	Journees Internationales de Siderurgie, Luxembourg, 1970, Paper B4.
(14)	A. RIST & N. MEYSSON	Journal of Metals, April, 1967.
(15)	C. STAIB et al	IRSID Report RE 189, Jan. 1968.
(16)	R. VIDAL et al	Journees Internationales de Siderurgie, Luxembourg, 1970, Paper B6.
(17)	H. RAKE	2nd IFAC Symposium, Prague, 1970.
(18)	T. BARBIERI et al	Journees Internationales de Siderurgie, Luxembourg, 1970, Paper B5.
(19)	I. MUCHI	Trans ISIJ Vol. 7, 1967, p.223.
(20)	J. YAGI & I. MUCHI	Trans ISIJ Vol. 10, 1970, p.392.

REFERENCES (cont.)

(21)	V. KOUMP et al	Process Simulation and Control in Iron and Steelmaking, Gordon & Breach, New York.
(22)	K. OKABE et al	Tetsu-to-Hagane, 55 (1969) S432.
(23)	H. BEER et al	Journees Internationales de Siderurgie, Amsterdam, 1965, Paper B3.
(24)	A. K. LAHIRI & V. SESHADRI	JISI March, 1969, p293.
(25)	H. W. St. CLAIR	United States Bureau of Mines Report RI 6975.
(26)	G. A. FLIERMAN & J. M. Van LANGEN	Journees Internationales de Siderurgie, Amsterdam, 1965, Paper B2.
(27)	H. TSUCHIYA & M. MORI	IFAC Symposium, Kyoto, Japan, August, 1970.
(28)	B. WATSON	Steel Times, June 24th 1966.
(29)	A. K. BISWUS & G. R. BASHFORTH	The Physical Chemistry of Metallurgical Processes, C & H, 1962.
(30)	E. SCHURMANN et al	Stal en Eisen Vol. 80, 1960, P.853.
(31)	C. BODSWORTH	Physical Chemistry of Iron and Steel Manufacture, Longmann.
(32)	R. JON et al	CNRM No. 15, 1968.
(33)	J. TAYLOR	JISI 1964, 202, 420.
(34)	J. KYLE et al	38th B.I.S.R.A. Blast Furnace Conference, Oct. 1970.
(35)	E. T. TURKDOGAN & L. E. LEAKE	JISI 1965, 179, 39.
(36)	B. I. WOOD	B.Sc. Thesis, The City University, London, 1967.
(37)	D. BULTER	Stal en Eisen, 1970, 90, (22), 1189.
(38)	B. PORTER	Synthesis of Dynamical Systems, Nelson, 1969, Chapter 8.
(39)	F. D. POWELL	IEEE Transactions October, 1969, p550.
(40)	J. D. HIGHAM	Control, February, 1968.
(41)	G. F. BRYANT et al	JISI Nov. 1971, p.869.

APPENDIX 1

The fundamental differential equations

To establish the form of the differential equations consider a mass balance over an elementary volume τ for any of the chemical components present in the furnace.

Let the flow /sec/m^2 at the general point P ($\vec{r}$) of one of the components

$= \vec{F}(\vec{r}, t)$

Then the flow out of the volume τ per sec $= \int_S \vec{F}.d\vec{s}$

and applying Gaus' Divergence Theorm this becomes

$$= \int_\tau \nabla.\vec{F}\, d\tau$$

The mass of this component within $\tau = \int_\tau c\, d\tau$

where c is the concentration (Mass/m^3)

A Mass balance can now be performed giving

$$\int_\tau \frac{\partial c}{\partial t} d\tau = - \int_\tau \nabla.\vec{F}\, d\tau + \int_\tau G d\tau$$

where G is the rate of generation of the component (Mass/sec/m^3)

Now letting $\tau \to 0$

$$\frac{\partial c}{\partial t} = - \nabla.\vec{F} + G$$

Consider next the case of unidimensional flow in the vertical direction, x being measured from the stockline. For this case

$$\vec{F} = c\vec{V}$$

where $\vec{V}(\vec{r}, t)$ is the velocity of gas or solid as appropriate

Thus

$$\frac{\partial c}{\partial t} = - \frac{\partial}{\partial x} (V_x c) + G$$

The equations relating to gas and solid temperatures are slightly different.

Let $\vec{H}(\vec{r}, t)$ = heat flow/sec/m^2 at the point $P(\vec{r})$ in the solids. Then the heat flow out of the volume τ

$$= \int_s \vec{H} . \vec{ds}$$

$$= \int_\tau \nabla . \vec{H} \, d\tau \qquad \text{(by Divergence Theorm)}$$

Now if the concentration of heat at $P(\vec{r})$ is denoted by $\rho(\vec{r}, t)$ a heat balance gives

$$\frac{\partial}{\partial t} \int_\tau \rho \, d\tau = - \int_\tau \nabla . \vec{H} \, d\tau + \int_\tau G_{H_s} \, d\tau$$

letting $\tau \to o$

$$\frac{\partial \rho}{\partial t} = - \nabla . \vec{H} + G_{H_s}$$

Now

$$\rho = \int_{Ts_o}^{Ts} W_s \, dT$$

and

$$\vec{H} = \int_{Ts_o}^{Ts} W_s \vec{V} \, dT$$

where W_s = water equivalent of solids cals/$^oC/m^3$

Thus

$$\frac{\partial}{\partial t} \int_{Ts_o}^{Ts} W_s \, dT = - \frac{\partial}{\partial x} \int_{Ts_o}^{Ts} W_s V_x \, dT + G_{H_s}$$

$$\therefore W_s \left(\frac{\partial Ts}{\partial t} + V_x \frac{\partial Ts}{\partial x}\right) = - \int_{Ts_o}^{Ts} \left(\frac{\partial W_s}{\partial t} + \frac{\partial}{\partial x} (W_s V_x)\right) dt + G_{H_s}$$

But

$$W_s = \sum_i S^i c_i^s$$

where the sumation ranges over the solid components and S^i are the individual specific heats and so

$$W_s \left(\frac{\partial Ts}{\partial t} + V_x \frac{\partial Ts}{\partial x}\right) = - \sum_i \int_{Ts_o}^{Ts} S^i G_i \, dT + G_{H_s}$$

The first term on the RHS represents the heat required to raise the temperature of materials generated in the volume τ from Ts_o to Ts. In fact, because these materials transfer from the gas to the solid stream or vice versa the temperature change is small ($< 250^{\circ}C$) and so this term can be ignored. Thus, the equation relating solid temperature to space and time is

$$W_s \left(\frac{\partial Ts}{\partial t} + V_x \frac{\partial Ts}{\partial x}\right) = G_{H_s}$$

APPENDIX 2

Error Calculations

These error calculations are aimed at estimating the effect of decoupling the gas and solid systems in order to handle boundary values at two points without iteration, as discussed in Chapter 3. Two examples are given of simplified systems which serve to give an initial estimate of the step length for the complete system:-

(1) heat transfer

$$\frac{\partial T_s}{\partial t} + V_s \frac{\partial T_s}{\partial x} = G_H/W_s$$

$$\frac{\partial T_g}{\partial t} - V_g \frac{\partial T_g}{\partial x} = -G_H/W_g$$

where

$$G_H = 88.0\,(T_g - T_s)$$

In this case $W_s \geq 0.16 \times 10^6$ and so

$$\% \text{ Error in } T_g \leq \frac{100 \times 88 \times \Delta t}{0.16 \times 10^6}$$

Thus if $\Delta t = 60s$ then the % Error in $T_g \leq 3\%$

(2) carbon solution loss i.e. $C + CO_2 \quad 2CO$

$$\frac{\partial C}{\partial t} + V_s \frac{\partial C}{\partial x} = -T$$

$$\frac{\partial CO}{\partial t} - V_g \frac{\partial CO}{\partial x} = 2T$$

$$\frac{\partial CO_2}{\partial t} - V_g \frac{\partial CO_2}{\partial x} = -T$$

where

$$T = 0.24 \times C \times CO_2 \times \exp(-2500/(T_s + 273))$$

In this case

$$\% \text{ Error in } CO_2 = 100 \times 0.24 \times CO_2 \times \exp(-2500/(T_s + 273))\ \Delta t$$

and is therefore less than 0.3% for $\Delta t = 60s$.

This corresponds to an error in $\% CO_2$ of $\pm$ 0.05% of the total gas volume.